DESIGN, SYNTHESIS, AND ASSAY OF POTENTIAL INHIBITORS OF *E. COLI* ASPARAGINE SYNTHETASE B

By

ANTHONY BRIAN DRIBBEN

A DISSERTATION PRESENTED TO THE GRADUATE SCHOOL
OF THE UNIVERSITY OF FLORIDA IN PARTIAL FULFILLMENT
OF THE REQUIREMENTS FOR THE DEGREE OF
DOCTOR OF PHILOSOPHY

UNIVERSITY OF FLORIDA

1997

This work is dedicated to my parents, whom I respect, admire, and love dearly. This dedication is extended to my brother, sister, grandparents, aunts, uncles, cousins, and others who have supported me during the course of my education.

ACKNOWLEDGMENTS

I would like to thank my advisor, Nigel G. J. Richards, for his guidance, patience, support, and valuable input throughout my graduate studies. The members of my supervisory commmittee, R. J. Bartlett, W. S. Brey, W. R. Dolbier, and S. M. Schuster, also have my appreciation. Thanks to John Stanton and John Watts for helping me get started using the ACES II *ab initio* program, and to Mike Bartberger for occasional advice with GAMESS. I thank Ian Parr, Jose Rosa, and Margaret Deyrup for helpful advice throughout the synthetic portion of this research. I thank Susan Boehlein and Tom Soper for results from various enzyme assays, and also for instructive conversations about the enzyme activity. I could not have done it without the help from these important people. They have my appreciation and best wishes for the future.

I also want to thank the professors in the chemistry department at UF, particularly Jon Stewart and Ben Horenstein, as well as all of the chemistry professors at Mississippi College, who have given me helpful advice regarding my future career in chemistry.

Next, I would like to thank all my colleagues in the Richards Group: Ian Parr, Jennifer Brown, Craig Porter, Jose

Rosa, Susan Rasmussen, Srini Iyengar, Rick Smith, Nagraj Bokinkere, Yannis Karayannis, Rajiv Moghe, Steven Nowicki, Astra Dinculescu, Maria Capobianco-Perez, Saul Jacchieri, Ramanan Thiurmoorthy, Mihai Ciustea, and Amy Boone for daily productive and nonproductive conversations in the topics of chemistry and life. I wish all of them the best in the future and hope to see them again. Special thanks to Yannis for his quick, but accurate, proofreading of this manuscript.

Sincere thanks go to my parents, Al and Mary Jo Dribben, who have been my primary support system throughout my studies. Thanks also to my sister, Traci, and my brother and sister-in-law, Taylor and Melanie. You have all been there to listen to my gripes and complaints, yet still, for some reason, love me anyway. Thanks also go to my grandparents and other extended family members who have kept me in their thoughts and prayers all this time. I also want to thank my pals Lucian, Melania, Nagraj, and Carlton for helping me spend my free time away from the lab. I also thank all my Mississippi pals for their support, and for at least feigning interest in what I have been doing. I truly appreciate it.

Finally, I would like to thank the Florida Section of the American Cancer Society, and the National Cancer Institute of the National Institutes of Health for funding for this research. Thanks also go to the Florida State Supercomputing Center for generous allocations of supercomputer time.

TABLE OF CONTENTS

Abstract of Dissertation Presented to the Graduate School of the University of Florida in Partial Fulfillment of the Requirements for the Degree of Doctor of Philosophy

DESIGN, SYNTHESIS, AND ASSAY OF POTENTIAL INHIBITORS OF *E. COLI* ASPARAGINE SYNTHETASE B

By

Anthony Brian Dribben

August, 1997

Chairman: Dr. Nigel G. J. Richards
Major Department: Chemistry

β-Alkylation of protected aspartate derivatives has allowed the preparation of a number of stereochemically defined aspartate analogs suitable for probing the molecular features of the aspartic acid binding site in *E. coli* asparagine synthetase B (AS-B). Further investigation of the alkylation reaction has determined that the addition appears to proceed via a Z-lithium enolate geometry, with complete stereochemical control in some cases. The use of substrate analogs has shown that AS-B appears to be extremely selective and that it can tolerate only relatively minor structural alterations in the aspartic acid substrate.

The computational modeling of possible AS-B reaction mechanisms and intermediates through semi-empirical and *ab initio* methodology has shown the feasibility of several

alternate mechanisms which do not involve nitrogen transfer via ammonia. Moreover, AS-B appears to behave in a similar manner as proteolytic enzymes which also utilize a catalytic sulfur nucleophile.

A route for the chemoenzymatic synthesis of L-4,4-difluoroglutamic acid has been developed which involves the enzymatic resolution of a racemic precursor. This fluorinated amino acid is a valuable precursor in the synthesis of other fluorinated substrate analogs. Potential applications of these fluorinated analogs include use as mechanistic probes of AS-B due to their enhanced reactivity, or use as possible suicide inhibitors of AS-B.

A series of protected phosphorus-based transition state analogs have been synthesized. These types of compounds, which contain a phosphonamidate functionality, are useful inhibitors of other hydrolytic enzymes, and may prove to be effective inhibitors of AS-B.

CHAPTER 1
STRUCTURE AND FUNCTION OF THE AMIDOTRANSFERASES AND *E. COLI* ASPARAGINE SYNTHETASE B

The Amidotransferases

The amidotransferases are a family of enzymes that use the amide functionality of glutamine **1** in the biosynthesis of other biomolecules. These biomolecules include amino acids (1), purine and pyrimidine bases (2), amino sugars (3), coenzymes (4), and antibiotics (5). The fate of the amide nitrogen atom in some of these biomolecules is illustrated in **Figure 1-1.** The amidotransferase family of enzymes has been thoroughly reviewed by Buchanan (6) and Zalkin (7).

Most of the amidotransferase enzymes catalyze at least three different reactions (6,7). They can use ammonia as the nitrogen source in the absence of glutamine (ammonia-dependent activity). They also can use glutamine as the nitrogen source, (glutamine-dependent activity), or hydrolyze it to form glutamic acid **2** and ammonia (glutaminase activity). The glutamine-dependent and glutaminase activities can be inactivated by alkylating an active site cysteine residue with a glutamine analog, or by replacing the cysteine residue with an alternate amino acid.

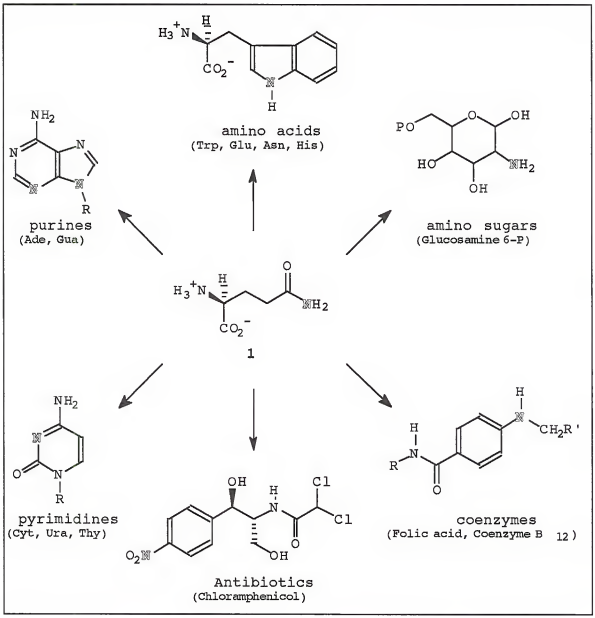

Figure 1-1. Fate of the amide nitrogen of L-glutamine **1** in several biosynthetic pathways.

These properties indicate the presence of two independent domains, or subunits, operating together for enzyme activity. The synthetase domain utilizes ammonia as the nitrogen source, and the glutamine amide transfer (GAT) domain utilizes glutamine as the nitrogen source. The

chemical reactions catalyzed by the synthetase domain (i) and the GAT domain (ii) are illustrated in **Figures 1-2** and **1-3**, respectively. These two domains are either fused together and present on a single protein chain, or present as independent subunits of the enzyme (6,7).

Based on the conservation of GAT domains throughout these enzymes, the amidotransferase family has been divided into two subfamilies. The first subfamily, known as Class I, was originally designated TrpG based on the *trpG* gene encoding the GAT domain of anthranilate synthase component II. Members of this family include anthranilate synthase (13), carbamoyl-phosphate synthase (14), cytidine triphosphate (CTP) synthetase (3), FGAM synthetase (15), guanosine monophosphate (GMP) synthetase (16), imidazole glycerol-phosphate synthase (1), and aminodeoxychorismate synthase (17). The second subfamily, known as Class II, was originally designated PurF based on the *purF* gene encoding the GAT domain of glutamine phosphoribosyl pyrophosphate amidotransferase (glutamine PRPP amidotransferase) (8,9). This family includes the enzymes asparagine synthetase (10), glucosamine 6-phosphate synthase (2), glutamate synthase (11), and glutamine PRPP amidotransferase (12). Other amidotransferases which have not yet been classified as Class I or Class II include arylamine synthetase (5), Gln-$tRNA^{Gln}$ amidotransferase (18), NAD synthetase (19), cobyrinic acid

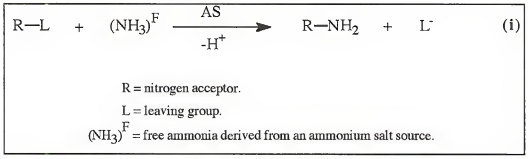

Figure 1-2. Reaction catalyzed by the synthetase domain of Amidotransferases.

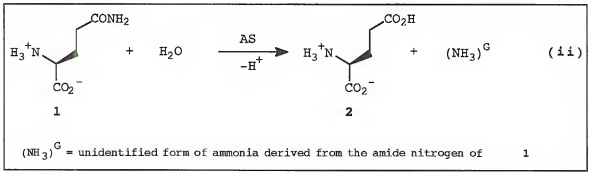

Figure 1-3. Reaction catalyzed by the glutamine amidotransferase domain (GAT) of Amidotransferases.

a,c-diamide synthetase (20), and cobyric acid synthetase (21).

The mechanism of amide nitrogen transfer from the GAT domain to the synthetase domain was initially investigated by Levitzki and Koshland (22) using the Class I enzyme CTP synthetase from *Escherichia coli* (*E. coli*). Through the use of kinetic assay experiments, it was found that ammonia derived from the glutamine amide functionality $(NH_3)^G$ remained bound to the enzyme prior to incorporation into the substrate. Ammonium sulfate was used in competition

experiments to demonstrate that free ammonia from solution $(NH_3)^F$ competed with $(NH_3)^G$ for a single site in the enzyme. Similar studies by Zalkin and Truitt (23) conducted using the Class I enzyme GMP synthetase also found that $(NH_3)^G$ remains enzyme bound. However, experiments using ammonium chloride as the $(NH_3)^F$ source to determine whether a single NH_3 site was common to $(NH_3)^F$ and $(NH_3)^G$ were inconclusive. These authors demonstrated that the results obtained by Levitzki and Koshland showing competition of $(NH_3)^F$ for $(NH_3)^G$ were probably due to SO_4^{2-} inhibition and not due to $(NH_3)^F$ inhibition derived from $(NH_4)_2SO_4$. Nevertheless, the specific form of $(NH_3)^G$ for these enzymes was not addressed in either of these studies and remains an open question. Also, since these experiments were based on Class I enzymes, the same conclusions cannot necessarily be extended to Class II enzymes.

The role of the ammonia-dependent activity has also been studied in other amidotransferases such as anthranilate synthase (24), glutamine (PRPP) amidotransferase (25), and carbamyl-P synthetase (26). In general, it was found that the ammonia-dependent activity of *E. coli* strains in which the GAT domain function had been inactivated by modification or deletion of the active site cysteine residue, remained unaltered but required higher concentrations of ammonium salts in the reaction medium. This observation is attributed to the low concentrations of NH_3 present in solution relative to NH_4^+ at pH 7.0-7.5 and from the high K_M of NH_3 relative to

the K_M of glutamine. From these studies, two ideas for the ammonia-dependent activity of the amidotransferases were proposed. One proposed idea is that the ammonia-dependent enzymes existed before the evolution of the GAT domain. This evolution resulted in the expansion of the specificity of these enzymes. The other proposed idea is that the ammonia-dependent activity resulted from utilization of an existing enzyme-bound ammonia site by NH_3[G]. However, no evidence has been presented to support either of these two proposals.

Asparagine Synthetase

Structure and Function

Asparagine Synthetase (AS) is a member of the Class II subfamily of amidotransferases, which are characterized by the location of the GAT domain in their polypeptide chain and an essential N-terminal cysteine residue (8). Asparagine synthetases which strictly use ammonia as the nitrogen source have been found in bacteria (27), whereas asparagine synthetases capable of utilizing both ammonia and glutamine as nitrogen sources have been found in more complex higher organisms. Bacterial AS has been isolated from *Streptococcus bovis* (28), *E. coli* (29), *Lactobacillus arabinosus* (30), and *Klebsiella aerogenes* (31). AS has also been isolated and purified from fungi such as *Neurospora crassa* (32), yeast such as *Saccharomyces cerevisiae* (33), plants (34), and various mammals (10,35-37).

Coding sequences for AS were first obtained from the Chinese hamster (38) and from human fibroblasts (10). They were found to encode primary sequences of 561 amino acids having 95% identity. Alignment of these sequences with *E. coli* glucosamine 6-phosphate synthase, *E. coli* PRPP amidotransferase, and yeast glutamine PRPP amidotransferase sequences confirmed that AS is a member of the Class II subfamily which has an N-terminal GAT domain followed by a synthetase domain (38).

Primary sequence alignment for several members of the Class II subfamily is shown in **Figure 1-4** (39). From this alignment, at least 11 residues seem to be conserved throughout the GAT domains of all Class II amidotransferases. These correspond to Cys_1, Gly_2, Ile_3, Arg_{30}, Gly_{31}, Asp_{33}, Arg_{49}, Asn_{74}, Gly_{75}, Asn_{79}, and Asp_{98} in *E. coli* asparagine synthetase B (see APPENDIX A for amino acid abbreviations). Although the crystal structure for any of the asparagine synthetase enzymes remains to be solved, the crystal structures for other Class II enzymes, namely *B. subtillus* glutamine PRPP amidotransferase (40), *E. coli* glutamine PRPP amidotransferase (41), and the GAT domain of glucosamine 6-phosphate synthase (42) have been determined. The crystal structure of the Class I amidotransferase GMP synthetase (43) has also been determined.

```
                  01[b]                                                  49
Ham ASase[a]  MCGIWALFGS DDCLSVQCL. .SAMKIA... .HRGPDAFRF ENVNGY....
Hum ASase[a]  MCGIWALFGS DDCLSVQCL. .SAMKIA... .HRGPDAFRF ENVNGY....
Eco ASase[a]  MCSIFGVFDI KTDAVELRK. .KALELSRLM RHRGPD...W SGIYAS....
Pea ASase[a]  MCGILAVLGC SDDSQAKRV. .RILELSRRL KHRGPD...W SGLHQH....
Pea AS II[a]  MCGILAVLGC SDPSRAKRV. .RVLELSRRL KHRGPE...W SGLHQH....
Hum GFat[a]   MCGIFAYLNY HVPRTRREIL ETLIKGLQRL EYRGYDSACV GFDGGNDKDW
Yst GFat[a]   MCGIFGYCNY LVERSRGEII DTLVDGLQRL EYRGYDSTGI AIDGD.....
Rhz NodM[a]   MCGIVGIV.. ....GHQPVS ERLVEALEPL EYRGYDSAGV A.........
PRPP[a]       MCGIVGIAGV M .....PVN QSIYDALTVL QHRGQDAAGI ISIDAN....

                  50                                                     99
Ham ASase     ..................... ..... ......TNCC FGFHRLAVVD
Hum ASase     ..................... ..... ......TNCC FGFHRLAVVD
Eco ASase     ..................... ..... ......DNAI LAHERLSIVD
Pea ASase     ..................... ..... ......GDNY LAHQRLAIVD
Pea AS II     ..................... ..... ......GDCY LAQQRLAIVD
Hum GFat      EANACKTQLI KKKGKVKALD EEVHKQQDMD LDIEFDVHLG IAHTRWATHG
Yst GFat      ..EAOSTFIY KQIGKVSALK EEITK.QNPN RDVTFVSHCG IAHTRWATHG
Rhz NodM      TMDAGTLQRR RAEGKLGNLR EKL....... KEAPLSGTIG IAHTRWATHG
PRPP          ....NCFRLR KANGLVSDVF EARHMQR... ....LQGNMG IGHVRYPTAG

                  100                                                    149
Ham ASase     P..LFGMQPI RVKKYPYLWL CYNGEIYNHK ALQQRF.... EFEYQTNVDG
Hum ASase     P..LFGMQPI RVKKYPYLWL CYNGEIYNHK KMQQHF.... EFEYQTKVDG
Eco ASase     V..NAGAQPL YNQQKTHV.L AVNGEIYNHQ ALRAEY..GD RYQFQTGSDC
Pea ASase     P..ASGDQPL FNEDKSII.V TVNGEIYNHE ELRKQL..PN H.KFFTQCDC
Pea AS II     P..ASGDQPL FNEDNPSI.V TVNGEIYNHE DLRKQL..SN H.TFRTGSDC
Hum GFat      EPSPVNSHPQ RSDKNNEFIV IHNGIITNYK DL.KKFLESK GYDFESETDT
Yst GFat      RPEQVNCHPQ RSDPEDQFVV VHNGIITNFR EL.KTLLINK GYKFESDTDT
Rhz NodM      APTERNAHPH FTE...GVAV VHNG.IENFA EL.KDELAAG GAEFQTETDT
PRPP          SSSASEAQPF YVNSPYGITL AHNGNLTNAH ELRKKLFEEK RRHINTTSDS

                  150                                                    199
Ham ASase     EIILHLYDK. ......... .....GGIEQ TICMLDGVFA FILLDTANKK
Hum ASase     EIILHLYDK. ......... .....GGIEQ TICMLDGVFA FVLLDTANKK
Eco ASase     EVILALYQE. ......... .....KG.PE FLDDLQGMFA FALYDSEKDA
Pea ASase     DVIAHLYEE. ......... .....HG.EN FVDMLDGIFS FVLLDTRDNS
Pea AS II     DVIAHLYEE. ......... .....YG.ED FVDMLDGIFS FVPLDTRDNS
Hum GFat      ETIAKLVKYM YDN..RESQD TS.FTTLVER VIQQLEGAFA LVFKSVHFPG
Yst GFat      ECIAKLYLHL YNTNLQNGHD LD.FHELTKL VLLELEGSYG LLCKSCHYPN
Rhz NodW      EVVAHLLAKY ......RRDG LG.RREAMHA MLKRVKGAYA LAVLFEDDPS
PRPP          EILLNIFASE LDNFRHYPLE ADNIFAAIAA TNRLIRGAYA CVAMIIGHGM
```

Notes: (a) Ham ASase = Hamster asparagine synthetase (EC 6 3 5 4)
Hum ASase = Human asparagine synthetase (EC 6 3 5 4)
Eco ASase = E. coli asparagine synthetase B (EC 6 3 5 4)
Pea ASase = Pea AS1 nodule asparagine synthetase (EC 6 3 5 4)
Pea AS II = Pea AS2 root asparagine synthetase (EC 6 3 5 4)
Hum GFat = Human D-fructose-6-phosphate amidotransferase
Yst GFat = *S. cerevisiai* D-fructose-6-phosphate amidotransferase
Rhz NodM = NodM encoded D-glucosamine synthetase (R. leguminosarum)
PRPP = K. coli purF amidophosphorthoxylransferase (EC 2.4.2.14)
(b) N-terminal methionine is not present in any of the mature proteins. Residue numbers correspond to those of human D-fructose-6-phosphate amidotransferase.

Figure 1-4. Primary sequence alignment of Class II glutamine-dependent amidotransferases (Taken from reference 39).

Asparagine synthetase catalyzes the ATP-dependent synthesis of L-asparagine **4** from L-aspartic acid **3** using either ammonia (**iii**) or L-glutamine (**iv**) as the nitrogen source (**Figure 1-5**). Glutaminase activity (**v**) has also been found in various sources of AS.

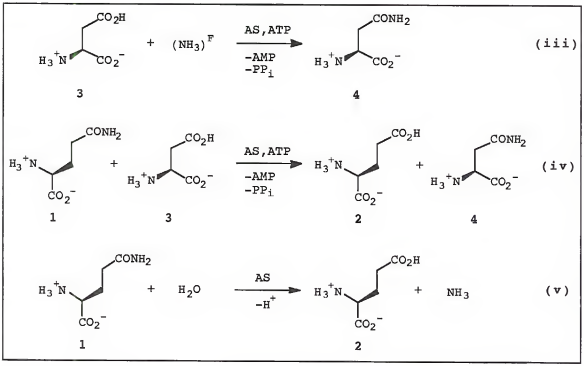

Figure 1-5. Reactions catalyzed by Asparagine Synthetase; (**iii**) ammonia-dependent activity; (**iv**) glutamine-dependent activity; (**v**) glutaminase activity.

Some asparagine synthetases, such as asparagine synthetase A (AS-A), can only use ammonia as the source of nitrogen to produce asparagine, while the glutamine-dependent enzymes can use glutamine or ammonia as the nitrogen source (7). Interestingly, the glutamine-dependent activity of the latter enzymes can be inactivated without affecting the

ammonia-dependent activity. This fact was demonstrated in a series of experiments by Van Heeke and Schuster using human AS expressed in *E. coli* (44) and *S. cerevisiae* (45). In these experiments, a mutant enzyme was expressed in which the N-terminal cysteine residue (Cys_1) was replaced with an alanine residue (C1A mutant). This mutation resulted in the loss of glutamine-dependent activity and a slight increase in ammonia-dependent activity. These results verify the presence of a GAT domain with an N-terminal cysteine residue essential for glutamine-dependent activity, as well as a synthetase domain which is responsible for the ammonia-dependent activity. Further studies by Schuster and coworkers demonstrated that these two domains are topographically separated from each other (46). This was shown through the use of monoclonal antibodies which selectively and specifically inhibited each of the two activities independently (46). It is the interaction between these two domains which allow the nitrogen transfer reaction to occur (**Figure 1-6**).

Reaction Mechanism

As a result of studies on mammalian AS and bacterial AS-A, ^{18}O isotopic labeling techniques have established that, in asparagine synthesis, the synthetase domain appears to catalyze formation of the β-aspartyl-AMP intermediate **6** (37,47). Cedar and Schwartz demonstrated the presence of **6**

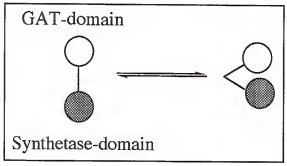

Figure 1-6. Schematic representation of the conformational reorganization of the GAT- and synthetase domains in the nitrogen transfer reaction of asparagine synthetase.

by incubating *E. coli* AS with ^{18}O-labeled aspartic acid **3** and ATP **5** (**Figure 1-7**) (47). These react to form ^{18}O-labeled **6** and release pyrophosphate (PP_i) with no ^{18}O-label. The resultant nucleophilic attack of ammonia on **6** forms ^{18}O-labeled L-asparagine **4** and releases ^{18}O-AMP **7** as a side product. This scheme of reactions illustrates the events taking place in the ammonia-dependent reaction **(iii)** which occur in the C-terminal synthetase domain of AS.

Of more interest is the function of the GAT domain. Sequence studies by Tso et al. (48) and Vollmer et al. (49) on glutamine PRPP amidotransferase established the presence of an N-terminal cysteine residue (Cys_1) essential for glutamine-dependent activity. This residue is conserved in all the members of the Class II family of amidotransferases. It was demonstrated that alkylation of Cys_1 with 6-diazo-5-oxo-L-norleucine **8** (DON) (**Figure 1-8**), or mutagenesis of the histidine (His_{101}) and aspartate (Asp_{29}) residues in glutamine PRPP amidotransferase each abolished the glutamine-dependent

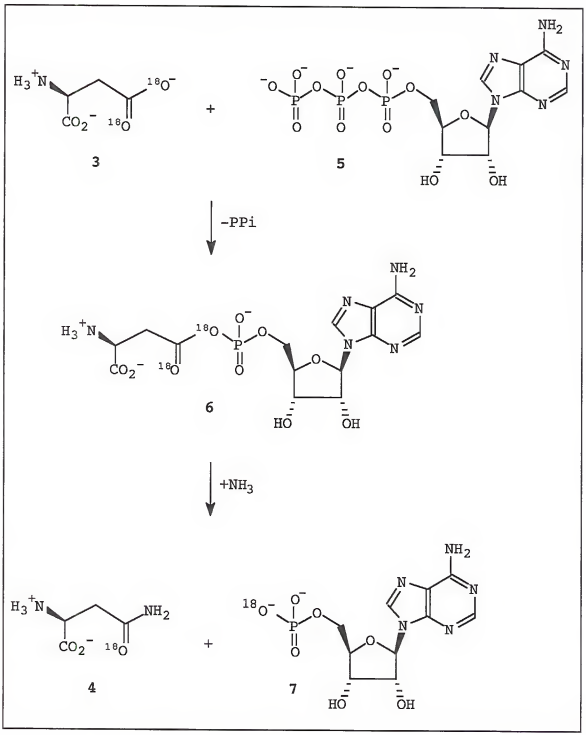

Figure 1-7. *E. coli* AS catalyzed biosynthesis of L-asparagine **4** from ^{18}O-labeled L-aspartic acid **3** and NH_3 via ^{18}O-β-asparty1-AMP intermediate **6**.

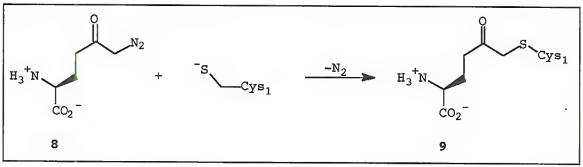

Figure 1-8. Alkylation of Cys_1 with 6-diazo-5-oxo-L-norleucine (DON) **8** to form inactivated Cys_1 residue **9** (12).

activity without affecting the ammonia-dependent activity (8). Schuster et al. replaced Cys_1 with alanine (C1A) on human AS and obtained a mutant enzyme with no glutamine-dependent activity and unaffected ammonia-dependent activity (45,50).

Mei and Zalkin (8) have proposed a mechanism for the Class II subfamily of amidotransferases, including AS, based on studies upon glutamine PRPP amidotransferase (**Figure 1-9**). In this enzyme, the active site is composed of a Cys_1, His_{101}, and Asp_{29} catalytic triad (glutamine PRPP amidotransferase numbering) which have a similar function to the Cys-His catalytic diad found in the thiol protease family of enzymes (51). In the proposed mechanism of AS, the nucleophilicity of the sulfur atom is increased by the presence of His_{101} in the active site, through polarization or deprotonation of Cys_1. The thiolate anion formed attacks the amide functionality of glutamine to form the tetrahedral intermediate **10**. The primary amine generated abstracts a proton from the imidazolium ion of His_{101} to form intermediate

11 which subsequently breaks down to give ammonia and γ-glutamyl-thioester enzyme intermediate **12**. The ammonia generated at this stage reacts with β-aspartyl-AMP intermediate **6** to generate asparagine and AMP (**Figure 1-7**). Nucleophilic attack of water, assisted by His_{101} as before, attacks intermediate **12** to form tetrahedral intermediate **13**. Breakdown of **13** releases glutamate and regenerates the initial state of the enzyme.

Recent evidence, however, has been presented which does not support this proposed mechanism. The primary sequence alignment of several Class II amidotransferases have failed to show conserved histidine residues (**Figure 1-4**) (39). Furthermore, primary sequence alignment of 20 asparagine synthetases from different sources have revealed no histidine residue cognate to His_{101} in glutamine PRPP amidotransferase (52). In addition, the crystal structures of *B. subtillus* glutamine PRPP amidotransferase (40), *E coli* glutamine PRPP amidotransferase (41), and the GAT domain of glucosamine 6-phosphate synthase (42) failed to reveal amino acid residues in close proximity to Cys_1 which can participate in acid-base catalysis. Therefore, residues His_{101} and Asp_{29}, which are implicated as catalytically important residues in glutamine PRPP amidotransferase, do not seem to play a role in catalysis by AS.

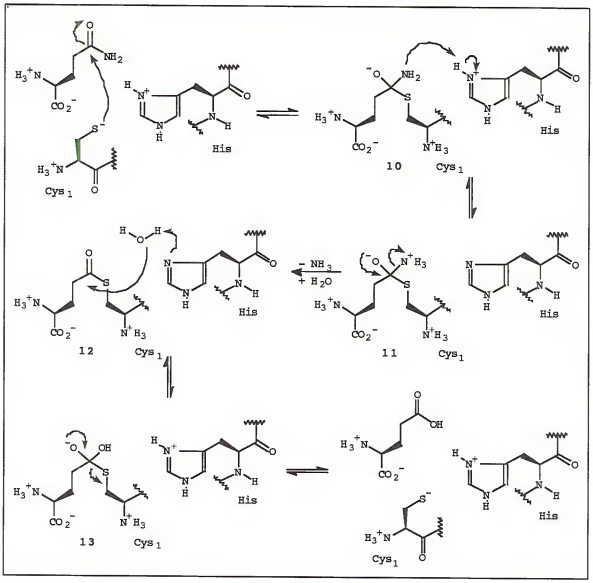

Figure 1-9. Proposed ammonia-mediated mechanism of Asparagine Synthetase based on studies of glutamine PRPP amidotransferase (8).

Milman et al. (53) kinetically characterized mouse pancreas AS and proposed a uni-uni-bi-ter ping-pong Theorell-Chance mechanism (54) for the glutamine-dependent activity (**Figure 1-10A**). In this mechanism, glutamine binds first followed by release of glutamate. Sequential binding of

aspartate and ATP follow, at which point nitrogen is transferred. The ordered release of PP_i, AMP, and Asn regenerate the original state of the enzyme. Markin et al. (55) kinetically characterized beef pancreas AS and proposed a bi-uni-uni-ter ping-pong mechanism (54) for the glutamine-dependent activity (**Figure 1-10B**). In this mechanism, glutamine and ATP bind sequentially, followed by release of glutamate and addition of aspartate. At this stage, nitrogen is transferred, followed by sequential release of PP_i, AMP, and Asn to regenerate the original state of the enzyme. In the ammonia-dependent activity of this enzyme, ammonia binds first followed by random binding of ATP and Asp. Nitrogen transfer then occurs, followed by sequential release of PP_i, AMP, and Asn (**Figure 1-10C**) (55).

It is difficult to reconcile the binding of glutamine and release of glutamate prior to the formation of β-aspartyl-AMP **6**. Since aspartate binds after hydrolysis of the putative γ-glutamyl enzyme intermediate **12**, it is not clear how the enzyme can sequester ammonia throughout the hydrolysis step, as well as maintain the unprotonated nucleophilic character needed for the subsequent reaction with β-aspartyl-AMP **6**. Recent studies by Habibzadegah-Tari on *E. coli* AS (56) have demonstrated that glutamine is the last reactant to bind to the enzyme before the nitrogen transfer step occurs, in contrast with previous results. If this is the case, β-aspartyl-AMP formation would precede glutamine hydrolysis.

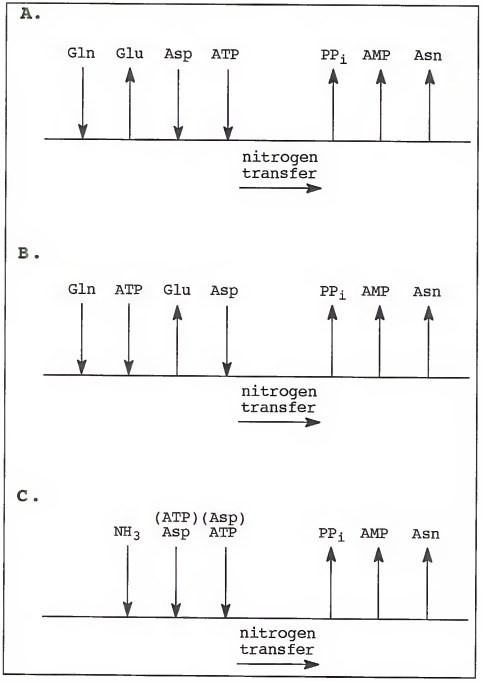

Figure 1-10. Kinetic mechanism of AS depicting order of substrate binding, nitrogen transfer, and product release; **A.** glutamine-dependent activity in mouse pancreas AS; **B.** glutamine-dependent activity in beef pancreas AS; **C.** ammonia-dependent activity in beef pancreas AS.

E. coli Asparagine Synthetase

Structure and Function

There are two different AS enzymes that have been isolated from *E. coli*. Asparagine synthetase A (AS-A) is encoded by the *asnA* gene and strictly catalyzes the ammonia-dependent reaction (**iii**) (**Figure 1-5**) (27). In contrast, asparagine synthetase B (AS-B) is encoded by the *asnB* gene and catalyzes all reactions (**iii**)-(**v**) independently (57). However, multiple asparagine synthetases contained in a single organism other than *E. coli* have not been reported (7).

The primary sequence of *E. coli* AS-A has been determined from the cloned *asnA* gene and found to be composed of 330 amino acids with an M_r of 36,700 (58). Similarly, the primary sequence of *E. coli* AS-B has been determined from the cloned *asnB* gene and found to be composed of 554 amino acids with an M_r of 62,700 (59). Inspection of the N-terminal amino acid sequence of AS-B identified it as being a member of the Class II subfamily. Also, the primary sequence of AS-B was found to have a high degree of homology (48%) with human AS and little or no homology with AS-A. Because of the dissimilarity between them, it is accepted that the *asnA* and *asnB* genes evolved independently. Thus, the ability of AS-B to possess glutamine-dependent activity probably did not

arise from fusion of an ancestral GAT gene with the *asnA* gene (59).

Site-directed mutagenesis on the GAT domain of AS-B has revealed no histidine residues which can participate in glutamine-dependent nitrogen transfer (39). Furthermore, crystal structures of other members of the Class II subfamily lack amino acid residues in close proximity to Cys_1 which can participate in acid-base catalysis. Unfortunately, no crystal structure is available for *E. coli* AS-B or any asparagine synthetase. Nevertheless, alternative pathways for the nitrogen transfer step in the mechanism of Class II enzymes have recently been made.

Reaction Mechanism

Richards and Schuster (60) have proposed a mechanism for glutamine-dependent nitrogen transfer in *E. coli* AS-B which operates without participation of histidine or aspartate residues in catalysis (**Figure 1-11**). In this mechanism, nucleophilic attack of the amide nitrogen on β-aspartyl-AMP **6** forms the unsymmetric acyclic imide **14** after breakdown of a presumed tetrahedral intermediate. Subsequent attack of Cys_1 thiolate anion upon imide **14** produces γ-glutamylthioester **12** and the hydroxyimine tautomer of asparagine **15** after protonation. Finally, water attacks intermediate **12** to ultimately form glutamate via intermediate **13** (**Figure 1-9**) and regenerates the initial state of the enzyme.

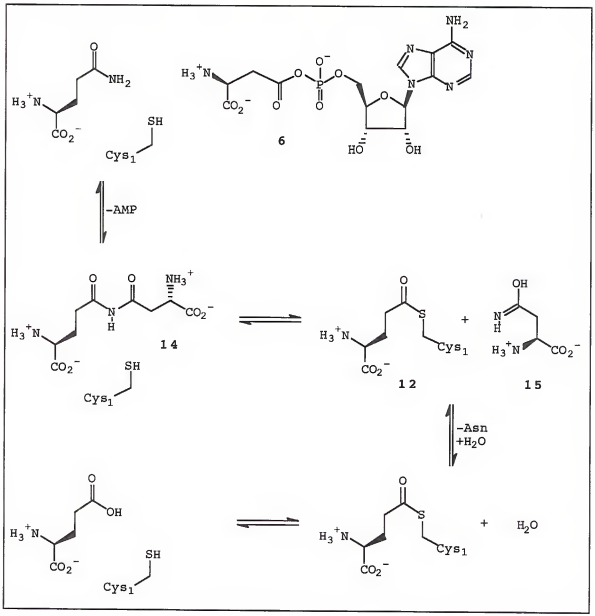

Figure 1-11. Proposed mechanism for glutamine-dependent nitrogen transfer in *E. coli* AS-B involving acyclic unsymmetric imide **14** as a reaction intermediate.

In this proposed imide-mediated mechanism, the need for an active site histidine to perform general acid protonation of the ammonia leaving group from tetrahedral intermediate **10** is eliminated (**Figure 1-9**). Furthermore, the transfer of

nitrogen via the imide intermediate **14** eliminates the possibility of ammonia diffusing from the active site to form unproductive NH_4^+. Additionally, there is no need for a separate ammonia binding pocket or an NH_3-enzyme complex intermediate.

There is some precedence for imide formation from primary amides in other biological systems as well as from synthetic organic methodology (61-63). Gibbs et al. have raised catalytic antibodies which catalyze the rearrangement of an asparaginyl-glycyl peptide sequence to an aspartyl-glycyl and an isoaspartyl-glycyl peptide sequence through the formation of a cyclic succinimide intermediate (61). Solid phase peptide synthesis using certain glutamine derivatives form peptide mixtures arising from coupling at the C_α-carboxyl group and the C_γ-carboxyl group via a cyclic glutarimide intermediate (62,63).

Recent mutagenesis studies on *E. coli* AS-B have investigated the glutamine-dependent nitrogen transfer reaction in more detail (39). Sequence studies have revealed that His_{29} and His_{80} are conserved in the Class II subfamily of amidotransferases. The His_{29} to alanine (H29A) and the His_{80} to alanine (H80A) mutants each demonstrated essentially no effect on the ammonia-dependent activity of AS-B, indicating that the mutant protein had folded in a similar manner to wild type AS-B. In the case of the glutamine-dependent reaction, for H29A and H80A, although k_{cat} was essentially unchanged by the amino acid replacements, the K_m

for glutamine was increased by a factor of approximately 4.5 relative to the wild type enzyme. These results suggest that neither of these histidine residues appear to be involved in mediating the nitrogen transfer reaction.

The Cys_1 to alanine (C1A) and serine (C1S) mutants of AS-B were constructed and determined to have no glutaminase or glutamine-dependent activity (60). Although the ammonia-dependent activity was unaffected, it was inhibited by glutamine. This observation was also made in the C1A and C1S mutants of human AS (52). Furthermore, the C1A mutant inhibition pattern was consistent with the formation of an abortive complex in a similar fashion as the human AS C1A mutant. These results are consistent with the proposed mechanism, in which the imide intermediate **14** (**Figure 1-11**) could represent the abortive complex.

Primary sequence alignment studies have also shown that Asp_{33} (D33) in AS-B is cognate to Asp_{29} in glutamine PRPP amidotransferase (**Figure 1-4**). Moreover, Asp_{33} is highly conserved in the Class II subfamily including asparagine synthetases from various sources (39). The Asp_{33} to asparagine (D33N) and Asp_{33} to glutamic acid (D33E) mutants of AS-B had little or no effect on the glutamine and ammonia-dependent activities, however.

In recent studies conducted by Habibzadegah-Tari (56), *E. coli* AS was kinetically characterized and a bi-uni-uni-ter ping-pong Theorell-Chance mechanism (54) was proposed for the glutamine-dependent activity (**Figure 1-12**). These results

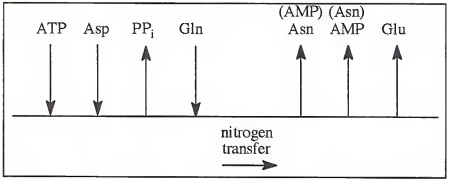

Figure 1-12. Kinetic mechanism of *E. coli* AS-B.

differ from the kinetic mechanisms reported for mouse pancreas (54) (**Figure 1-10A**) and beef pancreas AS (56) (**Figure 1-10B**). In this mechanism, ATP and aspartate bind sequentially, followed by release of PPi and addition of glutamine. At this stage, nitrogen is transferred, followed by random release of asparagine and AMP, then glutamate release to regenerate the original state of the enzyme. Contrasting with the mechanisms proposed by Milman et al. and Markin et al. (**Figure 1-10A,B**), this mechanism does not generate free ammonia while simultaneously interacting with Asp and ATP. Furthermore, these results are consistent with the mechanism for glutamine-dependent nitrogen tranfer proposed by Richards and Schuster (60) (**Figure 1-11**). Since the binding of glutamine and subsequent nitrogen transfer take place after formation of β-aspartyl-AMP **6**, this mechanism also allows for the possibility of forming imide intermediate **14**.

In related studies on human AS, Sheng et al. (50) pursued mutagensis studies to investigate the glutamine-

dependent nitrogen transfer reaction in more detail. The Cys_1 to alanine (C1A) and serine (C1S) mutants were constructed and determined to have no glutaminase or glutamine-dependent activity. The ammonia-dependent activity, although unaffected, was inhibited by glutamine, presumably through the formation of an abortive complex. Sequence studies on human AS carried out by the Boehlein, et al. (39) demonstrated that His_{102} of human AS is not cognate to His_{101} of glutamine PRPP amidotransferase as was previously believed. These results infer the possibility that human AS may also be operating by a mechanism analogous to the proposed mechanism for *E. coli* AS-B (**Figure 1-11**).

Sequence studies have revealed that the residues Arg_{30}, Asn_{74}, and Asn_{79} appear to be conserved throughout the Class II subfamily of amidotransferases (39). The roles of these highly conserved residues on the glutamine-dependent activity of *E. coli* AS-B were investigated through mutagenesis studies by Boehlein, et al (64). The Arg_{30} to alanine (R30A) mutant of AS-B resulted in a 182-fold increase of K_M for glutamine in the glutamine-dependent activity compared to wild-type AS-B. In addition, the ATP-dependent stimulation of the glutaminase activity was modified or completely lost when Arg_{30} is replaced by other amino acids. This observation suggests that Arg_{30} may mediate communication betweeen the synthetase and GAT domains of AS-B, in an analogous fashion to that observed for Glu_{841} in carbamoyl-phosphate synthetase (65). The kinetic parameters associated with the ammonia-

dependent and the glutamine-dependent activity of the Asn79 to alanine (N79A) mutant of AS-B were essentially unchanged compared to wild-type AS-B, indicating that this residue appears to possess no catalytic function in AS-B.

Three mutants of AS-B were constructed in which Asn_{74} was replaced by alanine (N74A), glutamine (N74Q), and aspartic acid (N74D). All three of these mutants displayed kinetic parameters associated with ammonia-dependent activity which are similar to those of wild-type AS-B. However, the N74A and N74Q mutants displayed a substantial difference in glutamine-dependent activity compared to wild-type AS-B, indicating that Asn_{74} plays a significant role in glutamine-dependent nitrogen transfer. Glutaminase activity of the N74A mutant was similar to that of wild-type AS-B; however, the activity of the N74Q mutant was only 10% relative to wild-type AS-B. Significantly, the glutaminase activities of both N74A and N74Q were stimulated by ATP. Interestingly, it has been determined that the N74D mutant confers nitrile hydratase activity upon the mutant enzyme (66).

These results obtained from these studies on Asn_{74} allow for further refinement of the proposed mechanism of *E. coli* AS-B shown in **Figure 1-11.** The Asn_{74} residue can play a catalytic role through polarization of the amide bond of glutamine, possibly by formation of low-barrier hydrogen bonding (67,68), to form the hydroxyimine tautomer **16** which now has a more nucleophilic nitrogen atom (**Figure 1-13**). This nitrogen atom can attack β-aspartyl-AMP **6** to form imide

intermediate **14**, followed by the subsequent attack of Cys_1 thiolate anion on imide **14** to form the tetrahedral intermediate **17**. The resultant breakdown of **17** to form the γ-glutamythioester enzyme intermediate **12** and asparagine tautomer **15** ultimately generates glutamate and asparagine (**Figure 1-11**).

A modified version of this mechanism which is also consistent with recent results on Asn_{74} has been proposed (64) (**Figures 1-14**). In this mechanism, Asn_{74} plays a catalytic role by stabilizing the oxyanion formed in intermediate **10** by the nucleophilic attack of Cys_1 on bound glutamine. The resulting primary amine nitrogen of **10** is nucleophilic, and can attack β-aspartyl-AMP **6** to form the intermediate **17**, which ultimately generates asparagine and glutamate as before (**Figure 1-11**).

Further studies on *E. coli* AS-B using alternate substrates have provided further evidence for the involvement of Asn_{74} in catalysis. Boehlein et al. (69) have investigated the ability of the enzyme to use glutamic acid γ-hydroxamate (LGH) and hydroxylamine as alternate substrates for glutamine and ammonia, respectively. Using wild-type AS-B and LGH as the substrate, the catalytic efficiency (k_{cat}/K_M) increased 3-fold in the glutaminase activity relative to glutamine, while it decreased 3-fold for the glutamine-dependent activity compared to glutamine. The catalytic efficiency for

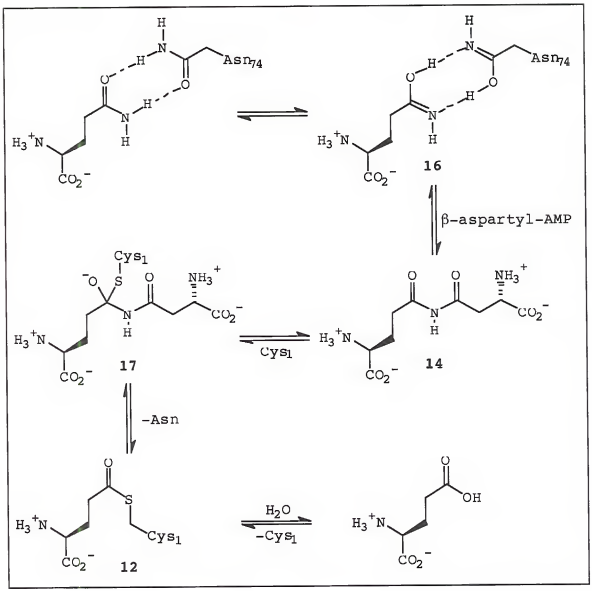

Figure 1-13. Proposed mechanism for nitrogen transfer in *E. coli* AS-B involving imide intermediate **14.**

hydroxylamine in the ammonia-dependent activity of wild-type AS-B increased 2-fold relative to ammonia. Using the N74A mutant, using both LGH and hydroxylamine in all three reactions catalyzed by AS-B (**Figure 1-5**) gave essentially no difference in catalytic efficieny as compared to using

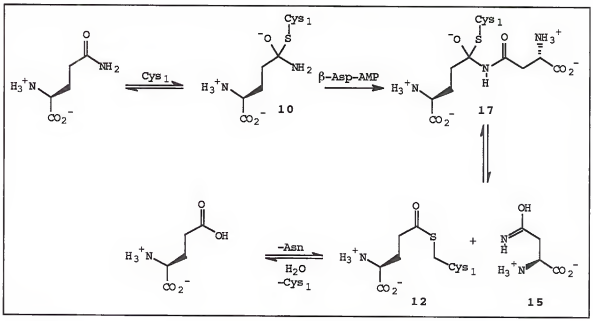

Figure 1-14. Proposed mechanism for nitrogen transfer in *E. coli* AS-B involving tetrahedral intermediate **10.**

glutamine and ammonia as substrates. However, because the nitrogen transfer with LGH proceeded with a turnover number (k_{cat}) that was 10-fold lower than that observed in glutamine-dependent asparagine synthesis, the results were interpreted to be further evidence against ammonia-mediated nitrogen transfer in *E. coli* AS-B.

Indirect support for the proposed polarization and tautomerization of the glutamine amide group has been obtained in model studies upon the glycosylation of asparagine residues in Asn-X-Ser/Thr sequences (70-72). Imperiali et al. evaluated several synthesized conformationally constrained peptides containing asparagine. The primary amide nitrogen of the Asn residue becomes N-glycosylated through nucleophilic attack on an electrophilic

oligosaccharide. This process is catalyzed by the enzyme oligosaccharyltransferase (70). Studies on this enzyme system indicated that the Ser and Thr residues in the active site presumably assist the tautomerization of the Asn primary amide group.

In experiments aimed at determining the mechanism of nitrogen transfer of *E. coli* AS-B, ^{13}C and ^{15}N kinetic isotope effects have been measured in the glutaminase and glutamine-dependent synthesis reactions (73). For the glutaminase reaction, substitution of heavy atom labels in the sidechain amide of the glutamine gave observed values of 1.0245 and 1.0095 for the amide carbon and amide nitrogen, respectively. In the glutamine-dependent synthesis of asparagine, the amide carbon and amide nitrogen isotope effects were 1.2031 and 1.0222, respectively. Based on comparison of these values with those obtained with papain and other thiol proteases, these results were interpreted to mean that nitrogen transfer does not proceed by free ammonia formation, rather, it probably involves a series of intermediates in which glutamine becomes covalently attached to aspartate. These results are consistent with the proposed mechanism for nitrogen transfer through the tetrahedral intermediate 17 (**Figure 1-14**) (64). However, these results are also consistent with the proposed mechanism for nitrogen transfer via the imide intermediate **14** (**Figure 1-13**) (60).

Further experiments aimed at determining the mechanism of *E. coli* AS-B were recently carried out by Rosa-Rodriguez,

et al. (74). A sample of the imide intermediate **14** was synthesized using synthetic organic methodology and screened for activity against AS-B. Incubation of **14** with wild-type AS-B did not form products L-Glu and L-Asn. Furthermore, incubation of L-Gln, L-Asp, and ATP with the C1A and C1S mutants of AS-B did not generate the imide **14**. These studies indicated that the lack of imide **14** was not dependent on the energetics of the enzyme-substrate complex. While these results are inconsistent with the imide-mediated nitrogen transfer mechanism (**Figure 1-11**), they do not necessarily rule it out as a possibility.

Specific Aims

The enzyme L-asparaginase (75,76) is often employed in the treatment of acute lymphoblastic leukemia (ALL). The mechanism of action for L-asparaginase is to deplete the level of circulating asparagine synthesized in the liver by asparagine synthetase (77,78). Resistance of human neoplasms to protocols involving L-asparaginase arises from the synthesis of endogenous asparagine in malignant cells (79,80), and there is also evidence to suggest that blood asparagine concentration may also play a role in T-cell response (81). Therefore, inhibitors of asparagine synthetase represent targets with potential application in treating leukemia, and in exploring cellular mechanisms of immunosuppression (82,83).

The first part of the present study involved the synthesis and use of constrained substrate analogs to probe the active site of *E. coli* AS-B. The lack of a crystal structure of the enzyme necessitates the use of probes to analyze the structural properties of the active site. Further studies were done to clarify several stereochemical features observed in the alkylations of aspartic acid.

The second part of the present study involved the computational modeling of possible reaction mechanisms and intermediates through semi-empirical and *ab initio* methodology. From the results of these calculations, a comparison of reaction energetics for the proposed mechanisms versus the currently accepted ammonia-mediated mechanism was performed.

The third part of the present study involved the chemoenzymatic synthesis of fluorinated glutamate substrate analogs. Potential applications of these fluorinated analogs include use as possible suicide inhibitors, or use as mechanistic probes of *E. coli* AS-B due to their enhanced reactivity.

Finally, the fourth part of the present study involved the development of synthetic routes toward the synthesis of phosphorus-based transition state analogs. Regardless of the mechanism of action, compounds that mimic a tetrahedral intermediate or transition state may prove to be effective inhibitors of the enzyme.

CHAPTER 2
PROBING THE ASPARTIC ACID BINDING SITE OF *E. COLI* ASPARAGINE SYNTHETASE B USING SUBSTRATE ANALOGS

Introduction

Functionalized aspartic acid analogs have proven useful tools in the elucidation of structure-function relationships associated with the N-methyl-D-aspartate (84) and glutamate receptors (85), and in the preparation of chiral intermediates in the synthesis of a number of complex natural products (86). This study involves the preparation and assay of a series of β-functionalized aspartates to probe the specificity and stereochemical preferences of the *E. coli* asparagine synthetase B active site. Additional studies have also probed the stereoselectivity of the aspartate alkylation reaction.

Synthesis of Constrained Aspartic Acid Analogs

The synthesis of the constrained aspartate analogs **18** and **19** begins with the commercially available N-benzyloxycarbonyl-L-aspartic acid **20** (**Figure 2-1**). Using the method of Wang et al. (87), formation of the N-protected diester **21** was achieved by reacting the dicarboxylate cesium salt of **20** with benzyl bromide (48% yield). Alkylation of the dianion of **21** has been shown to proceed without

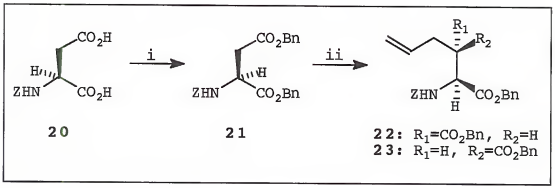

Figure 2-1. Synthesis of dibenzyl [2*S*,3*R*]-2-benzyloxycarbonylamino-3-propen-2'-yl-succinate **22** and dibenzyl [2*S*,3*S*]-2-benzyloxycarbonylamino-3-propen-2'-yl-succinate **23**. Z=$C_6H_5CH_2OCO$-; Bn=$C_6H_5CH_2$-. Reagents and conditions: i.) a. Cs_2CO_3, H_2O, b. BnBr, DMF, 48%; ii.) LiHMDS, allyl bromide, THF, -78 °C, 60%.

racemization at the chiral carbon using a wide variety of electrophiles (88-90). Treatment of **21** with lithium hexamethyldisilazide (LiHMDS) (2.0 eq.) in THF at -78 °C gave a 1:6 mixture of the diastereomers **22** and **23** after column chromatography. No N-alkylated product was observed, and the recovered starting material had an unchanged optical rotation, suggesting that the deprotonation at C-2 did not occur under these conditions. Two equivalents of base are needed in this reaction due to the relatively acidic carbamate N-H present. As the mixture of diesters **22** and **23** could only be separated through careful chromatography and fractional crystallization, it was decided that the separation of the diastereoisomeric products would be done at a later stage in the synthesis, if possible.

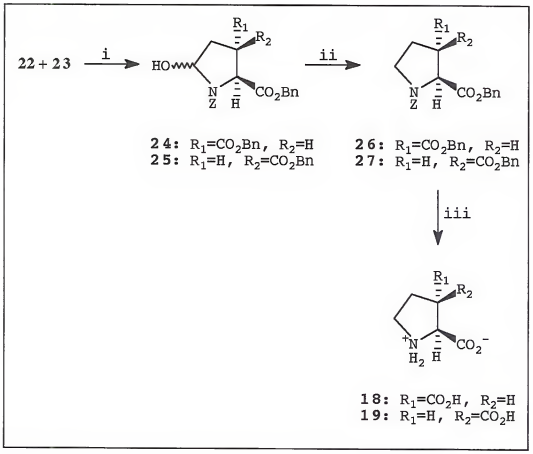

Figure 2-2. Synthesis of pyrrolidine-2(S),3(R)-dicarboxylic acid **18** and pyrrolidine-2(S),3(S)-dicarboxylic acid **19**. Z=$C_6H_5CH_2OCO$-; Bn=$C_6H_5CH_2$-. Reagents and conditions: i.) OsO_4, $NaIO_4$, MeOH, H_2O, RT, 85%; ii.) Et_3SiH, $CHCl_3$, TFA, RT, **26** 27%, **27** 40%; iii.) NH_4OCHO, Pd/C, EtOH, Δ, **18** 85%, **19** 25%.

Cleavage of the double bond and subsequent cyclization (**Figure 2-2**) was accomplished using sodium periodate and catalytic OsO_4 (91,92) in an aqueous methanol solvent, giving the mixture of substituted pyrrolidines **24** and **25** in a good yield. Dehydration and reduction of the resulting imine was done by treatment of **24** and **25** with triethylsilane and trifluoroacetic acid (93) in chloroform to give the

pyrrolidines **26** and **27** in moderate yields. At this time, it was possible to separate the diastereoisomers without too much difficulty by column chromatography. This purification afforded **26** and **27** as a 1:2.5 ratio. Removal of the N-benzyloxycarbonyl protecting group, as well as the benzyl esters, was performed independently on **26** and **27** with catalytic hydrogenation using palladium and ammonium formate in ethanol (94,95). Purification of the crude diacids using Dowex-1 strong anion exchange resin (97) gave purified **18** in a 85% yield, and **19** in a 25% yield.

During our experiments, a study by Humphrey et al. (97) appeared describing a synthesis of the enantiomers of **18** and **19** (synthesis began with D-aspartic acid) and their potential use as neurotransmitter conformer mimics. The alternate synthetic route is conceptually identical to the one described herein, employing a stereocontrolled β-alkylation of a protected aspartic acid derivative, except that the N-phenylfluorenyl protecting group was used. In this study, the relative stereochemistry of the alkylated material was proven by X-ray crystallography.

While the synthesis and use of constrained aspartic acid analogs to probe the aspartic acid binding site of *E. Coli* AS-B is the goal of this part of the project, the observation of diastereoselectivity in the alkylation reaction warrants further investigation.

Studies on the Alkylation of Aspartic Acid

The first reported alkylation of a protected aspartate derivative was done in a study by Seebach and Wasmuth (98) in which the N-formyl di-*tert*-butyl ester of L-aspartic acid was alkylated with a series of alkyl halides (Table 1, entry 1). Using lithium diethylamide as the base, β-alkylated products were produced with some stereoselectivity, however the product mixture also contained α-alkylated product, indicating that little regioselectivity existed for the reaction. Further work by Baldwin et al. (90) on β-methyl α-*tert*-butyl diester of aspartic acid found that increasing the steric bulk of the nitrogen protecting group and using sterically bulky bases would give the β-alkylated products as the sole regioisomer (Table 1, entry 2-3). However, little or no stereoselectivity was seen at the β-carbon, probably due to the smaller β-methyl ester that was used.

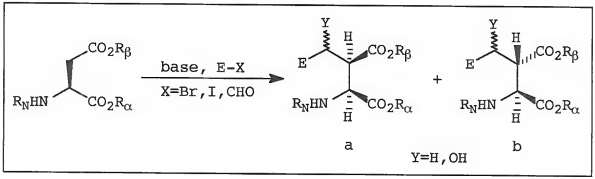

Figure 2-3. Alkylation of protected aspartic acid with various electrophiles (E-X) to produce diastereomers **a** and **b**.

Table 1. Examples of Alkylations of Protected L-Aspartic Acid (**Figure 2-3**)

	R_N	R_α	R_β	base[a]	electophile	a:b ratio[b]	yield (%)	Ref.
1	HCO	tBu	tBu	$LiEt_2NH$	CH_3I	>50:1	45	98
2	Cbz	tBu	Me	LiHMDS	PhCHO	1:1	50	90
3	Cbz	tBu	Me	LiHMDS	$PhCH_2Br$	5:1	50	90
4	Cbz	tBu	Me	LiHMDS	$CH_2=CHCH_2Br$	3:1	40	88
5	PhFl	Me	Me	KHMDS	$PhCH_2I$	7:1	69	100
6	PhFl	Me	Me	KHMDS	CH_3CH_2OTf	>50:1	87	99
7[c]	PhFl	Me	Me	KHMDS	$CH_2=CHCH_2I$	1:10	94	97
8[c]	PhFl	Me	Me	LiHMDS	$CH_2=CHCH_2I$	23:1	96	97
9[c]	PhFl	Me	Me	KHMDS	CH_3I	2:1	99	97
10[c]	PhFl	Me	Me	LiHMDS	CH_3I	>50:1	98	97
11[c]	PhFl	Me	Me	KHMDS	$PhCH_2Br$	>1:50	73	97
12	Cbz	tBu	Me	LiHMDS	$ClCH_2CO_2tBu$	>50:1	75	102
13	Cbz	tBu	Me	LiHMDS	$CH_2=CHCH_2Br$	>50:1	60	102
14	Cbz	tBu	Me	LiHMDS	$CH_2=CHCH_2I$	8:1	71	102
15	Cbz	tBu	Me	LiHMDS	CH_3CHO	>50:1	25	102
16	Cbz	tBu	Me	LiHMDS	PhCHO	>50:1	66	102
17	Cbz	tBu	Me	LiHMDS	propargyl Br	4:1	69	102
18	Cbz	tBu	Me	LiHMDS	$NCCH_2Br$	2:1	70	102
19	Cbz	tBu	Me	LiHMDS	CH_3I	1:1	95	102
20	Cbz	Me	Me	LiHMDS	$BrCH_2CO_2tBu$	5:2	86	102
21	Cbz	tBu	Me	LiHMDS	$BrCH_2CO_2tBu$	5:4	91	102
22	Cbz	CPh_3	Me	LiHMDS	$BrCH_2CO_2tBu$	4:5	98	102
23	Cbz	tBu	Me	LiHMDS	$ClCH_2CO_2tBu$	>50:1	50	-
24	Cbz	tBu	Me	LiHMDS	$PhCH_2Br$	2:1	12	-
25	Cbz	Bn	Bn	LiHMDS	$CH_2=CHCH_2Br$	6:1	60	-

[a] All reactions done in THF. [b] The products a and b correspond with diastereomers **a** and **b** in **Figure 2-3.** [c] Alkylations performed on D-aspartic acid.

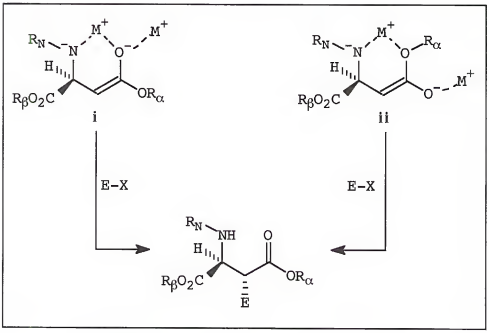

Figure 2-4. Proposed nitrogen-chelated enolate geometry for the alkylation of protected L-aspartic acid derivatives with various electrophiles; **i** (Z)-enolate; **ii** (E)-enolate.

Rapoport et al. (99,100) reported the stereoselective alkylation of 9-phenylfluoren-9-yl-N-protected L-aspartic acid derivatives with various electrophiles giving higher diastereomeric excess of the 2(S),3(R) products (Table 1, entries 5,6). The proposed explanation of this observation is alkylation through a chelation-controlled (Z)-potassium enolate in which the nitrogen group is involved in chelation with the cation to form a cyclic-chelated enolate (**Figure 2-4**). Precedence for this type of nitrogen-chelated enolate has been reported by Rapoport and Lubell (103) and Yamamoto et al. (104) in related systems.

Further work by Humphrey et al. (97) on the same system investigated the role of the cation of the base used. It was found that the potassium and lithium bases gave opposite diastereoisomer ratios (Table 1, entries 7-11). In this study, the respective potassium and lithium enolates were trapped with TMS-Cl, and their configurations were determined by ^{1}H NMR. The trapped potassium enolates were found to exist exclusively in the Z-configuration, while the trapped lithium enolates were exclusively in the E-configuration. Although the reasons for this difference were not given, the assigned geometries are consistent with reports that (Z)-lithium enolates are significantly more reactive than the corresponding (E)-lithium enolates (101). From the assigned enolate configurations (**Figure 2-5**), the facial selectivity of alkylation for the (Z)-potassium enolate was explained by a proposed α-ester chelation which gave a cyclic chelate. The electrophile presumably attacks preferentially opposite to the bulky protected nitrogen group. The (Z)-lithium enolate, in which the metal ion cannot form a cyclic chelate because of its (E)-geometry, assumes a hydrogen in the plane conformation (**Figure 2-5**) that is attacked opposite the bulky nitrogen group, giving rise to the opposite diastereomer product (Table 1, entries 7-11).

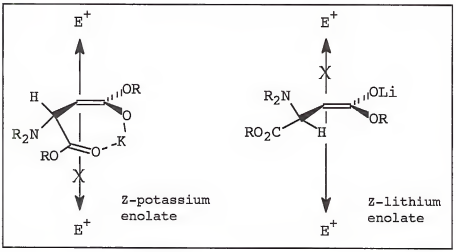

Figure 2-5. Proposed potassium and lithium enolate geometries for the alkylation of protected D-aspartic acid derivatives with various electrophiles (Taken from reference 97).

The results obtained by Parr (102) using the benzyloxycarbonyl-N-protected L-aspartic acid derivatives with LiHMDS and various nucleophiles (Table 1, entries 12-19) are in agreement with these previously reported studies. Exceptional diastereoselectivity was seen with several electrophiles, leading to an initially proposed enolate geometry similar to that seen by Seebach et al (98, 103), Rapoport and Lubell (104), and Yamamoto et al (105) on related systems. This proposed enolate involves chelation control by the nitrogen anion formed to give the corresponding (E) or (Z)-lithium enolate (**Figure 2-4**). Presumably, electrophilic attack on the least hindered face opposite the bulky α-ester group gives the product in diastereomeric excess.

To investigate this idea, further studies by Parr (102) were done to ascertain the effect of steric bulk at the α-ester position of N-protected L-aspartic acid derivatives with LiHMDS and tert-butyl bromoacetate (Table 1, entries 20-22). It was demonstrated that increasing the size of the α-ester substituent did little in determining the diastereoselectivity of the reaction. The relative stereochemistry of the products formed were established using NOE difference spectroscopy (106,107) and by examination of scalar coupling constants (108,109). These results appear to rule out the proposed nitrogen-chelated enolate, and favor a similar (Z)-lithium enolate geometry as proposed by Humphrey et al (**Figure 2-5**) (97).

While the studies by Parr (102) clearly demonstrated the relative stereoselective and regiospecific preference for the alkylation reactions, the absolute stereochemical assignment for the alkylated products remained ambiguous. It was determined that the enantiomeric purity of an alkylation product could be determined by a chemical resolution and subsequent ^{1}H NMR study. From the results of this resolution and stereochemical assignment, a tentative assignment of stereochemistry could then be made to the other alkylated products.

The synthesis of *tert*-butyl-2(S),3(R)-2-benzyloxy-carbonylamino-3-carbomethoxy-glutarate **28** begins with the protection of the commercially available L-aspartic acid, β-methyl ester **29** (**Figure 2-6**). Nitrogen protection with a

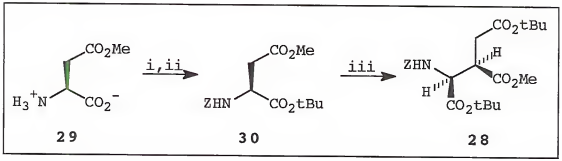

Figure 2-6. Synthesis of 1,5-di-*tert*-butyl-2(S)-(N-benzyloxycarbonyl)amino-3(R)-carbomethoxypentanoate **28**. Z=$C_6H_5CH_2OCO$-. Reagents and conditions: i.) Benzyl chloroformate, dioxane, H_2O, Na_2CO_3, RT, 70%; ii.) isobutylene, conc. H_2SO_4, RT, 45%; iii.) LiHMDS, *tert*-butyl chloroacetate, THF, -78 °C, 39%.

benzyloxycarbonyl group was done using literature methods (110) to give the Cbz-N-protected acid, which was subsequently subjected to isobutylene gas with catalytic H_2SO_4 in methylene chloride (111) to give the N-protected diester **30**. Alkylation using LiHMDS (2 eq.) and *tert*-butyl chloroacetate in THF gave **28** as the single diastereomer, as determined by ^1H NMR.

Semi-empirical calculations were made using the AM1 Hamiltonian (112) as implemented in MOPAC 6.0 (113) on the possible diastereomers of **28**. This study indicated that the 2(S), 3(R) diastereomer is more stable than its C3 epimer by 2.5 kcal/mol. While the alkylation of aspartate is an irreversible reaction which occurs under kinetic control, these calculations suggest that the reaction also produces the thermodynamically favored product.

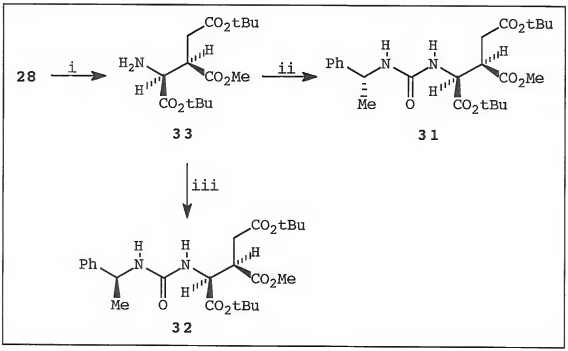

Figure 2-7. Synthesis of the (R)- and (S)-N-(α-methylbenzyl)urea triesters **31** and **32**. Reagents and conditions: i.) H_2, Pd/C, MeOH, RT, 66%; ii.) (R)-α-methylbenzyl isocyanate, THF, Δ; iii.) (S)-α-methylbenzyl isocyanate, THF, Δ.

The enantiomeric purity of **28** was ascertained after conversion to the (R)- and (S)-N-(α-methylbenzyl)urea triesters **31** and **32** (**Figure 2-7**). Hydrogenation of **28** was performed using hydrogen gas over catalytic palladium in methanol (94,95) to form the free amine **33** (**Figure 2-7**). The amine **33** was then acylated with either (R)- or (S)-α-methylbenzyl isocyanate in THF (109,114) to form **31** and **32**, respectively. Observation of the diastereomeric methyl ester singlets by 500 MHz ^1H NMR spectroscopy in $CDCl_3$ during incremental additions of the opposite isomer demonstrated **31**

and **32** to be of >95% purity (**Figure 2-7**). Hence **28** is presumed to be of >95% purity.

Mapping the Aspartic Acid Binding Site of *E. Coli* Asparagine Synthetase B Using Substrate Analogs

The inhibitory effects of a series of aspartic acid analogs on glutamine-dependent asparagine synthesis were determined using recombinant, wild-type AS-B[1] (115). Standard reaction solutions in these experiments contained 1 mM glutamine, 1 mM ATP, 1 mM aspartic acid and 10 mM $MgCl_2$ in TrisHCl buffer at pH 8. Asparagine production was assayed by measuring the amount of pyrophosphate formed under steady state conditions (39,64).

Initial studies focused on the commercially available compounds **34-39** (**Figure 2-8**). All of these compounds exhibited only low levels of inhibition even at 10 mM concentration. The inability of malic acid **36** to inhibit asparagine synthesis demonstrates that the hydroxyl cannot act as an isostere of the charged amino group, consistent with results reported for the asparagine synthetase present in RADA1, a murine leukemia (116). It therefore appears that AS-B requires the presence of all of the ionizable groups in aspartate for substrate binding. The significance of the β-carboxylate in recognition is underscored by the failure of L-proline **39** to inhibit AS-B, within the limits of the assay, at concentrations up to 50 mM.

---

[1] Enzyme assay experiments performed by Dr. Susan K. Boehlein (115).

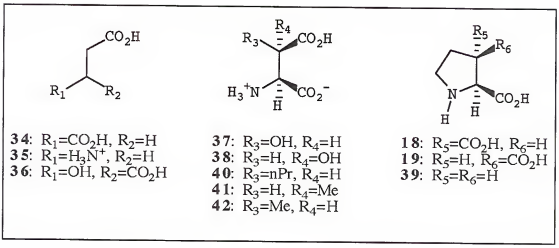

Figure 2-8. Aspartic acid analogs **18, 19, 34-42** used in inhibition studies of AS-B.

Having established that all three ionized functional groups were essential to the recognition of aspartate by AS-B, the β-functionalized aspartic acid analogs **18, 19, 40, 41,** and **42** were then assayed[2]. Previous experiments by Mokotoff et al. on asparagine synthetase isolated from asparaginase-resistant Novikoff hepatomas (117) demonstrated 27% AS inhibition in synthetase activity in the presence of the racemate of *erythro*-β-hydroxyaspartate **37** (**Figure 2-8**). However, no reduction in AS-B activity was observed for 3-*n*-propylaspartate **40**, and the remaining analogs were weak AS-B inhibitors (**Table 2**). Furthermore, there was a significant effect of stereochemistry at C-3 upon the level of AS-B inhibition. Again, this observation is consistent with reports that *threo*-ß-hydroxyaspartate **38** (**Figure 2-8**) cannot

[2] Compounds **40-42** synthesized by Dr. Ian B. Parr (102).

TABLE 2 Inhibition constants for selected aspartic acid analogs in the glutamine-dependent synthetase activity of *E. coli* AS-B

Inhibitor	Substrate varied	Inhibition pattern	K_{is}[a] (mM)	K_{ii}[a] (mM)
41	Asp	Non-competitive	18.0	>50
41	Gln	Non-competitive	93.0	16.5
41	ATP	Non-competitive	8.0	15.0
42	Asp	Competitive	0.25	n.a.[b]
42	Gln	Non-competitive	1.62	1.71
42	ATP	Non-competitive	0.45	3.28
19	Asp	Competitive	2.65	n.a.
19	Gln	Uncompetitive	n.a.	2.57
19	ATP	Non-competitive	2.65	4.80

[a] K_{is} and K_{ii} are the inhibition constants computed from the intercepts and slopes, respectively, of the double reciprocal plots of $1/v_o$ versus 1/[aspartate] obtained at various concentrations of the inhibitor (118). [b] n.a. = not applicable.

inhibit AS isolated from Novikoff hepatomas (117). The constrained aspartate analog **18** gave an apparent K_I of 60 mM.

In contrast, the constrained analog **19**, differing only in its C-3 configuration, was competitive with respect to aspartate, having a K_{IS} of 2.65 mM. A similar dependence of inhibitory properties upon C-3 stereochemistry was also observed for the methylated analogs **41** and **42** (**Table 2**). Detailed kinetic analysis confirmed that **42** and **19** were competitive only with respect to aspartate, suggesting that these compounds did indeed bind to the same form of the enzyme (probably the E.ATP complex) (56) as aspartic acid,

preventing the natural substrate from binding and taking part in subsequent chemical transformations (118).

Given the conformationally restricted nature of **18** and **19**, and the observation that these compounds are only competitive with respect to aspartate, it is reasonable to assume that **19** defines the bound conformation of aspartic acid. In addition, the identical correlation between C-3 stereochemistry and the ability to inhibit AS-B observed for the diastereoisomers of β-methylaspartate suggests that **42** adopts a bound conformation on the enzyme similar to that of **19**. Both **42** and **19** possess a carboxyl group capable of undergoing reaction with ATP to form reactive intermediates cognate to β-aspartyl-AMP **6** (**Figure 1-7**).

In the absence of detailed structural data upon the complexes between AS-B and these aspartate analogs, we also propose that **19** binds within the same pocket as **42**, especially given the correlation between C-3 stereochemistry and inhibition for the aspartate analogs. It is reasonable to suggest that aspartic acid binds, at least initially, to AS-B in a conformation that is identical to that of the rigid analog **19** (**Figure 2-9A**). In this shape, all of the polar functionality is placed upon one face of the molecule, with the hydrogen atoms defining a hydrophobic surface that makes contact with the enzyme (**Figure 2-9B**). Given that the methylated analog **42** also interacts with this site, there is some flexibility in the protein that can be used to

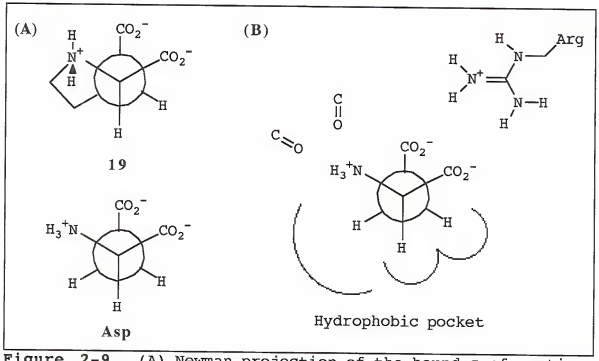

Figure 2-9. (A) Newman projection of the bound conformation of L-aspartate in the AS-B active site based on the constrained analog **19**. (B) Schematic model for the aspartic acid binding site in AS-B. (Taken from reference 117).

accommodate the larger substitutent. On the other hand, the inability of **40** to inhibit AS-B synthetase activity argues that this pocket in the enzyme cannot be distorted significantly.

There are now three examples of aspartate binding sites for which the X-ray structures have been reported (119-121). In all cases, arginine residues interact with the carboxylate groups of aspartate, although the number employed is variable. Given that both carboxylates are placed in close proximity in our model of the bound aspartate conformation, it is possible that only a single arginine residue will be present in the binding site of AS-B. Interactions that

stabilize the protonated amine of L-aspartate, however, seem less predictable. For example, the amino group is placed over the face of a tryptophan ring in adenylosuccinate synthetase, while in the bacterial aspartate receptor, backbone carbonyl groups are used to bind the amine. Our data suggest that while two of the three protons in aspartate are placed within a well-defined pocket on the surface of the enzyme, there is room in the site to accommodate a small hydrophobic substituent in place of the pro-(*R*) hydrogen at C-3 (**Figure 2-9B**).

Crystallization Studies of the Amidotransferases

To date, no X-ray crystal structure for *E. coli* asparagine synthetase B is available. The X-ray crystal structures are available for the Class II amidotransferases *E. coli* glutamine PRPP amidotransferase (41), *B. subtilis* glutamine PRPP amidotransferase (40), and the GAT domain of glucosamine 6-phosphate synthase (42), as well as the Class I amidotransferase GMP synthetase (43). However, neither of the Class II amidotransferases which have been crystallized have a high degree of homology with AS-B (39), making a structural prediction by comparison difficult. Therefore, obtaining crystals of sufficient quality for X-ray analysis has become a priority for future studies on AS-B.

Recent approaches in the crystallization of amidotransferase enzymes has been through the method of isomorphous replacement (122). Proteins and nucleic acids

crystallize with a large amount (30-90%) of water in the unit cell, so that there are aqueous channels in the crystals (123). These channels provide routes along which solutions of compounds containing heavy atoms may diffuse and interact with side chains on the surface of the protein. If the heavy atoms attach to the macromolecule in well defined positions that are the same from unit cell to unit cell, intensity differences due to the addition of the heavy atom will be observed in the X-ray diffraction pattern (124). This method allows one to derive phases for the "native" macromolecule (no heavy-atom binding). The isomorphism between the "native" protein structure and crystals soaked with the appropriate heavy-atom salt or reactant is the basis of the method of relative phase determination (123).

The method of isomorphous replacement with mercury ions (Hg^{++}) was used successfully in the structure determination of the Class I amidotransferase GMP synthetase (125). Salts containing mercury ions are common isomorphous replacement compounds because they readily bind to the sulfur atoms of cysteine residues (126). However, use of mercury salts has not produced viable crystal structures of AS-B.

Studies by Tesmer et al. have successfully determined the structure of the Class I amidotransferase GMP synthetase by forming a product complex of AMP and pyrophosphate (PP_i)

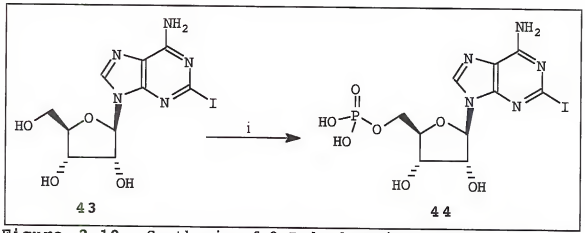

Figure 2-10. Synthesis of 2-Iodoadenosine monophosphate (2-I-AMP) **44**. Reagents and conditions: i.) $POCl_3$, H_2O, C_6H_5N, CH_3CN, 0° C, 34%.

with the enzyme (43). In this study, the adenine nucleotide analog 2-iodoadenosine triphophate (2-I-ATP) was probed as a possible heavy-atom derivative. While 2-I-ATP did bind to the protein, it gave a substantially different structure than the structure produced with AMP/PP_i, excluding the purine ring from the adenine-binding pocket.

In order to attempt to determine the crystal structure of *E. coli* AS-B, the heavy-atom nucleotide analog 2-iodoadenosine monophosphate (2-I-AMP) **44** has been synthesized and crystallization experiments attempted. It is hoped that 2-I-AMP will give a product complex as seen with GMP synthetase.

The synthesis of **44** begins with 2-iodoadenosine **43**[3] (**Figure 2-10**). The monophosphorylation of the unprotected nucleoside **43** was done with phosphoryl chloride in the

[3] 2-Iodoadenosine was a generous gift from Dr. V. J. Davisson, University of Purdue.

presence of water and pyridine in acetonitrile, following the procedure of Yoshikawa et al. (127,128). The reaction was purified by anion exchange high performance liquid chromatography (HPLC) using a water:methanol gradient to obtain pure **44** in a 34% yield.

Experiments to crystallize AS-B as a product complex with 2-I-AMP, to date, have not produced crystals of sufficient quality for structural analysis[4].

Conclusions

β-Alkylation of protected aspartate derivatives has allowed the preparation of a number of stereochemically defined aspartate analogs suitable for probing the molecular features of the aspartic acid binding site in *E. coli* AS-B. Further investigation of the alkylation reaction has determined that the addition appears to proceed via a Z-lithium enolate geometry, with complete stereochemical control in some cases.

The use of substrate analogs has shown that AS-B appears to be extremely selective and it is able to discriminate between metabolites that have similar structures to aspartic acid, which is clearly important in terms of cellular metabolism. However, the protein residues that are responsible for mediating this selectivity remain to be defined by site-directed mutagenesis or X-ray

[4] Crystallization experiments of 2-I-AMP **44** with *E. coli* AS-B performed by Dr. Todd Larsen, University of Wisconsin-Madison.

crystallography. Additional studies using heavy-atom labeled substrates and products, such as 2-I-AMP, have failed to give the structural information needed to aid in this assignment.

While it appears that AS-B can tolerate only relatively minor structural alterations in the aspartic acid substrate, these results suggest that functionalized aspartate analogs can be developed that are selective, tight-binding AS inhibitors.

CHAPTER 3
MODELING THE REACTION MECHANISM OF *E. COLI* ASPARAGINE SYNTHETASE B USING COMPUTATIONAL APPROACHES

Introduction

There are currently two proposed nitrogen transfer mechanisms for *E. coli* AS-B which do not involve free ammonia. One mechanism involves nitrogen transfer through formation of an imide intermediate (**Figure 1-13**), while the other involves nitrogen transfer through prior formation of a tetrahedral intermediate, followed by the nitrogen transfer step (**Figure 1-14**). In order to acquire additional information on the possible nitrogen transfer mechanisms, detailed, high-level *ab initio* calculations have been done in order to provide insight into the relative activation energies involved in the possible reaction mechanisms. These calculations include the effects of electron correlation (129), which is important in modeling processess involving bond formation and bond breaking. Because of the impracticality of modeling these large systems using current computational techniques, smaller model systems have been used in this analysis. This chapter describes the computational modeling of these two proposed mechanisms, as well as the accepted ammonia-mediated mechanism. A detailed

analysis of the structural properties of simple amides and imides is also described.

Structural Comparison of Amides and Imides

Computational Studies of Formamide

The formamide **45** and hydroxyimine tautomer **46** system (**Figure 3-1**) and similar species have been studied previously (130-133) as models for tautomerization in nucleic acid bases. Many theoretical studies employing a variety of methods have focused attention on the relative stabilities of tautomers **46-49**, and have examined the computed stabilities as functions of choice of basis set (134) and treatment of electron correlation (132). Several other workers (135,136) have examined the predicted geometry of **45** as a function of atomic basis set, in particular, the planarity (or lack thereof) at the H_2N center.

Studies by Wang et al. (137) on formamide **45** and the lowest energy hydroxyimine tautomer **46** employed higher levels of theory, using Dunning's "correlation consistent" polarized valence double-zeta basis set (PVDZ) (138). Vibrational frequency analysis and electron correlation techniques using single and double excitations from the single configuration reference function (CISD) method (139) and the second-order Møller-Plesset perturbation theory (MP2) method (140,141) were also utilized in this study. Using these methods, the

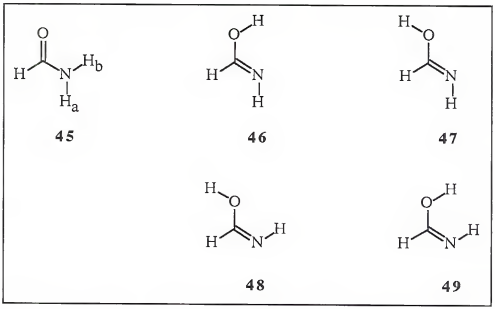

Figure 3-1. Formamide **45** and tautomers **46-49.**

energy difference between **45** and **46** was calculated to be 12.1 kcal/mol.

In the present study on **45** and the hydroxyimine tautomers **46-49**, geometry optimizations were done at the SCF level using Dunning double-zeta basis set (142) with polarization functions (DZP) (143) for all the atoms in the study. Vibrational analysis was used to verify that optimized structures were potential energy minima, and to compute the zero point energy correction. Single point correlation energies were calculated using CCSD(T) methods (144). These calculations were done using the ACES II *ab initio* software package (145,146).

The SCF-optimized bond lengths and angles of formamide and it's tautomers are given in Appendix B, Tables 7 and 8, respectively. For **45**, experimental structural data (147) are

included for comparison; analogous data for the hydroxyimine tautomers **46-49** is not available. Total and relative energies for **45** and tautomers are given in Table 3. The SCF-level energy difference between **45** and the lowest energy hydroxyimine tautomer **46** is calculated to be 12.6 kcal/mol using the DZP basis. The **45→46** correlation energy difference, which was obtained at the singles and doubles coupled cluster (CCSD(T)) level of correlation, is 10.8 kcal/mol. Consideration of the zero-point vibrational energies give a **45→46** correlated-electronic-plus-zero-point energy difference of 11.8 kcal/mol. This data indicates that the gas-phase electronic endothermicity for the tautomerization of **45** to the most likely formed tautomer, **46**, is 11.8 kcal/mol. This is the gas phase thermodynamic energy required to tautomerize the amide bond of formamide, and it gives an idea of the thermodynamic energy that will be required of the AS enzyme. Relative energies for the other tautomers were calculated in a likewise manner, and were also corrected for zero-point energies using the SCF harmonic vibrational frequencies (Appendix B).

The local harmonic vibrational frequencies of formamide, **45**, as well as comparison to experimental data (148,149) are given in Appendix B, Table 9. Included in this table are the calculated vibrational frequencies of a series of deuterated formamide structures, which were done to aid in the assignment of the vibrational frequencies which were in question. The SCF approximation often overestimates

Table 3. Total Energies (atomic units) for SCF and Correlated Wave Functions and Relative Energies (kcal/mol) for Formamide **45** and Tautomers **46-49**

species	SCF[a]	CCSD(T)[b]	Relative Energies[c]
45	-168.975 99	-169.534 60	0
46	-168.955 87	-169.517 34	11.796
47	-168.950 02	-169.512 34	17.917
48	-168.944 87	-169.506 99	15.064
49	-168.949 14	-169.511 62	14.749

[a] Hartree-Fock SCF-level calculation using DZP basis set. [b] With all electrons treated at the singles and doubles coupled cluster level. [c] Relative energy calculated by subtracting zero-point corrected CCSD(T) calculated energy of **45** from each zero-point corrected CCSD(T) calculated energy and converting to kcal/mol.

vibrational frequencies by 10%, especially for low-frequency vibrations like the H_2N out-of-plane bending motion (137). Although anharmonicities were likely to be important, their treatment was not included in this study. Therefore, caution should be used when using these results. All the data in Table 9 (Appendix B) pertain to the C_1 symmetry case (i.e. - all structures were calculated as planar).

Computational Studies of Formimide

In the proposed mechanism of *E. coli* AS-B which involves nucleophilic attack of glutamine on β-aspartyl AMP **6** (**Figure 1-13**), the subsequent loss of AMP produces an imide intermediate. This intermediate can exist as several conformational isomers, with the imide proton (N-H) and the

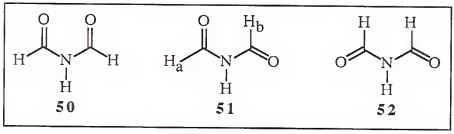

Figure 3-2. Formimide conformational isomers **50-52.**

carbonyl oxygen(s) existing in either the cis or trans orientation.

A search of the literature revealed that little work has been done in calculating the expected form of formimide, or N-formylformamide, and the relative energy between the "keto" and "enol" forms. Radom, et al. (150), using a STO-3G basis set SCF optimization (151), calculated the E,E (**Figure 3-2**) conformational isomer, or conformer, **52** to be lower in energy than either the E,Z (**51**) or Z,Z (**50**) conformers by 0.05 kcal/mol and 2.63 kcal/mol, respectively. Kupfer, et al. (152), using a 3-21G basis set (155) SCF optimization calculated the relative energy of **52** to be higher in energy than **51** by 1.37 kcal/mol and lower than **50** by 5.16 kcal/mol (Table 4).

Experimental results have not been in agreement either. Steinmetz (156) used microwave spectroscopy to assign the major conformer of formimide in the gas phase as the asymmetric conformer **51**. Noe, et al. (157) assigned the E,E configuration **52** as the predominant conformer in acetone

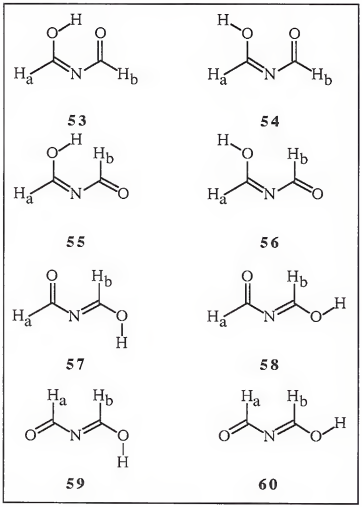

Figure 3-3. Formimide tautomers **53-60.**

solution using NMR. A ratio of 85:15 (E,E : E,Z) was found in the study.

Because of the conflict of data, both computational and experimental, it was decided to determine the relativeenergies of formimide and tautomers (**Figure 3-3**) using high level *ab initio* calculations. The calculations on the formimide system were done using the same methods as the formamide system. Geometry optimizations were done at the

SCF level using the DZP basis set. Vibrational analysis was used to verify that optimized structures were potential energy minima, and to compute the zero point energy correction. Electron correlation energies were obtained using CCSD(T) methods. All structures were optimized as planar, but upon scrutiny of vibrational analysis output (Appendix C, Table 3), it was seen that the tautomers of **51** contained an imaginary vibrational frequency, indicating that the optimized structures were not at a minimum.

The relative energy differences between the formimide conformers **50-52** can be best seen in Table 4. Previous calculations done on this system by Radom et al. (150) and Kupfer et al. (152) are given for comparison. Data from a second set of calculations on the three conformers of formimide which uses the MBPT(2) gradient (153) while using a TZ2P basis set (154) are also included in this table. The calculations done in this work, which utilize the higher degrees of theory, along with the larger basis sets, are the most comprehensive calculations done on this system to date. Note that in both sets of calculations on the formimide conformers done in this study, the E,E conformer **52** was calculated as the lowest energy structure in the gas phase.

The SCF-optimized bond lengths and angles of the formimide conformers and tautomers are given in Appendix C, Tables 10 and 11, respectively. Total and relative energies for **50-60** are given in Table 5. As before, this relative energy is the difference between the SCF optimized structures

Table 4. - Calculated Relative Energies of Formimide Conformers (kcal/mol)

	 **50**	 **51**	 **52**
STO-3G	2.63	0.05	0
3-21G	5.16	0	1.37
DZP - CCSD[T]	6.40	0.51	0
TZP - MBPT(2)	6.25	0.67	0

which were treated with all the electrons at the CCSD(T) level done with the DZP basis set less the calculated energy of the lowest energy formimide conformer, **52**. Zero-point corrections using the SCF harmonic vibrational frequencies (Appendix C, Table 12) have also been made.

The local harmonic vibrational frequencies of the formimide conformers are given in Appendix C: Table 12. As before, to aid in the assignment of vibrational frequencies in question, the calculated vibrational frequencies of a series of deuterated formimide structures are also given. All the data in Appendix C: Table 12 pertains to either the C_{2v} (**50** and **52**) or C_1 (**51**) case.

Also of interest is the higher energy of the hydroxyimine tautomer **53** (**Figure 3-4**). The higher energy of **53** is in accord with the experimental findings of Allenstein et al. (158), who deduced from the gas-phase infrared spectrum of formimide that the enol form is not present in

Table 5. Total Energies (atomic units) for SCF and Correlated Wave Functions and Relative Energies (kcal/mol) for Formimide Conformers and Tautomers **50-60**

species	SCF[a]	CCSD(T)[b]	MBPT(2)[c]	Relative Energies[d]
50	-281.724 60	-282.625 80	-282.758 77	6.40
53	-281.714 75	-282.616 85		12.74
54	-281.695 32	-282.596 86		24.51
51	-281.736 58	-282.635 57	-282.767 65	0.51
55	-281.694 79	-282.597 38		24.02
56	-281.697 48	-282.599 01		23.02
57	-281.712 60	-282.611 62		15.41
58	-281.703 08	-282.602 77		20.74
52	-281.736 42	-282.636 29	-282.768 72	0
59	-281.708 98	-282.610 04		16.39
60	-281.697 67	-282.599 75		22.54

[a] Hartree-Fock SCF-level calculation using DZP basis set. [b] With all electrons treated at the singles and doubles coupled cluster level. [c] Second order many body perturbation level calculation using TZ2P basis set. [d] Relative energy calculated by subtracting zero-point corrected CCSD(T) calculated energy of **52** from each zero-point corrected CCSD(T) calculated energy and converting to kcal/mol.

significant amounts, as well as the work of Noe et al. (157), who obtained no evidence for the presence of **53** from NMR experiments with formimide (in acetone solvent). The decreased tendency of imides to tautomerize, as compared with β-ketones, is not surprising in view of the fact that conjugation is significant even in the "keto" form of imides.

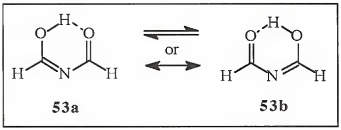

Figure 3-4. Formimide tautomer **53.**

Modeling the Reaction of AS-B

In the proposed imide-mediated nitrogen transfer mechanism of asparagine synthetase (**Figure 1-13**), the breakdown of the imide intermediate occurs with nucleophilic attack of a thiolate anion to form the tetrahedral intermediate **17.** The resultant loss of asparagine anion gives a thioester intermediate **12,** which is subsequently hydrolyzed by water to release glutamate. In the alternate proposed mechanism (**Figure 1-14**), the primary amine of the tetrahedral intermediate **10** formed from thiolate attack on glutamine undergoes nucleophilic attack on β-aspartyl AMP **6** to form intermediate **17.** Because both of these proposed mechanisms involve the nucleophilic attack of the thiolate anion of Cys_1, it was determined that this reaction should be analyzed in more detail using computational methodology.

Preliminary Studies

Previous studies by Kollman et al. (159,160) involved modeling the attack of hydroxide (OH^-) and thiolate (SH^-)

anions on formamide as a model for proteolytic enzymes. In these studies, no local minimum for a tetrahedral adduct structure involving thiolate was found, in contrast to similar calculations with hydroxide. Instead, only an ion-dipole complex minimum was found. Further studies were done by the same authors (161) to examine the possibility for concerted proton transfer in the sulfhydryl protease, but no definite mechanism was determined.

Before carrying out similar studies on the formimide/thiolate system, it was necessary to duplicate the previous work in order to "calibrate" the methods being used. Preliminary semi-empirical studies were made using MOPAC 6.0 (113) as implemented on the CACHE Scientific worksystem. Using the geometry optimized structures obtained from this AM1 (112) calculation as an input structure for the *ab initio* calculation, a SCF geometry optimization was done using a 4-31G basis set (162), as implemented in the ACES II *ab initio* software package.

All degrees of freedom were relaxed during the optimization calculations except the C-S distance. This value was constrained to several values to simulate nucleophilic thiolate attack on the carbonyl carbon of formamide. The selected C-S distances were: 1.5, 2.0, 2.63, 2.68, 3.0, 3.87, 4.0, and 6.0Å. As in the case of Kollman (160), it was necessary to include further constraints on the 6.0Å C-S distance calculation, in order to insure nucleophilic attack was under investigation, and not simply a

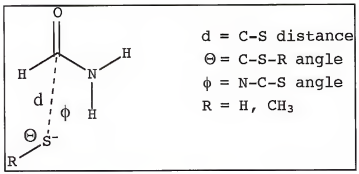

Figure 3-5. Thiolate attack on Formamide.

proton abstraction. These constraints included the CSH angle (99°), the NCS angle (90°), as well as the NCSH dihedral angle (0°) (**Figure 3-5**).

Once it was established with the formamide system that the calculation method being used was valid, and that previous results could be duplicated, the investigation of nucleophilic attack of thiolate on formimide was done using the same procedure. The first formimide isomer chosen for the calculation was the Z,Z conformer **50**, for a couple of reasons. First, **50** was calculated as the highest energy conformational isomer, which may be the most likely choice for an enzymatic-type reaction. Also, with larger groups on the imide, namely the Asp and Gln residues, the Z,Z structure **50** should be the favored isomer (74). However, the nucleophilic attack of thiolate on the E,Z conformer **51** was also done, for comparative purposes.

Semi-empirical calculations, as well as a few trial *ab initio* calculations, showed that, as in the case of

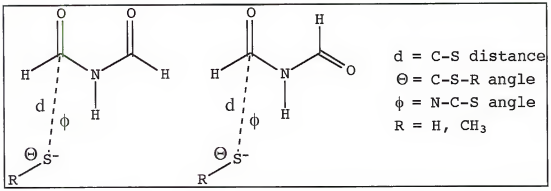

Figure 3-6. Thiolate attack on Formimide.

formamide, further constraints would be needed to insure nucleophilic attack of the thiolate anion on the carbonyl carbon of formimide was taking place, not proton abstraction of the relatively acidic N-H. The CSH bond angle and the NCS bond angle were constrained to 99° and 90°, respectively (**Figure 3-6**). It was determined that the NCSH dihedral angle constraint used in the formamide system was not necessary in the formimide system.

Further studies were done to investigate the nature of the attacking nucleophile. In AS-B, the attacking nucleophile is the N-terminal cysteine residue. For this reason, it was felt that perhaps the thiolate (SH^-) nucleophile used in these calculations is not the best choice. Therefore, the calculations were repeated using the same procedure with methylthiolate (CH_3S^-) as the attacking nucleophile. Methylthiolate was chosen because it incorporates an alkyl group so as to be more similar to the

Table 6. *Ab initio* (4-31G) Calculated Relative Energies (kcal/mol) for the Nucleophilic Attack of (Methyl)Thiolate on Formimide (gas phase)[a]

C-S distance (Å)	**50** with ^-SH	**51** with ^-SH	**50** with CH_3S^-	**51** with CH_3S^-
1.50		+45.61		
2.00		+1.13	-3.65	-3.63
2.63	-18.14	-17.86	-17.19	-18.21
2.68	-19.24	-19.32	-19.26	-18.99
3.00	-22.42	-26.15	-25.61	-25.63
3.45	-29.10	-30.52	-30.63	-29.75
3.87	-26.45	-26.61	-27.02	-25.96
4.00	-25.06	-24.94	-25.45	-24.35
6.00	-9.40	-8.21		-8.06

[a] Calculated energies are not corrected for zero-point energies.

natural cysteine residue, while still being small enough to be a feasible *ab initio* calculation.

The *ab initio* energies calculated for the attack of thiolate and methylthiolate on the two conformers (**50,51**) of formimide are shown in Table 6. The corresponding semi-empirical calculations are shown in Appendix D: Table 13. As can be seen, the energies for the thiolate and methylthiolate systems are comparable, indicating that the thiolate and methylthiolate nucleophiles behave similarly. The shift of calculated minima from 3.0 Å for the semi-empirical calculation (Appendix D: Table 13) to 3.45 Å (Table 6) for the *ab initio* calculated structure is presumably a function of the more complete electronic

contributions calculated using *ab initio* methods. From these studies, it was determined that replacing the hydrogen of thiolate with the methyl group of methylthiolate gave little difference in the energetics calculated for each system.

Methylthiolate Attack Calculations

Once the preliminary studies were completed, a systematic computational study of the nucleophilic attack of methylthiolate on formamide and formimide was undertaken. These studies were done using the angle constraints outlined above. A comparative study on the effect of protonating the carbonyl oxygen of formamide and formimide with the corresponding nonprotonated species was also done (**Figure 3-7**). For comparison, the protonated studies were done with the NCOH dihedral angle initially set at 0° or 180°, but this angle was not constrained.

Semi-empirical studies were made using MOPAC 6.0 as implemented on the CACHE Scientific worksystem. Using the geometry optimized structure obtained from the AM1 calculation as the input structure for the *ab initio* calculation, a SCF geometry optimization was done using a 6-31G basis set (163), as implemented in the GAMESS *ab initio* software package (164,165). Upon locating the stationary points, the local harmonic vibrational frequencies were calculated and zero-point energy corrections were obtained. The second-order Møller-Plesset (MP2) perturbation theory method was used to evaluate the single point electron

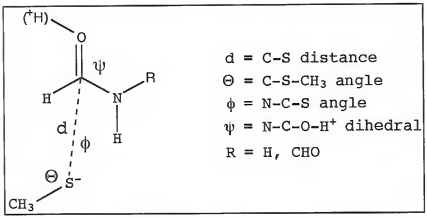

Figure 3-7. Methylthiolate attack on Protonated Formamide **45** and Formimide **50,51.**

correlated energies of the species using a 6-31G** basis set (166,167).

The overall reaction profile of the nucleophilic attack of methylthiolate on formamide **45** is shown graphically in **Figure 3-8**, and the total and relative energies for the complexes are given in Appendix D, Table 14. The corresponding semi-empirical calculated reaction profile can be found in Appendix E. A gradual decrease in energy occurs as the sulfur-carbon distance is reduced from infinity to ~4 Å. The energy subsequently steadily increases as the sulfur-carbon distance is further reduced. As before, this minimum at 4.0 Å corresponds to an ion-dipole complex. No local minimum for a tetrahedral adduct structure involving methylthiolate was found for nonprotonated formamide.

In the case of protonated formamide **45**, a local minimum for a tetrahedral adduct structure was found at 1.75 Å, and a higher energy structure was found at 2.5 Å. While this

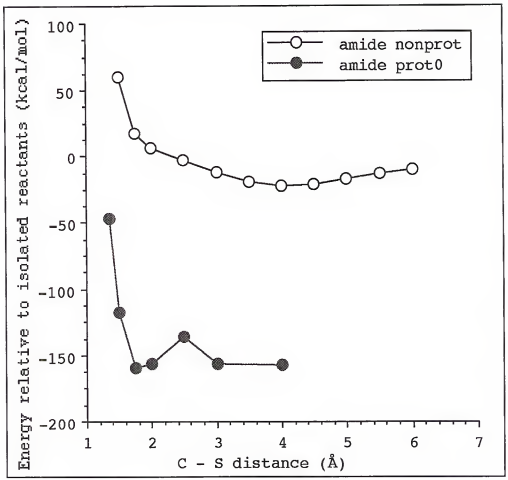

Figure 3-8. *Ab initio* calculated gas phase reaction coordinate for methylthiolate ion + formamide **45.**

higher energy structure is not a true transition state, as no saddle-point analysis was done to find the true transition state, presumably the complex at 2.5 Å closely resembles the transition state. Therefore, the difference in relative energies can be calculated and used to predict the gas phase energy of activation (E_{act}) for the nucleophilic addition of methylthiolate to protonated **45.** From this calculation, E_{act} for the nucleophilic addition of methylthiolate to protonated

45 is 21.7 kcal/mol. The energy difference between the higher energy structure at 2.5 Å and the tetrahedral adduct local minimum structure is 23.9 kcal/mol.

As seen in **Figure 3-8**, the relative energies were calculated as the energy of the respective reaction coordinate structure less the energies of the isolated reactants. The shift between the nonprotonated and protonated reaction coordinate paths occurs because the energies of the protonated species have not been corrected for gas-phase proton affinities (161,168).

The overall reaction profile of the nucleophilic attack of methylthiolate on Z,Z formimide conformer **50** is shown graphically in **Figure 3-9**, and the total and relative energies for the complexes are given in Appendix D, Table 15. The corresponding semi-empirical calculated reaction profile can be found in Appendix E. As in the case of formamide, no local minimum for a tetrahedral adduct structure involving methylthiolate was found for nonprotonated formimide **50**, rather, an ion-dipole complex minimum was found at 4.0 Å. For protonated formimide **50**, the structures along the reaction coordinate were initially protonated with the HOCN dihedral angle at 0° and 180°. For most points along the reaction coordinate, these structures optimized to identical or nearly identical structures, however, the local minimum for a tetrahedral adduct structure was found at 1.75 Å and 2.0 Å for the 0° and 180° initially-protonated species, respectively. A higher energy "transition-state-like"

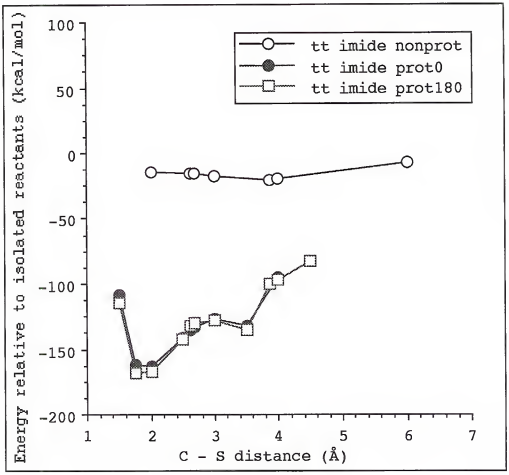

Figure 3-9. *Ab initio* calculated gas phase reaction coordinate for methylthiolate ion + formimide **50.**

structure was found at 3.0 Å for both species. From these calculations, the gas phase E_{act} for the nucleophilic addition of methylthiolate to protonated **50** is 5.7 and 6.5 kcal/mol for the 0° and 180° initially-protonated species, respectively. The energy difference between the higher energy structure at 3.0 Å and the tetrahedral adduct local minima structures is 36.8 and 39.7 kcal/mol, respectively.

The overall reaction profile of the nucleophilic attack of methylthiolate on formimide conformer **51** is shown

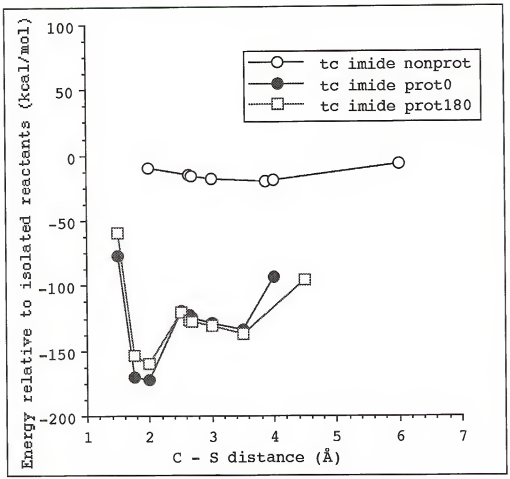

Figure 3-10. *Ab initio* calculated gas phase reaction coordinate for methylthiolate ion + formimide **51**.

graphically in **Figure 3-10**, and the total and relative energies for the complexes are given in Appendix D, Table 16. The corresponding semi-empirical calculated reaction profile can be found in Appendix E. Again, no local minimum for a tetrahedral adduct structure involving methylthiolate was found for nonprotonated Z,E formimide conformer **51**, just the ion-dipole complex minimum at 4.0 Å. One would not expect the orientation of the nonreacting-carbonyl group of formimide to cause a substantial difference in the energies

of nucleophilic addition of methylthiolate. This is true in the case of the nonprotonated species, as both **50** and **51** gave nearly identical results. However, while a local minimum for a tetrahedral adduct structure was found at 2.0 Å, as in the Z,Z conformer **50**, the higher energy "transition-state-like" structure was found at 2.5 Å. The reason for this shift can be attributed to the lack of intramolecular hydrogen bonding which can exist between the carbonyl oxygens in **50**, but cannot happen in **51**. This is similar to the intramolecular hydrogen shift seen in formimide tautomer **53** in the initial structural studies done on formimide (**Figure 3-4**). From these calculations of methylthiolate + protonated **51**, the gas phase E_{act} for the nucleophilic addition is 16.1 kcal/mol. The energy difference between the higher energy structure at 2.5 Å and the tetrahedral adduct local minimum structure is 52.7 and 39.3 kcal/mol for the 0° and 180° initially-protonated species, respectively.

Tetrahedral Intermediate Breakdown Calculations

Once the thiolysis studies were completed, a systematic computational study of the breakdown of the tetrahedral intermediates was done. In this case, the carbon to nitrogen bond was constrained at different values to simulate the lengthening and eventual bond breakage to form the thioester intermediate. Again, semi-empirical studies were made using MOPAC 6.0, and the geometry optimized structure obtained from the AM1 calculation was used as an input structure for the *ab*

initio calculation. As before, a SCF geometry optimization was done using a 6-31G basis set, as implemented in the GAMESS *ab initio* software package. Upon locating the stationary points, the local harmonic vibrational frequencies were calculated and zero-point energy corrections were obtained and MP2 calculations were done using a 6-31G** basis set to evaluate the single point electron correlated energies of the species.

The overall reaction profile of the breakdown of the tetrahedral intermediate formed by the nucleophilic attack of methylthiolate on formamide **45** is shown graphically in **Figure 3-11**, and the total and relative energies for the complexes are given in Appendix D, Table 17. The corresponding semi-empirical calculated reaction profile can be found in Appendix E. In the series of breakdown calculations on formamide **45**, the nitrogen was protonated to $-^{+}NH_3$. For the nonprotonated carbonyl species, a gradual decrease in energy occurs as the nitrogen-carbon distance is increased from 1.35 Å to 3.0 Å. The energy subsequently increases slightly as the nitrogen-carbon distance is further lengthened. However, no local minimum for a tetrahedral adduct structure was found for nonprotonated formamide, and the minimum at 3.0 Å corresponds to an ion-ion complex.

For the breakdown of the tetrahedral intermediate formed from methylthiolate attack on protonated formamide **45**, two local minima were found on the reaction coordinate (**Figure 3-11**). The minimum found at 1.5 Å corresponds to the

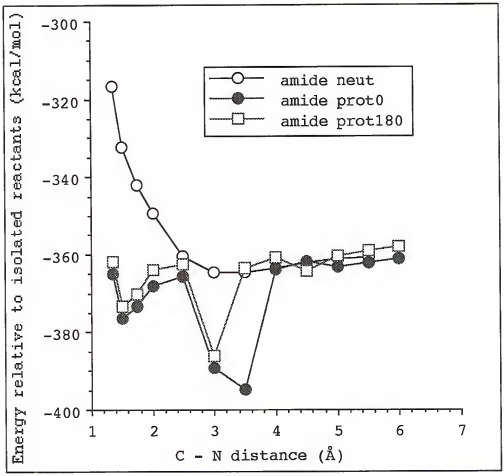

Figure 3-11. Ab initio calculated gas phase reaction coordinate for breakdown of methylthiolate ion + formamide **45** tetrahedral intermediate.

tetrahedral intermediate. Lengthening the nitrogen-carbon bond gives a higher energy structure at 2.5 Å, which resembles the transition state for the breakdown of this complex. A second minimum is seen at 3.0 Å and 3.5 Å, for the protonated species at 180° and 0°, respectively. While both of these species correspond to an intermolecular complex, the 0° protonated species (**Figure 3-6**) has involved a proton exchange from the carbonyl to the leaving ammonia

group, and results in a shift of the minimum. From these calculations, E_{act} for the breakdown of the tetrahedral intermediate formed from the nucleophilic attack of methylthiolate on protonated **45** is 10.7 kcal/mol. The energy difference between the higher energy structure at 2.5 Å and the second intermolecular complex minima at 3.0 Å and 3.5 Å for the 180° and 0° protonated species is 23.4 and 28.9 kcal/mol, respectively.

The overall reaction profile of the breakdown of the tetrahedral intermediate formed by the nucleophilic attack of methylthiolate on formimide **50** is shown graphically in **Figure 3-12**, and the total and relative energies for the complexes are given in Appendix D, Table 18. The corresponding semi-empirical calculated reaction profile can be found in Appendix E. For this species, a tetrahedral intermediate structure is seen at 1.35 Å, with a higher energy species at 2.0 Å. A second minimum is found at 3.0 Å, which corresponds to the intermolecular complex. The activation barrier calculated for the breakdown of the nonprotonated formimide **50** is 25.5 kcal/mol. The energy difference between the higher energy structure at 2.0 Å and the second intermolecular complex minima at 3.0 Å is 2.2 kcal/mol.

For the breakdown of the tetrahedral intermediate formed from methylthiolate attack on protonated formimide **50**, the higher energy structure corresponding to the transition state

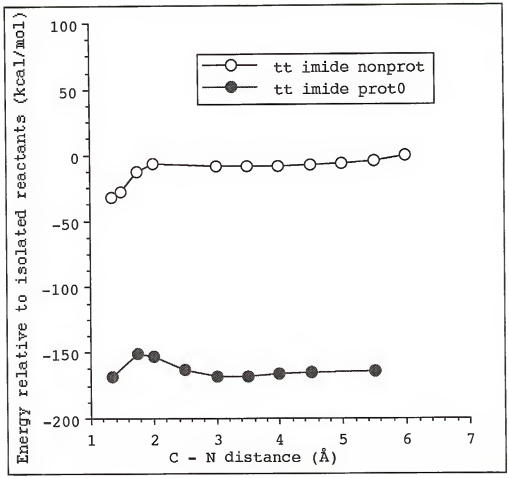

Figure 3-12. Ab initio calculated gas phase reaction coordinate for breakdown of methylthiolate ion + formimide **50** tetrahedral intermediate.

was shifted to 1.75 Å, as compared to 2.0 Å for the unprotonated calculation (**Figure 3-12**). From these calculations, E_{act} for the breakdown of the tetrahedral intermediate formed from the nucleophilic attack of methylthiolate on protonated **50** is 17.7 kcal/mol, which is significantly lower than that seen for the nonprotonated species. A second minimum is found at 3.0 Å, which corresponds to a intermolecular complex. The energy

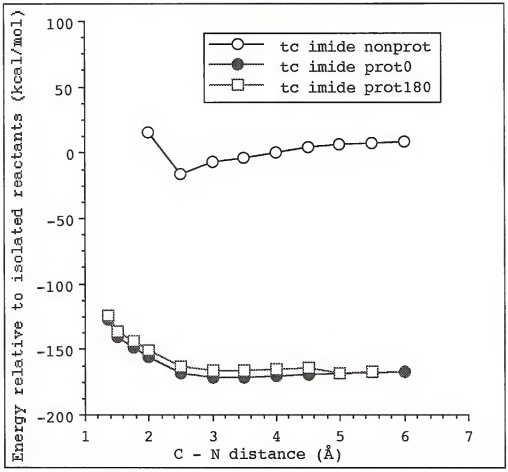

Figure 3-13. Ab initio calculated gas phase reaction coordinate for breakdown of methylthiolate ion + formimide **51** tetrahedral intermediate.

difference between the higher energy structure at 1.75 Å and the second intermolecular complex minimum at 3.0 Å is 18.2 kcal/mol. The stability of this second complex, as compared to the nonprotonated species, is due to an intermolecular proton transfer which has occurred between the protonated carbonyl of the forming thioester, and the amide anion leaving group.

The overall reaction profile of the breakdown of the tetrahedral intermediate formed by the nucleophilic attack of methylthiolate on nonprotonated and protonated formimide **51** is shown graphically in **Figure 3-13,** and the total and relative energies for the complexes are given in Appendix D, Table 19. The corresponding semi-empirical calculated reaction profile can be found in Appendix E. No stable tetrahedral species was found for either the nonprotonated or protonated species. However, a stable intermolecular complex minimum was found at 2.5 Å and 3.0 Å for the nonprotonated and protonated species, respectively.

Conclusions

The point of these calculations is to assess the feasibility of the two proposed mechanisms of *E. coli* AS-B which preclude the use of ammonia. The calculations on the thiolysis of formamide and formimide suggest that a proton transfer from an active site residue may be necessary prior to or concerted with the nucleophilic attack of Cys_1 on the reaction substrates or formed imide intermediate. This result is in agreement with that seen in similar studies performed on the thiol protease papain (161). Moreover, the activation barriers calculated for the thiolysis reaction were significantly lower for the Z,Z conformational isomer of formimide than for formamide.

The activation barriers calculated for the breakdown of the resultant tetrahedral intermediates are similar for both

formamide and the Z,Z conformational isomer of formimide. This would seem to indicate that the energetics involved in the loss of the amide anion is very similar to that needed for the loss of ammonia. Moreover, the activation barriers calculated for the resultant breakdown of the tetrahedral intermediates formed was greater than the activation barriers calculated to reform the starting materials. This observation is consistent with the mechanisms of other protease enzymes that utilize sulfur as the nucleophile (161,169).

CHAPTER 4
CHEMOENZYMATIC SYNTHESIS OF L-4,4-DIFLUOROGLUTAMIC ACID

Introduction

Historical Perspective

The synthesis of 9α-fluorohydrocortisone acetate **61** (**Figure 4-1**) by Fried and Lobo (170) in 1954 represents the first significant report of a successful application of selective fluorination to modify biological activity. The publication served to ignite a new era for medicinal and biological chemists to use fluorine as a substituent to modify reactivity in a variety of biochemically interesting molecules.

The attractiveness and utility of fluorine as a substituent in these molecules results from the pronounced electronic effects that can occur, without any substantial steric penalty. With its small Van der Waals radius (1.35 Å), fluorine closely resembles hydrogen (Van der Waals radius 1.20 Å), while the carbon-fluorine bond length, 1.39 Å, is comparable to that of the carbon-oxygen bond, 1.43 Å (171). The Pauling electronegativity of fluorine (4.0 vs. 3.5 for oxygen) can have a pronounced effect on the electron distribution in the molecule, affecting the acidity or

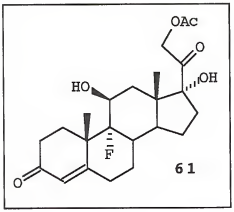

Figure 4-1. 9α-Fluorohydrocortisone acetate **61**.

basicity of the neighboring groups, dipole moments within the molecule, and overall reactivity and stability (172). Also, fluorine can function as a hydrogen bond acceptor because of its available electron density (173,174).

Biological Studies

Fluorinated analogs of naturally occurring biologically active compounds often exhibit unique physiological activities. For example, the introduction of fluorine into a pharmacologically active substance often leads to the development of more potent agonists or antagonists (175).

Fluorine-containing amino acids have been synthesized and studied as potential enzyme inhibitors and therapeutic agents. Specifically, β-fluorinated amino acids have been found to be irreversible inhibitors of certain pyridoxal phosphate-dependent enzymes (176,177). α-Monofluoromethyl and difluoromethyl amino acids have been recognized as potent

enzyme-activated irreversible inhibitors of parent α-amino acid decarboxylases (178,179). Other fluorinated amino acids have been found to exhibit antibacterial and cytotoxic activity (180). Some of these fluorinated amino acids may also be useful in the treatment of central nervous system disorders (172,181).

Fluorinated glutamic acid analogs have been used to probe several glutamic acid metabolic pathways. L-3-Fluoroglutamic acid has seen extensive use as an inhibitor of pyridoxal phosphate dependent enzymes that use glutamic acid as a substrate (177). These enzymes include transaminases, glutamate racemase, and glutamate decarboxylase. Racemic 4-fluoroglutamic acid has been studied as a potential antimetabolite in certain strains of *Mycobacterium tuberculosis* (182). While 4-fluoroglutamate alone proved to be inefficient as a cancerostatic agent (183), its derivative fluoromethotrexate **63** (**Figure 4-2**) has shown promising cancerostatic activity (184,185). 4-Fluoroglutamic acid has also become a focus of interest in studies of its effects on central neuronal mechanism (181,186,187).

4-Fluoroglutamic acid, 3,3-difluoroglutamic acid, and 4,4-difluoroglutamic acid have been used to probe the role of glutamic acid in folate-dependent one carbon biochemistry (188-191). The predominant forms of intracellular folate cofactors exist as pteroyl γ-glutamyl polypeptides (192), which contain a long γ-glutamic acid polypeptide chain (peptide formation involves the γ-carbonyl of glutamic acid,

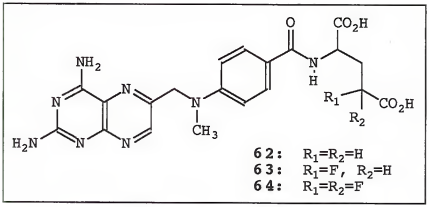

Figure 4-2. Methotrexate **62** and fluorinated methotrexate analogs **63,64.**

rather than the normal α-carbonyl-peptide linkage). One of the more important folate cofactors is N^5,N^{10}-methylene-tetrahydrofolate (N^5,N^{10}-methylene-THF), which is critical for the biosynthesis of deoxythymidine nucleotides by the enzyme thymidylate synthase. It is also essential for the biosynthesis of inosine monophosphate, the precursor for both adenosine and guanosine nucleotides, as well as the amino acids histidine and methionine (193).

In the course of deoxythymidine monophosphate synthesis, N^5,N^{10}-methylene-THF is oxidized to dihydrofolate (DHF). DHF is then recycled back to N^5,N^{10}-methylene-THF by reduction of DHF to THF by the enzyme dihydrofolate reductase, then hydroxymethylation of THF by the enzyme serine hydroxymethyl transferase. Inhibition of dihydrofolate reductase quickly results in all of a cell's limited supply of THF being converted to DHF by the thymidylate synthase reaction. Therefore, inhibition of dihydrofolate reductase not only

prevents synthesis of the nucleotide deoxythymidine monophosphate, but also blocks all other THF-dependent biological processes. Thus, dihydrofolate reductase offers an attractive target for chemotherapeutic agents.

Methotrexate **62** (**Figure 4-2**) is an excellent inhibitor of dihydrofolate reductase, and it has proven to have wide potential utility as an antitumor agent (194). However, extended use can give problems because of its relatively high toxicity (190). Introduction of fluorine into the amino acid moiety (**Figure 4-2**) enhances the acidity of the γ-carboxylic acid group, and thereby diminishes the toxicity of methotrexate (180). This enables the fluorinated analogs to be used in high-dose treatment regimens (195).

This enhancement of activity caused by the introduction of fluorine offers several potential uses in elucidating mechanistic information about *E. coli* AS-B (196). The hydrolysis of γ-fluorinated L-glutamine analogs, for instance, should occur very quickly with AS-B, due to the enhanced electrophilicity of the neighboring carbonyl carbon (195). If this chemistry step is sufficiently rapid, one can obtain mechanistic information for AS-B based solely on conformational changes of the enzyme that occur during the course of the reaction.

Formation of the γ-fluorinated L-glutamine analogs needed for this type of study require the development of a viable synthetic route for the formation of necessary precursors. This study describes efforts made in the

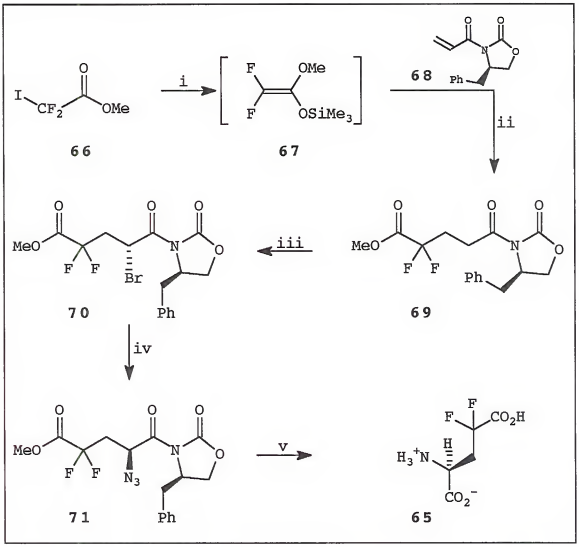

Figure 4-3. Stereospecific synthesis of L-4,4-difluoroglutamic acid **65**. Taken from reference 197. Ph=C_6H_5-. Reagents and conditions: i.) Zn, TMS-Cl, CH_3CN; ii) acryloyloxazolidinone **68**, RT, 15hr; iii.) Bu_2BOTf, iPr_2NEt, CH_2Cl_2, NBS; iv.) NaN_3, DMF; v.) a. LiOH, THF; b. H_2, Pd(C), EtOH.

development of synthetic routes for the stereospecific synthesis of L-4,4-difluoroglutamic acid.

Synthesis of L-4,4-Difluoroglutamic Acid

A stereospecific synthesis of L-4,4-difluoroglutamic acid **65** has been reported by Kitagawa and coworkers (197) (**Figure 4-3**). Their method, however, requires a commercially unavailable starting material, methyl difluoroiodoacetate **66**, which is costly to prepare (198,199). The key step in this asymmetric synthesis involved a Michael addition of the 2,2-difluoroketene silyl acetal **67** to the chiral oxazolidinone **68**. The fluorinated oxazolidinone **69** was then stereoselectively brominated through a boron enolate and NBS (200). The bromide **70** was subsequently converted to the azide **71** with inversion of stereochemistry. The oxazolidinone group of **71** was then removed by hydrolysis, and the azide group was reduced to the amine through catalytic hydrogenation with palladium to give **65**.

Because of the unavailability of the iodoacetate **66**, an alternate route for the synthesis of **65** must be taken. At first glance, the synthesis of **65** seems to be analogous to the stereospecific synthesis of L-4-fluoroglutamic acid **72** reported by Hudlicky and coworkers (**Figure 4-4**) (201,202).

This synthesis takes advantage of a relatively cheap and readily available starting material, 4-hydroxyproline. Using the appropriate starting material, the authors were able to make all four stereoisomers of 4-fluoroglutamic acid. The

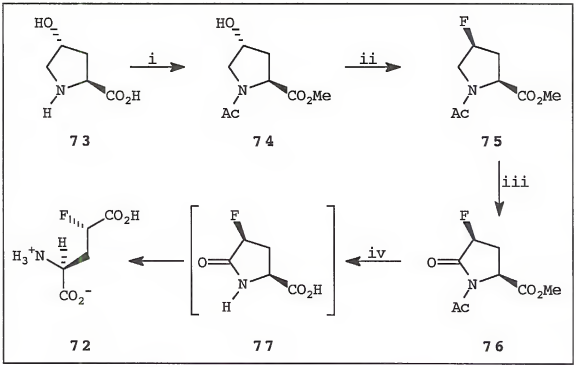

Figure 4-4. Stereospecific synthesis of (+)-threo-L-4-fluoroglutamic acid **72**. Taken from reference 201. Ac=CH_3CO-. Reagents and conditions: i.) a. Ac_2O, AcOH; b. CH_2N_2; ii) DAST; iii.) RuO_2, $NaIO_4$, H_2O; iv.) conc. HCl.

key step in this sequence involved the oxidation of the fluoroproline **75** (**Figure 4-4**) to give the fluorinated pyrrolidine-5-one **76**. Subsequent hydrolysis in concentrated hydrochloric acid afforded the desired diastereomer **72**.

Tsukamoto and coworkers (191) attempted to synthesize L-4,4-difluoroglutamic acid **65** using similar reaction conditions as in the reported stereospecific synthesis of monofluorinated glutamate **72**. In this study, the 4-oxoproline derivative **78** (**Figure 4-5**) was successfully converted to the difluoroproline derivative **79** by (diethylamido)sulfur trifluoride (DAST)-mediated fluorination

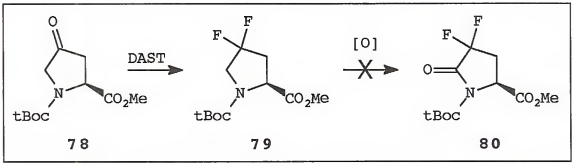

Figure 4-5. Attempted synthesis of L-4,4-difluoroglutamic acid **72** through oxidation of N-protected difluoropyrrolidone **79.** Taken from reference 191.

(203). Oxidation of **79** with ruthenium tetraoxide for extended reaction periods failed to yield the oxidized pyrrolidinone **80,** presumably as a result of the strong electron-withdrawing effect of the two adjacent fluorine atoms (191).

An alternate route for the synthesis of L-4,4-difluoroglutamic acid **65** involves the resolution of the racemic DL-4,4-difluroglutamic acid **81.** While this route may not be as elegant as an asymmetric synthesis, it should produce the target enantiomer desired.

Synthesis of DL-4,4-Difluoroglutamic Acid

The proposed synthetic route for the preparation of L-4,4-difluoroglutamic acid **65** is illustrated in **Figure 4-6.** The synthesis of **81** has been reported by Tsukamoto and coworkers (191). The key step in this synthesis is the

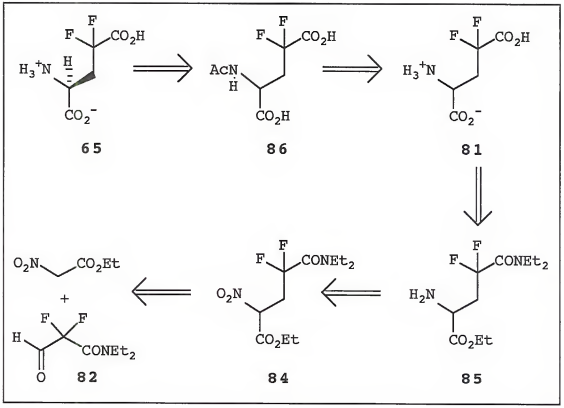

Figure 4-6. Retrosynthetic analysis for the formation of L-difluoroglutamic acid **65** starting from the difluorinated malonaldehydic acid derivative **82** and ethyl nitroacetate.

Knoevenagel condensation of the ethyl nitroacetate anion to the difluorinated malonaldehydic acid derivative **82** (**Figure 4-7**) to give the fluorinated nitroalcohol **83**. Subsequent transformations of **83** gave racemic **81** in a 15% overall yield. While a leading method for the synthesis of difluoromethylene-containing compounds has been the fluorination of ketones with DAST, in contrast to the reaction with alcohols, DAST-mediated fluorination of ketones generally requires higher temperatures and reaction times, and often gives low yields of the desired product (191). This synthetic approach

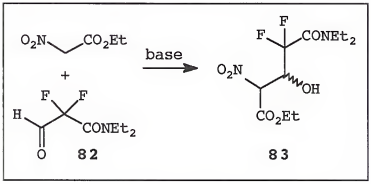

Figure 4-7. Synthesis of racemic 4,4-difluoroglutamic acid precursor **83** via the Knoevenagel condensation of ethyl nitroacetate anion with difluorinated malonaldehydic acid derivative **82**.

relies on the use of a small molecule already bearing the difluoromethylene group as a building block, and offers an alternate route to the desired product that cannot be obtained through the DAST approach.

The synthetic route depicted in **Figure 4-6** begins with the difluorinated malonaldehydic amide **82**, which was prepared according to literature methods (204). The synthesis of this compound begins with the commercially available chlorodifluoroacetic anhydride **87** (**Figure 4-8**). N,N-Diethyl chlorodifluoroacetamide **88** was prepared in quantitative yield by stirring **87** with diethylamine (Et_2NH) in diethyl ether. The Reformatsky reaction (205) of **88** with dimethyl formamide (DMF) in the presence of zinc and diethyl sulfate gave the aminal **89** in moderate to low yields after vacuum distillation. The relatively low yield of this reaction is presumably due to the partial hydrolysis of the relatively

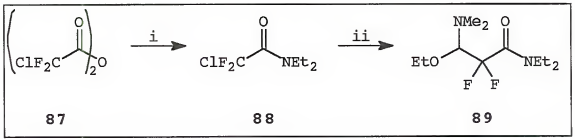

Figure 4-8. Synthesis of 3-(Dimethylamino)-3-ethoxy-N,N-diethyl-2,2-difluoropropionamide **89**. Reagents and conditions: i.) Et_2NH, Et_2O, 0 °C, 97%; ii.) Et_2SO_4, DMF, Zn, 70 °C, 24%.

unstable tetrahedral hemiaminal function upon aqueous workup, and is comparable to yields reported in the literature (204).

Regardless, **89** was hydrolyzed to the hemiacetal **90** using catalytic acid in a mixture of water and ethanol (**Figure 4-9**). The difluorinated hemiacetal **90** product contained a detectable amount of the corresponding aldehyde **82**, and was used as a mixture in the next reaction. The Knoevenagel condensation (206) of ethyl nitroacetate with **90** in the presence of diethylamine followed by acid treatment afforded the nitroalcohol **83** as a mixture of diastereomers.

This diastereomeric mixture **83** was acetylated with acetic anhydride in methylene chloride to give the corresponding acetate **91** (**Figure 4-10**). Due to the instability of the nitroalcohol **83** and the corresponding acetate **91**, these intermediates were carried through the synthesis in crude form. The acetate **91** was treated with sodium borohydride in THF (207) to give the deoxygenated

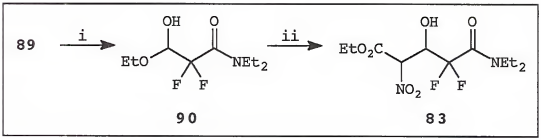

Figure 4-9. Synthesis of N,N-diethyl-4-carbethoxy-2,2-difluoro-3-hydroxy-4-nitrobutanamide **83**. Reagents and conditions: i.) H_2SO_4, H_2O, EtOH, 75%; ii) $EtO_2CCH_2NO_2$, Et_2NH, THF, 0°C, 98%.

product **84**, a key amino acid precursor. This compound was readily purified by flash column chromatography (208) on silica gel to afford pure material in 52% overall yield from **83**.

Reduction of the nitro group of **84** by Raney nickel-catalyzed hydrogenation at 40 psi, followed by purification by flash column chromatography on alumina gave the amine **85** (**Figure 4-11**). Hydrolysis of the amine **85** in concentrated HCl followed by anion-exhange chromatography on BioRad AG1-X2 anion-exhange resin gave the racemic DL-4,4-difluoroglutamate **81** in 40% overall yield from **84**.

Resolution of DL-4,4-difluoroglutamic Acid

The synthesis of chiral fluorine-containing amino acids can follow one of three possible routes: asymmetric synthesis, the fluorination of a homochiral starting material, or the resolution of the racemic amino acid derivative (209). In order to pursue the resolution of

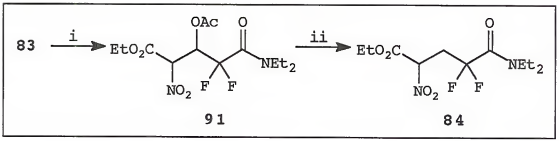

Figure 4-10. Synthesis of N,N-diethyl-4-carbethoxy-2,2-difluoro-4-nitrobutanamide **84**. Reagents and conditions: i.) Ac_2O, CH_2Cl_2, H_2SO_4, 83%; ii.) $NaBH_4$, THF, 0°C, 64%.

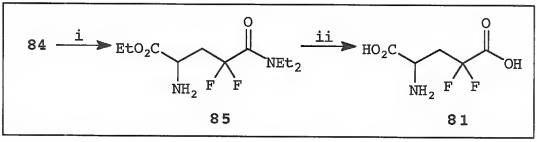

Figure 4-11. Synthesis of DL-4,4-difluoroglutamic acid **81**. Reagents and conditions: i.) Raney Ni, H_2, 40 psi, 52%; ii.) concentrated HCl, Δ, 77%.

DL-4,4-difluoroglutamic acid **81**, it is first necessary to determine which resolution method to employ. While chemical methods of resolution based on the formation of diastereomeric salts or derivatives are available, the use of an enzyme-mediated resolution offers several advantages, such as stereoselectivity, relatively mild reaction conditions, and acceleration of reaction rate.

Several enzyme-based resolution methods have been used to resolve racemic mixtures of amino acids (210). Typically, these resolutions involve the enzymatic formation or

breakdown of an amide bond, or the stereoselective hydrolysis of an ester.

Acylase I (aminoacylase, EC 3.5.1.1.4) from porcine kidney (PKA1) and *Aspergillus sp.* (AA) are two commercially available enzymes which are commonly used in the resolution of amino acids (210). These metalloprotease enzymes catalyze the enantioselective hydrolysis of N-acetyl-L-amino acids (211), using a zinc (Zn^{2+}) ion as a Lewis acid in the catalytic step. PKA1 has found broad application as an enzymatic catalyst in the kinetic resolution of unnatural and rarely occurring α-amino acids. Its enantioselectivity for the hydrolysis of N-acetyl-L-amino acids is nearly absolute, yet it has been found to accept substrates having a wide range of structure and functionality (212).

The resolution of DL-difluoroglutamic acid **81** requires a prior acetylation of the amino functionality. Attempts to acetylate **81** using standard Schotten-Baumann conditions (acetyl chloride and 4 M NaOH) (213) failed to yield the N-acetylated product **92** (**Figure 4-12**). Further attempts to acetylate **81** using acetic anhydride in acetic acid (212) were also unsuccessful. However, the N-acetylated product **92** was successfully synthesized using recently reported methods describing amino acid acylations in organic solvents through the use of ultrasound (214). Using a modification of this procedure, the amino acid **81** was combined with acetic anhydride in the presence of triethylamine in EtOAc. The reaction mixture was sonicated at 55 KHz for 45 minutes, then

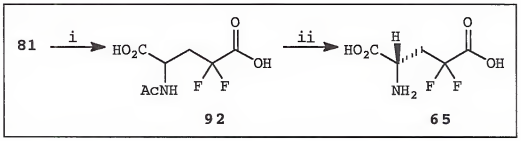

Figure 4-12. Chemoenzymatic resolution of racemic 4,4-difluoroglutamic acid **81** to produce L-4,4-difluoroglutamic acid **65**. Reagents and conditions: i.) Ac_2O, Et_3N, EtOAc, sonication, Δ, 94%; ii.) porcine kidney acylase I, H_2O, pH 7.5; 2.1%.

refluxed for 4 hours to yield the N-acylated racemic amino acid **92** in a quantitative yield.

Initial problems using porcine kidney acylase I (PKA1) in the resolution of **92** warranted the repeating of a literature example to serve as a "calibration" for the methods being used. Thus, the enzymatic resolution of racemic N-acetyl glutamic acid **93** (**Figure 4-13**) with PKA1 was performed (212) to yield L-glutamic acid **2** in a moderate yield (35%) after cation-exchange chromatography. The optical rotation ($[\alpha]_D^{22}$) of the resolved acid was +3.3° (c=0.1, 6M HCl), and is comparable with the reported optical rotation values for L-glutamic acid ($[\alpha]_D^{20}$=+31.5°, c=1.0, 6M HCl) (215). During the course of the resolution reaction, the pH of the reaction mixture decreases due to the buildup of released acetic acid. Higher yields for the reaction were obtained by maintaining a constant pH of 7.5-8.0 through frequent addition of dilute LiOH. The reported rate of PKA1

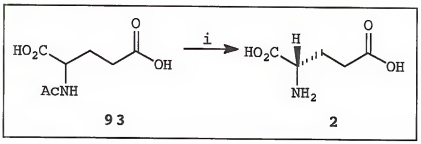

93 2

Figure 4-13. Chemoenzymatic resolution of racemic N-acetyl glutamic acid **93** to produce L-glutamic acid **2**. Reagents and conditions: i.) porcine kidney acylase I, H_2O, pH 7.5; 35%.

with amino acids having charged substituents (i.e., Glu, Asp) is significantly lower than for amino acids having neutral substituents (i.e., Met, Ala) (212). Therefore, extended reaction times (48 hrs) were found to increase the percent yield of the reaction dramatically.

The enzymatic resolution of racemic N-acetyl 4,4-difluoroglutamic acid **92** (**Figure 4-12**) with PKA1 was performed using the same procedures as the non-fluorinated glutamic acid to yield L-4,4-difluoroglutamic acid **65** in a low yield (2%) after cation-exchange chromatography. The optical rotation ($[\alpha]_D^{22}$) of the resolved acid was +2.1° (c=0.04, 6M HCl). The reported optical rotation values for L-4,4-difluoroglutamic acid ($[\alpha]_D$=+5.4°, c=1.0, H_2O) (197) are available, however, contrary to these reports, the purified acid from this procedure was not completely soluble in water at neutral pH. This phenomenon was also seen with the non-fluorinated glutamic acid compound **2**. Regardless, the fact that **65** prepared from this method does rotate

polarized light is promising, and the lack of confidence in the reported optical rotation is due to the limited amount of purified resolved compound available.

The low yields obtained in the resolution of **65** are attributed to problems encountered in the cation-exchange chromatography purification. This purification procedure involved loading the crude mixture on the Dowex-50 (H+) resin at pH=1.5, rinsing the resin with H_2O until neutral, then eluting with 1M ammonia. While this purification procedure provides a satisfactory separation for the non-fluorinated **2**, the fluorinated **65** does not appear to bind to the resin, and is eluted off with the initial fractions containing the N-acetylated compound **92** (as seen in ^1H NMR and ^{19}F NMR). Thus, the first fractions contain a mixture of acetylated material **92**, and presumably resolved non-acetylated material **65**. Careful collection of these first few fractions allows for the separation of a small amount of the resolved non-acetylated product **65**, however this method of purification is inefficient, and difficult to duplicate.

These separation problems are a direct result of the pK_a difference between non-fluorinated glutamic acid **2**, and the 4,4-difluorinated glutamic acid **65**. The pK_a for the γ-carboxylic acid functionality of **2** is 4, while the pK_a for the γ-carboxylic acid functionality of the fluorinated acid **65** is between 0 and 1. At pH=1.5, **2** is fully protonated, and has a net total charge of +1 (both carboxylates protonated, amine protonated). At pH=1.5, **65** has a net total charge of 0

(α-carboxylate protonated, γ-carboxylate deprotonated, amine protonated), and therefore does not bind to the ion-exchange resin.

Conclusions

Fluorinated amino acids are an important class of unnatural molecules which have been successfully used in a wide variety of biological applications. These compounds owe their unique biological properties to the profound electron-withdrawing effect caused by the fluorine atom(s) present. In order to develop potential fluorinated substrates for use as mechanistic probes for *E. coli* AS-B, a route for the synthesis of L-4,4-difluoroglutamic acid has been developed which relies on the enzymatic resolution of N-acetylated DL-4,4-difluoroglutamic acid. Using this method, purified L-4,4-difluoroglutamic acid has been synthesized, in low yields. The purification of the crude resolved reaction mixture using ion-exchange chromatography has not been straightforward, and will require future optimization before this synthetic route can be used to successfully produce useful quantities of this nonnatural amino acid (see Future Work, Chapter 6).

CHAPTER 5
STUDIES TOWARD THE SYNTHESIS OF TRANSITION-STATE BASED INHIBITORS OF *E. COLI* ASPARAGINE SYNTHETASE B

Introduction

Acute lymphoblastic leukemia (ALL) is often treated with the enzyme L-asparaginase, which functions by decreasing the concentration of circulating asparagine synthesized by asparagine synthetase in the liver (75-78). However, human neoplasms can become resistant to protocols involving L-asparaginase due to the synthesis of endogenous asparagine in malignant cells (79,80). There is also evidence to suggest that blood asparagine concentration may also play a role in T-cell response (81). Therefore, inhibitors of asparagine synthetase represent targets with potential application in treating leukemia, and in exploring cellular mechanisms of immunosuppression (82,83).

Whatever the details of the AS reaction mechanism, the role of Cys_1 in catalyzing the hydrolysis of the substrate glutamine primary amide appears firmly established (Chapter 1). Moreover, it is well established that enzymes are designed to bind transition state structures so as to lower the energy of activation for a reaction (C34). Therefore, structures which are isolable, ground-state analogs of

critical transition states are excellent targets for potential inhibitors of *E. coli* asparagine synthetase B.

Phosphonate esters and phosphonamidates have found great utility as stable mimetics of tetrahedral transition states (216). Transition state analogs incorporating these functionalities have been used as inhibitors for angiotensin converting enzymes (ACE) (217), aspartic proteinases (218-219), glutamine synthetase (220-223), carboxypeptidase A (224), and thermolysin (225-226). Phosphorus-centered transition state analogs have also been used as haptens for the generation of catalytic antibodies (227-228). The molecular basis for the activity of these compounds results from their steric and electrostatic resemblance to the tetrahedral intermediate formed in amide bond hydrolysis (229).

Phosphonate esters and phosphonamidates are generally prepared by the reaction of phosphonochloridates or phosphonodichloridates with alcohols or amines (230). Use of monochloridates is the more common practice. Phosphonochloridates are typically prepared by reaction of phosphonate diesters with 1 equiv. of phosphorus pentachloride (231), by treatment of monoesters with thionyl chloride or oxalyl chloride (224,232), or by oxidative chlorination of phosphinate esters with carbon tetrachloride (233).

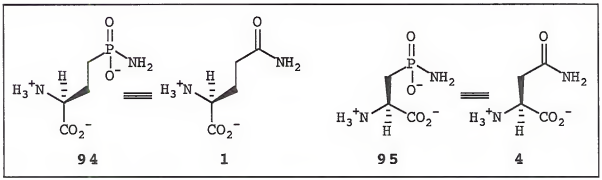

Figure 5-1. Glutamine phosphonamidate analog **94** and asparagine phosphonamidate analog **95.**

Synthesis of Phosphorus-centered Transition State Analogs

There are two target phosphorus-centered analogs which are to be synthesized in this study. The glutamine analog **94** is analogous to the transition state for glutamine **1** hydrolysis (**Figure 1-9**). The corresponding asparagine analog **95** should mimic the transition state for attack at β-aspartyl-AMP **6** (**Figure 1-7**).

Synthesis of Glutamine Phosphonamidate Analog **94**

The initial retrosynthetic strategy to form the glutamine analog **94** is shown in **Figure 5-2.** This strategy is based on the work of Valerio and coworkers (234) and involves the synthesis of the aspartylaldehyde **99** from commercially available L-aspartic acid, β-methyl ester. Reaction of this protected aldehyde with dimethyl trimethylsilyl phosphite using methodology developed by Evans and coworkers (235) should give the corresponding 2-amino-4-

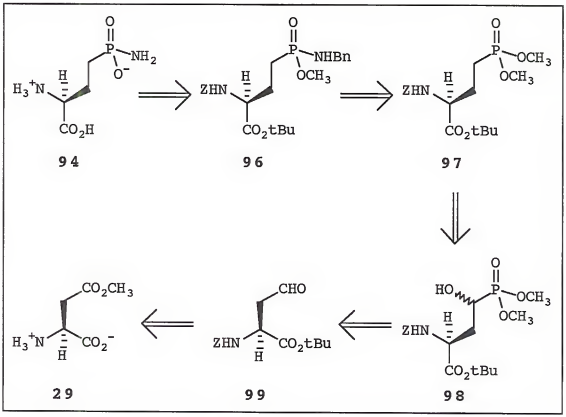

Figure 5-2. Retrosynthetic analysis for synthesis of glutamine phosphonamidate analog **94**.

(dimethoxyphosphoryl)-4-trimethylsilyloxybutanoic acid derivative **98**. This approach is reported to be favored over the classical Arbuzov methodology, since the reaction conditions are very mild and give reaction products in higher yields (234). Deoxygenation using standard radical deoxygenation methods should yield the dimethylphosphonate ester **97**. Selective demethylation of the phosphonate ester, followed by treatment with oxalyl chloride should yield the phosphonochloridate, which can subsequently be used to form the phosphonamidate **96** after treatment with the appropriate

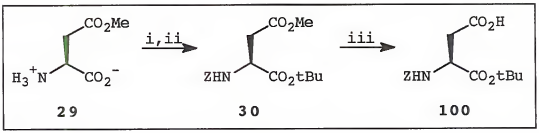

Figure 5-3. Synthesis of 1-*tert*-Butyl 2(S)-(N-benzyloxycarbonyl)amino-butanoate **100.** Z=$C_6H_5CH_2OCO$-. Reagents and conditions: i.) Benzyl chloroformate, dioxane, H_2O, Na_2CO_3, RT, 70%; ii.) isobutylene, conc. H_2SO_4, RT, 45%; iii.) NaOH, MeOH, RT, 58%.

amine. A series of deprotections should then afford the desired phosphonamidate **94.**

The synthesis of the N-protected aspartylaldehyde **99** begins with commercially available L-aspartic acid, β-methyl ester **29.** Nitrogen protection with a benzyloxycarbonyl group was done using literature methods (110) to give the Cbz-N-protected acid, which was subsequently subjected to isobutylene gas with catalytic H_2SO_4 in methylene chloride (111) to give the N-protected diester **30.** (**Figure 5-3**). Subsequent hydrolysis of the β-methyl ester functionality with hydroxide gives the diprotected aspartic acid derivative **100,** which was purified by column chromatography (207) to give a 20% overall yield from **29.**

Formation of the protected homoserine derivative **101** (**Figure 5-4**) was performed through borohydride reduction of the mixed carbonic anhydride of **100** (236), followed by column chromatography purification. Oxidation of the alcohol **101** with chromium (IV) oxide-pyridine in methylene chloride (237)

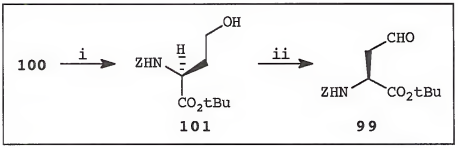

Figure 5-4. Synthesis of 1-*tert*-Butyl 2(S)-(N-benzyloxycarbonyl)amino-4-oxo-butanoate **99**. Z = $C_6H_5CH_2OCO$-. Reagents and conditions: i.) Ethyl chloroformate, N-methyl morpholine, THF, -10 °C; b. $NaBH_4$, H_2O, 0 °C, 69%; ii.) CrO_3, pyridine, CH_2Cl_2, RT, 30%.

affords the L-aspartylaldehyde t-butyl ester **99** in 30% yield after column chromatography. While reported yields (234) for this reaction are higher, attempts to optimize this yield further were unsuccessful.

Addition of dimethyl trimethylsilylphosphite to the aldehyde **99** gave the corresponding dimethyl trimethylsilyloxy phosphonate **102** as a mixture of diastereoisomers after column chromatography (**Figure 5-5**) (235). The 4-trimethylsilyloxy group is stable to treatment with aqueous extraction and chromatography on silica. This stability has been attributed to the possible steric hindrance at the silicon atom by the phosphonate ester functionality, which would hinder hydrolysis at the silicon-oxygen bond (234). Nevertheless, subsequent hydrolysis of the silyl protecting group was accomplished by stirring **102** in concentrated acetic acid (238) for 24 hours to afford **98** in a 52% overall yield from **99**.

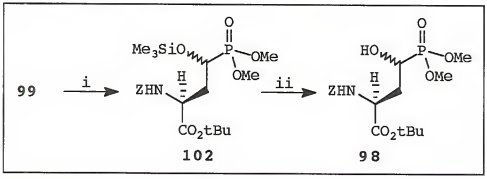

Figure 5-5. Synthesis of Dimethyl (3(S)-(N-benzyloxycarbonyl)amino-2(R,S)-hydroxy-4-carbobutoxybutyl) phosphonate **98**. Z=$C_6H_5CH_2OCO$-. Reagents and conditions: i.) Dimethyl trimethylsilylphosphite, C_6H_6, Δ, 56%; ii.) AcOH, RT, 92%.

Shortly after beginning the synthetic path to the glutamine analog **94** outlined in **Figure 5-2**, another route for the synthesis of the fully protected dimethyl phosphonate derivative **97** was reported (239), except that a different carboxylate ester was employed. The attractiveness of this route becomes apparent after comparison of number of steps and yields of key reactions for the synthesis of this intermediate. Furthermore, the acidic deprotection needed to remove the α-t-butyl ester in the final stages of the synthesis of **94** using the current route is worrisome in light of the reported lability of the phosphonamidate functionality in acidic media (240). In order to investigate the possible advantages of this reported route, a new scheme for the synthesis of **94** was devised (**Figure 5-6**) and a concurrent synthesis of **94** using this pathway was undertaken.

The alternate retrosynthetic scheme for the synthesis of **94** is shown in **Figure 5-6.** This strategy is based on the

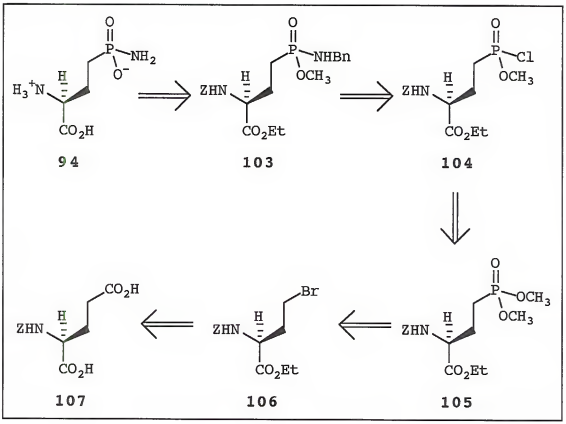

Figure 5-6. Alternate retrosynthetic scheme for the synthesis of glutamine phosphonamidate analog **94**.

work of Coward and coworkers (239) and involves the synthesis of the bromide derivative **106**, using methodology developed by Barton (241), from commercially available N-benzyloxycarbonyl L-glutamic acid **107**. Formation of the dimethyl phosphonate **105** should be obtained via a Michaelis-Arbuzov reaction of trimethylphosphite with **106**. Selective hydrolysis of the phosphonate ester followed by treatment with oxalyl chloride (232) should yield the phosphonochloridate **104**, which can subsequently be used to form the phosphonamidate **103** after treatment with the appropriate amine. A series of

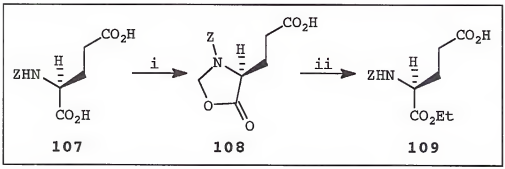

Figure 5-7. Synthesis of 1-Ethyl 2(S)-(N-benzyloxycarbonyl)aminopentanoate **109**. Z=$C_6H_5CH_2OCO$-. Reagents and conditions: i.) para-formaldehyde, p-TSA, C_6H_6, Δ, 88%; ii.) NaOEt, EtOH, 0 °C, 87%.

deprotections should then afford the desired phosphonamidate **94**.

The synthesis the N-protected bromide derivative **106** begins with commercially available N-benzyloxycarbonyl L-glutamic acid **107** (**Figure 5-7**). The differential protection of the α-carboxylate functionality of **107** was accomplished via formation of the N-benzyloxycarbonyl-5-oxazolidinone intermediate **108** according to literature methods (242). Subsequent reaction of **108** with sodium ethoxide in ethanol (243) afforded the N-protected α-ethyl ester glutamic acid derivative **109** after column chromatography purification in a 78% overall yield from **107**.

Glutamic acids with different α-carboxylic acid protective groups have been reported to yield the desired alkyl bromides via a modified Hunsdieker reaction (244,245). Using this method, the N-protected glutamic acid derivative **109** was converted to the N-hydroxypyridine-2-thione ester

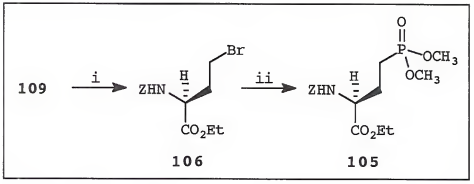

Figure 5-8. Synthesis of Dimethyl (3(S)-(N-benzyloxycarbonyl)amino-4-carbethoxybutyl) phosphonate **105**. $Z=C_6H_5CH_2OCO$-. Reagents and conditions: i.) a. 1-oxa-2-oxo-3-thiaindolizinium chloride, CH_2Cl_2, RT; b. $CBrCl_3$, hυ, RT, 40%; ii.) $P(OMe)_3$, Δ, 78%.

(Barton ester), followed immediately by the addition of bromotrichloromethane ($CBrCl_3$) and irradiation with a standard 150W flood lamp (**Figure 5-8**). The mechanism of this transformation involves the decomposition of the Barton ester formed from **109** with $CBrCl_3$ as the solvent and halogen atom source to form **106** in a radical chain reaction. Using this methodology, **106** was produced in moderate yields after purification by column chromatography. Reaction of the bromide **106** with trimethylphosphite in a Michaelis-Arbuzov reaction (246), followed by column chromatography purification, affords the dimethyl phosphonate **105** in higher yields than previously reported (239), and in a 34% overall yield from **109**. The well-know tendency of the alkyl halide product (CH_3Br) to react with the trimethylphosphite reagent was minimized by removal of CH_3Br via a warmed (hot water) condenser (247).

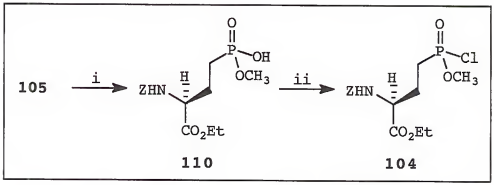

Figure 5-9. Synthesis of Methyl (3(S)-(N-benzyloxycarbonyl)amino-4-carbethoxybutyl) phosphonochloridate **104**. Z=$C_6H_5CH_2OCO$-. Reagents and conditions: i.) a. *t*-$BuNH_2$, Δ, b. Dowex 50W-X8, $CHCl_3$, RT, 66%; ii.) oxalyl chloride, DMF, CH_2Cl_2, 0 °C.

Having achieved an efficient synthesis of the dimethyl phosphonate **105** (**Figure 5-8**), this phosphonate was subjected to aminolysis by *tert*-butyl amine (248). The desired phosphonic acid monomethyl ester *tert*-butyl amine salt was formed in quantitative yield (**Figure 5-9**). The carboxylic acid ethyl ester functionality of **105** was stable to the nucleophilic demethylation conditions, and permitted differentiation between carboxylic acid ester and the phosphonate ester. The *tert*-butyl amine salt was subsequently converted to the free monomethyl phosphonic acid **110** in a 66% yield through the use of Dowex 50W-X8 cation exchange resin.

Initial attempts to form the phosphonochloridate intermediate **104** and subsequent coupling with an amine were unsuccessful. A detailed investigation determined that success in formation of **104** was directly related to the

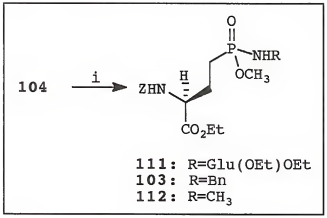

Figure 5-10. Coupling of Methyl (3(S)-(N-benzyloxycarbonyl)amino-4-carbethoxybutyl) phosphonochloridate **104** with various amines. Z=$C_6H_5CH_2OCO$-. Reagents and conditions: i.) amine, THF, 0 °C; yields: **111**, 12%; **103**, 60%; **112**, 42%.

quality of oxalyl chloride used, as well as the use of rigorously dry equipment and solvents. Regardless, the monomethyl phosphonate **110** was efficiently converted to **104** when treated with oxalyl chloride and catalytic DMF in CH_2Cl_2 (239) (**Figure 5-9**). Analysis of a reaction aliquot by ^{31}P NMR demonstrated complete conversion of **110** to **104**. The phosphonochloridate **104** is not extremely stable, and was used immediately in the coupling reaction with the appropriate amine.

Initial problems coupling benzyl amine with **104** warranted the repeating of a literature example to serve as a "calibration" for the methods being used. Thus, coupling of **104** with the diethyl ester of glutamic acid in THF (239) produced **111** in a relatively low yield after column chromatography purification on silica (**Figure 5-10**). A

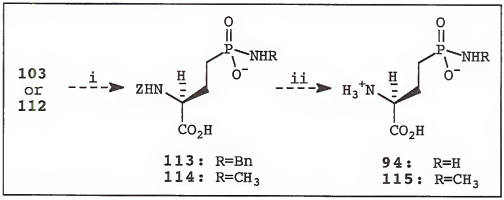

Figure 5-11. Deprotection of fully protected phosphonamidates **103** and **112**. Z=$C_6H_5CH_2OCO$-. Reagents and conditions: i.) LiOH, MeOH, 0 °C; ii.) H_2, Pd(C), EtOH, $NaHCO_3$.

substantial loss of product was seen during this column chromatography purification, and led to the use of alumina as the solid phase media in subsequent coupling reaction purifications. The coupling of benzyl amine with **104** successfully produced the protected phosphonamidate derivative **103** in a 60% yield following column chromatography. The coupling of methyl amine with **104** also successfully formed the corresponding protected phosphonamidate **114** in a 40% yield. Attempts to couple the phosphonochloridate with a simple secondary amine, dibenzyl amine, failed to yield the corresponding N,N-dibenzyl phosphonamidate, a result similar to that seen by others (239).

Removal of the phosphonate and carboxylate ester protecting groups using procedures analogous to those used in the synthesis of thermolysin phosphapeptide phosphonamidate

inhibitors (224) has been problematic. This procedure involves the base hydrolysis (3 equiv.) of the ester functionalities, followed by chromatographic purification using BioRad AG1-X2 anion-exchange resin (**Figure 5-11**). While the base hydrolysis of **103** has produced some of the desired compound **113** (as determined by ^{1}H NMR, ^{31}P NMR, and MS) in the reaction mixture, it is not the only compound present. The ion-exchange purification has, thus far, failed to provide purified **113**. This purification problem is not surprising, as it is similar to that seen in phosphonamidate syntheses reported by others (217,239). Further analysis of this purification using reverse-phase HPLC chromatography, or other chromatographic methods may need to be explored (see Future Work, Chapter 6).

Once the hydrolysis sequence is optimized, removal of the Cbz and benzyl protecting groups from the phosphonamidate **113** using procedures analogous to those used in the synthesis of ACE phosphapeptide phosphonamidate inhibitors (217) should afford the desired phosphonamidate **94**. This procedure involves palladium-catalyzed hydrogenation in the presence of sodium bicarbonate. (**Figure 5-11**). Similar conditions should also provide the N-methyl analog **115**.

Synthesis of Asparagine Phosphonamidate Analog **95**

The initial retrosynthetic strategy to form the asparagine analog **95** is shown in **Figure 5-12**. This strategy involves the synthesis of the β-lactone **119** of N-

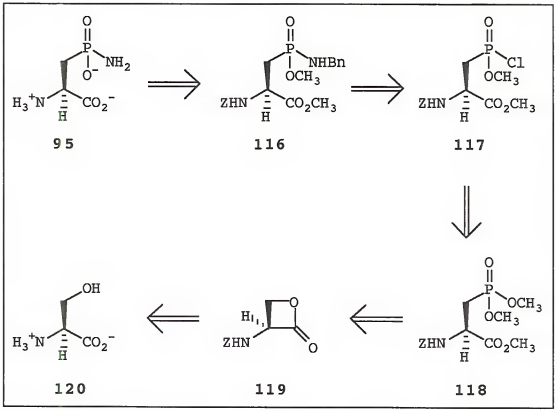

Figure 5-12. Retrosynthetic analysis for synthesis of asparagine phosphonamidate analog **95.**

protected serine, followed by the opening of the lactone with trimethylphosphite using modified Arbuzov methodology. Selective demethylation of the phosphonate ester, followed by treatment with oxalyl chloride should yield the phosphonochloridate **117,** which can subsequently be used to form the phosphonamidate **116** after treatment with the appropriate amine. A series of deprotections should then afford the desired phosphonamidate **95.**

The synthesis the N-protected serine β-lactone begins with commercially available L-serine **120** (**Figure 5-13**).

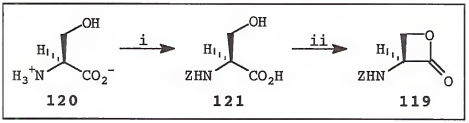

Figure 5-13. Synthesis of 2(S)-(N-benzyloxycarbonyl) amino-3-hydroxypropanoic acid lactone **119**. Z=$C_6H_5CH_2OCO$-. Reagents and conditions: i.) Benzyl chloroformate, MgO, H_2O, Et_2O, 0 °C, 76%; ii.) Ph_3P, DMAD, THF, RT, 45%.

Protection of the amino group with a benzyloxycarbonyl group using benzyl chloroformate is performed according to literature methods (249). Formation of the four-membered lactone **119** is done with triphenylphosphine and dimethyl azodicarboxylate (DMAD) in a modified Mitsunobu reaction developed by Vedras and coworkers (250,251). Formation of the dimethyl phosphonate **118** (**Figure 5-14**) is accomplished by opening the lactone with trimethylphosphite (252), in a 34% overall yield from **120**.

In order to form the phosphonamidate **116**, it is necessary to first selectively demethylate the dimethyl phosphonate, then form the phosphonochloridate precursor. However, attempts to selectively hydrolyze the phosphonate methyl ester were not successful. Use of dilute NaOH (224), trimethylsilyl bromide (253), or t-butyl amine (248) all failed to selectively demethylate the phosphonate ester.

It was determined that a more stable carboxylate ester protecting group was necessary in order to carry this

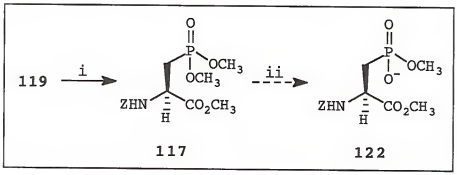

Figure 5-14. Attempted synthesis of Methyl (2(S)-(N-benzyloxycarbonyl)amino-3-carbomethoxypropyl) phosphonate **122.** Z=$C_6H_5CH_2OCO$-. Reagents and conditions: i.) $P(OCH_3)_3$, Δ, 76%.

synthetic route any further. The modified retrosynthetic route to form the asparagine analog **95** is shown in **Figure 5-15.** This strategy involves the synthesis of fully protected L-β-bromo-alanine **125** followed by formation of the phosphonate ester **124** using Michaelis-Arbuzov methodology (246). Since a more stable carboxylate protecting group is now present, selective demethylation of the phosphonate ester, followed by treatment with oxalyl chloride should yield the phosphonochloridate (239), which can subsequently be used to form the phosphonamidate **123** after treatment with the appropriate amine. A series of deprotections should then afford the desired phosphonamidate **95.**

The synthesis of the fully protected L-β-bromo-alanine also begins with commercially available L-serine **120** (**Figure 5-15**). Formation of the N-protected ester **126** was achieved using the method of Wang et al. (87) by reacting the carboxylate cesium salt of **121** with benzyl bromide, followed

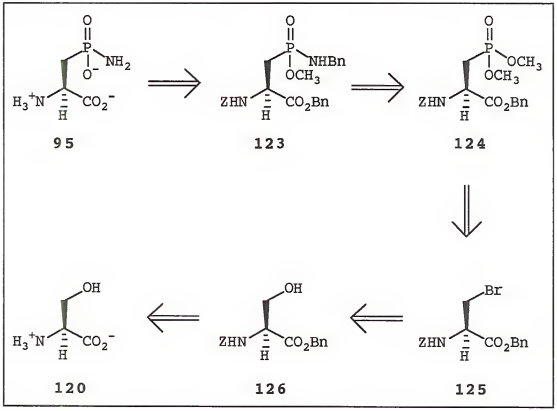

Figure 5-15. Modified retrosynthetic strategy for the synthesis of the asparagine phosphonamidate analog **95**.

by purification using column chromatography (60% yield) (**Figure 5-16**). The fully protected serine derivative **126** was then converted to the tosylate **127** with p-toluenesulfonyl (tosyl) chloride in pyridine at -10 °C (254), followed by column chromatography purification.

The serine tosylate **127** is relatively unstable, as it can easily undergo elimination to give vinylglycine **128** (**Figure 5-17**). This elimination was found to occur if the reaction temperature exceeded -10 °C, or if the reaction was allowed to occur over prolonged times (i.e., 4 hours or

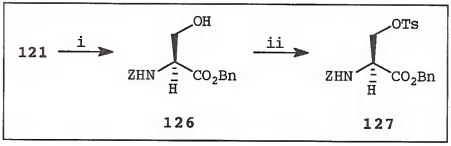

Figure 5-16. Synthesis of Benzyl 2(S)-(N-benzyloxycarbonyl)amino-3-(4'-toluenesulfon-oyl)propanoate **127**. Z=$C_6H_5CH_2OCO$-, Bn=$C_6H_5CH_2$-, Ts=$CH_3C_6H_5SO_3$-. Reagents and conditions: i.) a. Cs_2CO_3, H_2O, b. BnBr, DMF, 60%; ii.) Tosyl chloride, C_6H_5N, -10 °C, 43%.

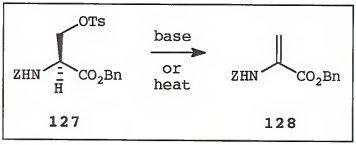

Figure 5-17. Formation of vinyl glycine **128** via elimination reaction of tosylate **127**.

more). Concentration of the reaction mixture under reduced pressure also caused the elimination reaction to occur. Optimum yields for **127** could be obtained if the cold reaction mixture was immediately placed on a prepared silica gel column, and purified by flash chromatography (207). Once in purified form, **127** proved to be relatively stable, even at room temperature.

The brominated derivative **125** was formed by nucleophilic displacement of the tosylate functionality of **127** with

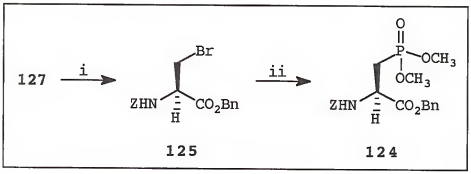

Figure 5-18. Synthesis of Dimethyl (2(S)-(N-benzyloxycarbonyl)amino-3-carbobenzoxypropyl) phosphonate **124**. Z=$C_6H_5CH_2OCO$-, Bn=$C_6H_5CH_2$-. Reagents and conditions: i.) nBu_4NBr, acetone, 0 °C, 93%; ii.) $P(OCH_3)_3$, Δ, 96%.

bromide (**Figure 5-18**). After several experiments with various bromide sources, the use of tetrabutylammonium bromide (*n*-Bu_4NBr) in neat acetone was found to give the best results in the nucleophilic displacement reaction. Therefore, the reaction of **127** with *n*-Bu_4NBr in neat acetone, followed by column chromatography purification afforded the bromide **125** in nearly quantitative yield, and in a 26% overall yield from **121**. A Michaelis-Arbuzov reaction (246) of the bromide **125** in refluxing trimethylphosphite with a heated reflux column (247), followed by column chromatography purification, afforded the dimethyl phosphonate **124** in a nearly quantitative yield (**Figure 5-18**).

The phosphonate **124** was subjected to aminolysis by *tert*-butyl amine (248) to form the desired phosphonic acid monomethyl ester *tert*-butyl amine salt in a quantitative yield (**Figure 5-19**). The carboxylic acid benzyl ester functionality of **124** was stable to the nucleophilic demethy

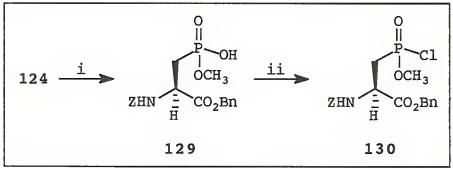

Figure 5-19. Synthesis of Methyl (2(S)-(N-benzyloxycarbonyl)amino-3-carbobenzoxypropyl) phosphonochloridate **130**. Z=$C_6H_5CH_2OCO$-, Bn=$C_6H_5CH_2$-. Reagents and conditions: i.) a. t-$BuNH_2$, Δ, b. Dowex 50W-X8, $CHCl_3$, RT, 85%; ii.) oxalyl chloride, DMF, CH_2Cl_2, 0 °C.

lation conditions, and permitted differentiation between carboxylic acid ester and the phosphonate ester. The *tert*-butyl amine salt was subsequently converted to the free monomethyl phosphonic acid **129** in a 85% overall yield from **124** after purification using Dowex 50W-X8 cation exchange resin.

Treatment of the monomethyl phosphonate **129** with oxalyl chloride and catalytic DMF in CH_2Cl_2 (239) (**Figure 5-19**) afforded the protected phosphonochloridate **130**. Analysis of a reaction aliquot by ^{31}P NMR demonstrated complete conversion of **129** to **130**. As described earlier (**Figure 5-9**), the phosphonochloridate **130** is not extremely stable, and was used in subsequent coupling reactions without purification.

The coupling of benzyl amine with **130** (**Figure 5-20**) successfully produced the protected phosphonamidate derivative **123** in a 52% yield following column chromatography

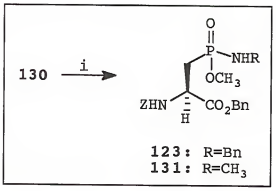

Figure 5-20. Synthesis of N-Benzyl-methoxy-(2(S)-(N-benzyloxycarbonyl)amino-3-carbo-benzoxypropyl) phosphonamidate **123** and N-Methyl-methoxy-(2(S)-(N-benzyloxycarbonyl)amino-3-carbo-benzoxypropyl) phosphonamidate **131**. Z=$C_6H_5CH_2OCO$-, Bn=$C_6H_5CH_2$-. Reagents and conditions: i.) amine, THF, 0 °C; yields: **123**, 52%; **131**, 89%.

on alumina. Likewise, the coupling of methyl amine with **130** also successfully formed the corresponding protected phosphonamidate **131** in a 89% yield.

Conclusions

The use of phosphonamidates and other phosphorus-based transition state analogs have been shown to be effective inhibitors in several enzyme systems. To that end, the synthetic routes for a series of potential glutamine and asparagine phosphonamidate inhibitors of *E. coli* AS-B have been described.

The routes developed for these syntheses involve the nucleophilic displacement of bromide through the use of Michaelis-Arbuzov methodology, followed by subsequent substitution about the phosphorus functionality using proven P(V) chemistry. Using these developed routes, the protected

glutamine analogs **103** and **112** have been synthesized, in 10% and 8% overall yields, respectively. Likewise, the protected asparagine analogs **123** and **131** have been synthesized, in 11% and 17% overall yields, respectively.

Deprotection of these protected phosphonamidates has proven to be a non-trivial step in the synthetic reaction schemes, and will require future exploration (see Future Work, Chapter 6).

CHAPTER 6
FUTURE WORK

Chemoenzymatic Synthesis of L-4,4-Difluoroglutamic Acid

The immediate goal for this project is the improvement of purification procedures developed for the isolation of L-4,4-difluoroglutamic acid. While it is tempting to attempt the purification of the crude resolved reaction mixture using Dowex-50 cation-exchange resin at a lower pH (<1), preliminary studies have shown that the degradation of the resin in the presence of strong acid is a potential problem. Alternate possibilities include purification using an anion-exchange resin, such as Dowex-1. At pH=1.5, the net total charge of the N-acetylated compound is -1 (protonated α-carboxylate, deprotonated γ-carboxylate), while the net total charge of the deprotected amino acid is 0 (protonated α-carboxylate, protonated amine, deprotonated γ-carboxylate). This difference in net charges should allow for the separation of the two components of the reaction mixture. Another possible separation procedure involves precipitation of the free L-amino acid from methanol with propylene oxide. This method of separation was successful in the preparation of several resolved nonnatural amino acids by Whitesides and coworkers (212).

Once a viable purification procedure is obtained, a determination of the enantiomeric purity of the resolved L-4,4-difluoroglutamic acid will be performed through ^{1}H NMR and ^{19}F NMR analysis of the (R)- and (S)-N-(α-methylbenzyl) ureas formed by reacting the free amino acid with (R)- or (S)-α-methylbenzyl isocyanate (as done in Chapter 2) (109,114).

The long-term goal of this project is to develop potential fluorinated substrates, such as L-4,4-difluoroglutamine, for use as mechanistic probes of *E. coli* and human AS-B. L-4,4-Difluoroglutamine should be readily available in one step from L-4,4-difluoroglutamic acid via an enzyme-catalyzed biosynthetic transformation using *E. coli* glutamine synthetase (255). Alternately, a relatively straightforward synthesis of L-4,4-difluoroglutamine using standard organic methodology should provide this analog in six steps using established literature methods (196).

Synthesis of Transition-State Based Inhibitors of *E. Coli* Asparagine Synthetase B

An obvious area for future work on this project is further studies into the removal of the acid protecting groups of the synthesized glutamine and asparagine phosphonamidate analogs. A systematic analysis of the reaction conditions, including equivalents of base used, temperature of the reaction, and reaction time will need to be done to obtain the best procedure for this deprotection. The

problems encountered in this deprotection are not surprising, considering the difficulties that have been reported by others on similar systems (217,224,256,257). While Dowex-1 anion-exchange purification has failed to provide purified phosphonamidate products following the hydrolysis reaction, several other possible purification procedures are available. These compounds appear to be prime candidates for purification by reverse-phase high performance liquid chromatography (HPLC). The presence of the benzyloxycarbonyl chromophore, as well as the negatively charged carboxylate and/or phosphonamidate anion should allow for the separation of the various components of the reaction mixture. This approach was taken by Portoghese and coworkers (217) in the synthesis of ACE phosphapeptide inhibitors. A final possibility is the use of diethylaminoethyl-cellulose (DEAE-cellulose) anion-exchange chromatography (257). DEAE-cellulose chromatography is a common purification procedure for negatively charged proteins and peptides, and offers the advantage of being less acidic than the Dowex-1 anion-exchange resins. The removal of the N-benzyloxycarbonyl protecting group and benzyl group(s) via catalytic hydrogenation should be straightforward, as several examples on similar compounds exist in the literature (217,224,239).

The long-term goal of this project is to test the inhibitory ability of the deprotected phosphonamidate analogs with *E. coli* and human AS-B. Once the deprotection steps

have been optimized, the target compounds will be assayed for activity with these enzymes.

CHAPTER 7
EXPERIMENTAL

Materials, Instruments, and Methods

L-aspartic acid, L-serine, L-glutamic acid, N-acetyl-DL-glutamic acid, N-Cbz-L-glutamic acid and N-Cbz-L-aspartic acid were obtained from Sigma Chemical Co. and used without further purification. All other reagents were obtained from Aldrich Chemical Co. or Fisher Scientific and were used without further purification unless otherwise specified. 2-iodoadenosine was a generous gift from Prof. V. J. Davidson at Purdue University. Tetrahydrofuran (THF) and diethyl ether (Et_2O) were distilled from sodium/benzophenone prior to use, and used immediately. Methanol (MeOH) was distilled from magnesium prior to use. Chloroform ($CHCl_3$), dichloromethane (CH_2Cl_2), acetonitrile (CH_3CN), and dimethyl formamide were distilled from calcium hydride prior to use. Diethylamine, *tert*-butyl amine, benzyl amine, and pyridine were distilled from potassium hydroxide prior to use. Zinc powder was freshly activated by the acid treatment (259) and used within a few hours. Chromic anhydride (CrO_3) was dried for 16 hours over sodium hydroxide in a vacuum dessicator prior to use. Analytical thin layer chromatography (TLC) analysis was performed on Whatman silica gel 60 Å F-254 nm

plates with polyester backing and visualized with a Mineralight model UVG-54 shortwave UV lamp at 254 nm, or by charring with (A) 4% ninhydrin in ethanol or (B) aqueous ceric sulfate/sulfuric acid solution. Column chromatography was performed on Davisil^{R} silica gel (Fisher) 60 Å; 200-425 Mesh, using standard flash methods (207), unless otherwise indicated. High performance liquid chromatography (HPLC) was done using a Dynamax analytical weak anion exchange column (AX 83-603-ETI, 250 mm. x 4.6 mm. ID). A Dynamax anion exchange guard column (AX 83-603-GTI, 15 mm. x 4.6 mm. ID) was connected in series and used with a Ranin HPXL dual pump solvent delivery system. Solvent gradients, flow rates, and other run conditions are reported with the specific compound purifications. Product content in the effluent was monitored using a Ranin Dynamax UV-1 UV/Visible absorbance detector set at 254 nm, with an 8 mm. flow cell light path. Melting points were obtained using a Fisher-Johns Melting Point Apparatus and are uncorrected. pH 4, 7, and 10 buffer solutions were obtained from Fisher Scientific. pH measurements were recorded using a ORION Model 250A pH Meter and a Mettler Toledo Process Analytical, Inc. Model 6030-M3/180/1M/BNC pH electrode. IR spectra were recorded on a Perkin-Elmer 1600 FTIR spectrophotometer. Optical rotations were determined at ambient temperature using a Perkin-Elmer 241 polarimeter, using a water-cooled 1 dm cell. Sonications were done using a Fisher Scientific model FS3 22-watt sonicator operating at 55KHz. Lypholizations were done on a

Labconco Lyph-Lock 6 Freeze Dry System at -50 °C and 10μ or lower pressure. ^{1}H NMR spectra were recorded at 300 or 500 MHz with a Varian VXR-300 spectrometer, a Gemini-300 spectrometer, or a Varian Unity-500 spectrometer, using deuterated chloroform / 0.3% TMS, deuterium oxide with DSS or DMSO-d_6, acetone-d_6, or methanol-d_4. ^{13}C NMR spectra were recorded at 75.4 MHz with a Varian VXR-300 spectrometer or a Gemini-300 spectrometer. ^{19}F NMR spectra were recorded at 282.2 MHz with a Varian VXR-300 spectrometer using hexafluorobenzene as an external reference. ^{31}P NMR spectra were recorded at 121.4 MHz with a Varian VXR-300 spectrometer using 85% phosphoric acid as an external reference.

Theoretical Calculations

All semi-empirical calculations were done using a CAChe Molecular Modeling system. Molecular structures were constructed using CAChe Molecular Editor software. Geometry optimizations and heats of formation (ΔH_f) were calculated using MOPAC 6.0 (113) with AM1 parameters (112), and the CONH correction. Relative heats of formation ($\Delta\Delta H_f$) correspond to the difference between the questioned structure and its lowest energy isomer or, in the case of modeled reactions between molecules, the heats of formation of the isolated reactants.

All *ab initio* calculations were done using ACES II (145) or GAMESS (164) software on either a Cray YMP-90 or Silicon Graphics Power Challenge supercomputer. Starting geometries

were obtained from semi-empirical output files, and translated into the correct *ab initio* software input file. Geometry optimizations were done at the SCF level using 4-31G (162), 6-31G (163), or DZP (143) basis sets, as specified. Vibrational analysis was used to verify that optimized structures were potential energy minima, and to compute the zero point energy correction. Single point correlation energies were calculated using MP2 (140) or CCSD(T) methods (144) using DZP, TZ2P (154), or 6-31G** (166) basis sets, as specified. Relative energies correspond to the difference between the questioned structure and its lowest energy isomer or, in the case of modeled reactions between molecules, the energies of the isolated reactants.

Synthetic Procedures and Chemical Data of Compounds

Pyrrolidine-2(S),3(R)-dicarboxylic acid **18.** The N-protected diester **26** (160 mg, 0.34 mmol) was dissolved in a MeOH (10 mL) together with ammonium formate (1.49 g, 23.7 mmol). 10% Pd/C (12 mg) was added and the reaction mixture was stirred at RT for 4 hours. Filtration through celite, followed by removal of the solvent under reduced pressure, yielded the crude aspartic acid analog **18** This hygroscopic solid was redissolved in a minimum amount of water and purified using Bio Rad Ag-1-X2 anion exchange resin (5 g, wet weight) by elution with 1% AcOH. Ninhydrin positive fractions were collected and freeze-dried to give **18** as a white solid: 29 mg, 25%; ^{1}H NMR (D_2O, 300 MHz) δ 2.22-2.35 (1 H, m), 2.35-2.49

(1 H, m), 3.40-3.50 (2 H, m), 3.51-3.63 (1 H, m), 4.40 (1 H, d, J=6.9 Hz); ^{13}C NMR (D_2O, 125.6 MHz) δ 26.38 (t), 42.09 (t), 43.80 (d), 61.95 (d), 169.70 (s), 174.62 (s); MS (FAB glycerol + TFA 5%) m/e (relative intensity) 160 (MH^+ 66), 130(17), 115 (100), 104 (25), 102 (37); exact mass calcd. for MH^+ $C_6H_{10}NO_4$ requires 160.0610, found 160.0609 (FAB NBA).

Pyrrolidine-2(S),3(S)-dicarboxylic acid **19**. The N-protected diester **27** (0.15 g, 0.31 mmol) was dissolved in MeOH (10 mL) together with ammonium formate (0.56 g, 8.8 mmol). 10% Pd/C (5 mg) was added and the reaction mixture was stirred at RT for 4 hours. Filtration through celite, followed by removal of the solvent under reduced pressure, yielded the crude aspartic acid analog **19**. This hygroscopic solid was redissolved in a minimum amount of water and purified using Bio Rad Ag-1-X2 anion exchange resin (5 g, wet weight) by elution with 1% AcOH. Ninhydrin positive fractions were collected and freeze-dried to give **19** as a white solid: 42 mg, 85%; mp >300 °C dec. (lit.[42] 333 °C dec.); IR (KBr) υ 3600-2800, 1702, 1618, 1460, 1102 cm^{-1}; ^1H NMR (D_2O, 300 MHz) δ 2.19-2.40 (2 H, m), 3.32-3.51 (3 H, m), 4.46 (1 H, d, J=5.6 Hz); ^{13}C NMR (CD_3CN, 75.4 MHz) δ 28.11 (t), 45.33 (t), 47.34 (d), 62.91 (d), 172.64 (s), 176.06 (s); MS (FAB: Glycerol + 5% TFA) *m/e* (relative intensity) 160 (MH^+ 10), 154 (15), 133 (100), 93 (41); exact mass calcd. for MH^+ $C_6H_{10}NO_4$ requires 160.0610, found 160.0440 (FAB). Elemental Analysis ($C_6H_9NO_4$) C, H, N. requires C 45.28, H 5.70, N 8.80, found C 45.25, H 6.02, N 8.57.

1,4-Dibenzyl 2(S)-(N-benzyloxycarbonyl)amino-butanoate **21**. N-benzyloxycarbonyl L-aspartic acid **20** (2.148 g, 8.0 mmol) was added to a solution of $CsCO_3$ (5.11 g, 15.7 mmol) dissolved in H_2O (42 mL, 2333 mmol). Solution was lypholyzed and the residue was dissolved in N,N-dimethylformamide (75 mL) followed by addition of benzyl bromide (2 mL, 16.8 mmol). Removal of solvent under reduced pressure yielded an oil which was dissolved in H_2O and extracted with EtOAc (3 x 30 mL). The organic layer was washed with aqueous 5% $NaHCO_3$ (1 x 30 mL), H_2O (1 x 30 mL), and dried with anhydrous $MgSO_4$. Removal of solvent under reduced pressure yielded a yellowish oil which solidified on standing. Recrystallization from EtOAc/40-60 °C Petroleum ether yielded a white solid: 1.65 g, 48%; mp 62-63 °C (lit.[209] 61-63 °C); $[\alpha]^{22}_D$ +14.1° (*c*=6.9 g/100 mL, $CHCl_3$); IR ($CHCl_3$) υ 3429, 3357, 3033, 1733, 1506, 1456, 1338 cm^{-1}; ^1H NMR ($CDCl_3$, 300 MHz) δ 2.82-3.15 (2 H, dq, *J*=17.1, 4.5, 4.5 Hz), 4.69 (1 H, m), 5.05 (2 H, s), 5.11 (2 H, s), 5.13 (2 H, s), 5.80 (1 H, d, *J*=8.4 Hz), 7.3-7.36 (15 H, m); ^{13}C NMR ($CDCl_3$, 75.4 MHz) δ 36.76 (t), 50.57 (d), 66.83 (t), 67.12 (t), 67.54 (t), 126.97 (d), 127.56 (d), 128.06 (d), 128.19 (d), 128.25 (d), 128.33 (d), 128.44 (d), 128.52 (d), 128.59 (d), 131.27 (s), 135.15 (s), 135.32 (s), 140.99 (s), 156.00 (s), 170.50 (s); MS (EI): *m/e* (relative intensity) 448 (11), 404 (6), 219 (2), 181 (10), 91 (100); HRMS exact mass calcd. for $C_{26}H_{26}NO_6$ requires 448.1760, found 448.1763 (FAB NBA). Elemental analysis ($C_{26}H_{25}NO_6$) C, H, N,

requires C 69.79, H 5.63, N 3.13, found C 69.70, H 5.64, N 3.03.

1,4-Dibenzyl 2(S)-(N-benzyloxycarbonyl)amino-3(S)-propen-2'-yl-butanoate **22** and 1,4-dibenzyl 2(S)-(N-benzyloxycarbonyl) amino-3(R)-propen-2'-yl-butanoate **23**. A solution of LiHMDS (1.0 M in THF) (8.0 mL, 8.0 mmol) dissolved in dry THF (10 mL) was cooled to -78 °C before the addition of diester **21** (1.69 g, 3.8 mmol) dissolved in dry THF (30 mL) to give a pale-yellow solution. The reaction mixture was stirred at -78 °C for 30 min, then warmed slowly to -30 °C, and stirred for 2 h to ensure formation of the dianion. After re-cooling the resulting orange solution to -78 °C, neat allyl bromide (1.6 mL, 18.5 mmol) was added at such a rate that the solution temperature did not exceed -75 °C. Stirring was continued for 16 h, at -78 °C, before the reaction was quenched by pouring it into aqueous 1 M HCl (120 mL) at RT. After extraction using Et_2O (4 x 50 mL), the organic phases were dried ($MgSO_4$) and the solvent evaporated under reduced pressure. The crude material was purified by flash chromatography (eluant: 30% EtOAc/40-60 °C petroleum ether) to yield a clear oil, which was a mixture of epimers at C-3: 1.09g, 60%; mp 82-83 °C; $[\alpha]^{20}_D$ +29.4° (c=2.3 g/100 mL, $CHCl_3$); IR ($CHCl_3$) υ 3428, 3019, 1733, 1507, 1456 cm^{-1}; ^1H NMR ($CDCl_3$, 300 MHz) δ 2.26-2.38 (1 H, m), 2.47-2.58 (1 H, m), 3.21-3.29 (1 H, m), 4.68 (1 H, dd, J=9.9, 3.7 Hz), 5.04-5.14 (8 H, m), 5.68-5.84 (2 H, m), 7.25-7.36 (15 H, m); ^{13}C NMR ($CDCl_3$, 75.4 MHz) δ 32.86 (t), 46.56 (d), 54.12 (d), 66.93

(t), 67.14 (t), 67.39 (t), 118.35 (t), 128.00 (d), 128.06 (d), 128.13 (d), 128.22 (d), 128.40 (d), 128.46 (d), 128.51 (d), 128.55 (d), 128.60 (d), 133.99 (d), 135.29 (s), 135.33 (s), 136.34 (s), 156.55 (s), 170.76 (s), 172.76 (s); MS (FAB) m/e (relative intensity) 488 (MH^+ 100), 444 (58), 308 (19), 181 (96); exact mass calcd. for MH^+ $C_{29}H_{30}NO_6$ requires 488.2073, found 488.2082 (FAB NBA). Elemental analysis ($C_{29}H_{29}NO_6$) C, H, N requires C 71.44, H 6.00, N 2.87, found C 71.30, H 5.99, N 2.81.

Dibenzyl 1-(N-benzyloxycarbonyl)-5(R,S)-hydroxy-pyrrolidine-2(S),3(S)-dicarboxylate **24** and dibenzyl 1-(N-benzyloxycarbonyl)-5(R,S)-hydroxy-pyrrolidine-2(S),3(R)-dicarboxylate **25.** OsO_4 (1.4 mL of a 1.0% solution in THF, 0.014 mmol) and $NaIO_4$ (1.39 g, 6.5 mmol) were added to a solution of the mixture of diastereoisomeric diesters **22** and **23** (0.98 g, 2.0 mmol) in MeOH (50 mL) and water (25 mL). The resulting reaction mixture was stirred at RT for 16 hr. The reaction mixture volume was concentrated under reduced pressure to half of the original volume, and the solution was poured into water (140 mL) and extracted with EtOAc (3 x 50 mL). The organic extracts were dried ($MgSO_4$) and the solvent removed under reduced pressure to yield the crude product as a brown oil. This material was purified by flash chromatography (eluant: 50% EtOAc/40-60 °C petroleum ether) to yield a mixture of the diastereoisomers **24** and **25**, which solidified on standing. ^1H NMR analysis showed that this material was a

9:1 ratio of **25:24**, which was used in the subsequent reduction reaction: 0.84 g, 85%; mp. 71-72 °C; $[\alpha]_D^{20}$ +31.3° (*c*=0.64 g/100 mL, $CHCl_3$); IR ($CHCl_3$) υ 3446, 3019, 1749, 1734, 1715, 1699, 1558, 1540, 1507, 1457, 1419 cm^{-1}; ^1H NMR ($CDCl_3$, 300 MHz) δ 2.05-2.15 (1 H, m), 2.48-2.62 (1 H, m), 3.65-3.80 (1 H, m), 3.83 (1 H, br. s), 4.68-4.78 (1 H, m), 4.80-5.20 (6 H, m), 5.72 (1 H, d, *J*=5.6 Hz), 7.16-7.22 (5 H, m), 7.25-7.36 (10 H, m); ^{13}C NMR ($CDCl_3$, 75.4 MHz) δ 34.73 (t), 44.43 (d), 60.96 (d), 67.18 (t), 67.41 (t), 67.62 (t), 81.43 (d), 127.76 (d), 128.06 (d), 128.14 (d), 128.26 (d), 128.35 (d), 128.47 (d), 128.50 (d), 128.68 (d), 128.78 (d), 135.13 (s), 135.18 (s), 135.74 (s), 154.31 (s), 169.54 (s), 169.69 (s); MS (FAB NBA) m/e (relative intensity) 490 (MH^+ 2), 472 (30), 428 (100), 338 (15); HRMS exact mass calcd. for MH^+ $C_{28}H_{28}NO_7$ requires 490.1866, found 490.1858 (FAB NBA).

Dibenzyl 1-(N-benzyloxycarbonyl)-pyrrolidine-2(S),3(S)-dicarboxylate **26** and dibenzyl 1-(N-benzyloxycarbonyl)-pyrrolidine-2(S),3(R)-dicarboxylate **27**. The mixture of diastereoisomeric diesters **24** and **25** (872 mg, 1.78 mmol) and Et_3SiH (0.45 mL, 2.82 mmol) were dissolved in dry $CHCl_3$ (25 mL). Neat TFA (1.4 mL, 18.2 mmol) was then added dropwise to this solution with vigorous stirring. Upon completion of the addition, the reaction mixture was stirred at RT for a further 90 min before the solvent volume was reduced under reduced pressure. This gave an oily residue which was redissolved in EtOAc (20 mL). After washing with 5% aqueous

$NaHCO_3$ (3 x 5 mL), the organic layer was dried ($MgSO_4$) and the solvent removed to yield the mixture of **26** and **27** as a pale-yellow oil. Purification by gravity column chromatography using (eluant: 25% EtOAc/40-60 °C petroleum ether) allows for separation of two diasteromers and gives desired products as clear oils: **26:** 0.177g, 20%; $[\alpha]_D^{20}$ +28.8 (c=1.7 g/100 mL, $CHCl_3$); ^1H NMR ($CDCl_3$, 300 MHz) δ 3.2-3.32 (1 H, m), 3.66-3.74 (2 H, m), 4.85-4.92 (1 H, dd, J=18.8, 3.66 Hz), 5.1-5.3 (7 H, m), 7.15-7.25 (15 H, m); ^{13}C NMR ($CDCl_3$, 75.4 MHz) δ 27.1 (t), 45.4 (t), 47.9 (d), 61.5 (d), 66.9 (t), 127.5 (d), 126.6 (d), 127.7 (d), 127.8 (d), 127.9 (d), 128.0 (d), 128.05 (d), 128.2 (d), 128.25 (d), 128.3 (d), 128.4 (d), 135.0 (s), 135.2 (s), 136.1 (s), 136.2 (s), 153.7 (s), 154.4 (s), 170.5 (s), 171.1 (s), 171.2 (s); IR (neat) υ 3065, 3034, 2958, 2893, 2360, 1715, 1608, 1587, 1497, 1456, 984 cm^{-1}; MS (FAB NBA) m/e (relative intensity) 474 (MH^+ 100), 430 (67), 338 (33), 294 (35), 181 (45); exact mass calcd. for MH^+ $C_{28}H_{28}NO_6$ requires 474.1917, found 474.1937 (FAB, NBA). **27:** 0.401g, 47%; $[\alpha]_D^{20}$ +14.7° (c=4.0 g/100 mL, $CHCl_3$); ^1H NMR ($CDCl_3$, 300 MHz) δ 2.5-2.56 (1 H, t, J=9.0), 3.34-3.46 (1 H, m, J=8.5 Hz), 3.48-3.61 (1 H, m, J=9.0 Hz), 3.83-3.94 (1 H, m, J=10.2 Hz), 4.75-5.0 (2 H, m, J=8.5 Hz), 5.1-5.25 (6 H, m), 7.15-7.25 (15 H, m); ^{13}C NMR ($CDCl_3$, 75.4 MHz) δ 25.9 (t), 45.7 (t), 47.0 (d), 60.3 (d), 66.8 (t), 127.6 (d), 127.7 (d), 127.8 (d), 127.9 (d), 128.1 (d), 128.2 (d), 128.25 (d), 128.3 (d), 128.4 (d), 135.0 (s), 135.1 (s), 136.1 (s), 136.3 (s), 153.7 (s), 154.4 (s), 169.6

(s), 169.7 (s), 169.8 (s); IR ($CHCl_3$) υ 3065, 3034, 2957, 2894, 1748, 1716, 1700, 1498, 1456, 1418, 1361, 1188 cm^{-1};.MS (FAB NBA) m/e (relative intensity) 474 (MH^+ 100), 430 (67), 338 (33), 294 (35), 181 (45); exact mass calcd. for MH^+ $C_{28}H_{28}NO_6$ requires 474.1917, found 474.1942 (FAB, NBA).

1,5-di-*tert*-butyl-2(S)-(N-benzyloxycarbonyl)amino-3(R)-carbomethoxypentanoate **28**. A solution of LiHMDS (1.0 M in THF) (6.7 mL, 6.7 mmol) dissolved in dry THF (20 mL) was cooled to -78 °C before the addition of diester **30** (1.08 g, 3.2 mmol) dissolved in dry THF (15 mL) to give a pale-yellow solution. The reaction mixture was stirred at -78 °C for 30 min, then warmed slowly to -40 °C, and stirred for 45 min. to ensure formation of the dianion. After re-cooling the resulting orange solution to -78 °C, neat *tert*-butyl chloroacetate (2.2 mL, 15.4 mmol) was added at such a rate that the solution temperature did not exceed -74 °C. Stirring was continued for 14 h at -78 °C before the reaction was quenched by pouring it into 1 M HCl (120 mL) at RT. After extraction using Et_2O (3 x 50 mL), the organic phases were dried ($MgSO_4$) and the solvent evaporated. The crude material was purified by flash column chromatography (eluant: 20% EtOAc/40-60 °C petroleum ether) initially yielding the desired triester **28** as a yellow oil which solidified upon standing. Recrystallization from EtOAc/40-60 °C petroleum ether gave the desired product **28** as a pale white solid: 551 mg, 39%; mp 56-58 °C; $[\alpha]_D^{20}$ +4.5° (c=5.3 g/100 mL,

$CHCl_3$); IR (neat) υ 3358, 2979, 1732, 1506, 1456, 1223, 1155 cm^{-1}; ^1H NMR ($CDCl_3$, 300 MHz) δ 1.48 (18 H, s), 2.47 (1 H, dd, *J*=16.85, 5.86 Hz), 2.68 (1 H, dd, *J*=16.85, 8.54 Hz), 3.54-3.62 (1 H, m), 3.70 (3 H, s), 4.62 (1 H, dd, *J*=8.79, 3.66 Hz), 5.16 (2 H, s), 5.61 (1 H, d, *J*=8.79 Hz), 7.30-7.40 (5 H, m); ^{13}C NMR ($CDCl_3$, 75.4 MHz) δ 27.61 (q), 27.76 (q), 33.64 (t), 43.40 (d), 51.79 (q), 54.65 (d), 67.87 (t), 80.86 (s), 82.54 (s), 127.90 (d), 127.94 (d), 128.28 (d), 136.01 (s), 156.11 (s), 168.75 (s), 170.17 (s), 170.98 (s); MS (FAB) *m/e* (relative intensity) 452 (MH^+, 8), 396 (7), 340 (48), 296 (35), 91 (100); HRMS exact mass calcd. for MH^+, $C_{23}H_{34}NO_8$ requires 452.2284, found 452.2285. Elemental analysis ($C_{23}H_{33}NO_8$) C, H, N. requires C 60.87, H 7.32, N 3.03 found C 60.87, H 7.32, N 3.03.

4-Methyl-2(S)-(N-benzyloxycarbonyl)amino-butanoate **29a.** Solid L-aspartic acid, β-methyl ester **29** (4.3 g, 29.2 mmol) was dissolved in solution of dioxane (50 mL, 588 mmol) and H_2O (25 mL, 1390 mmol) and cooled to 0 °C. To this solution was added Na_2CO_3 (4.0 g, 38 mmol) with stirring, followed by dropwise addition of benzyl chloroformate (9.2 mL, 64.4 mmol). After stirring for 2 hours, additional Na_2CO_3 was added (pH9) and solution was stirred at RT for an additional 48 hours. Solution was concentrated, and poured onto 100 mL of a water/ice mixture. Solution was washed with Et_2O, acidified with an aqueous saturated $NaHSO_4$ solution (pH2), extracted into Et_2O, and dried with anhydrous $MgSO_4$. Removal

of solvent under reduced pressure gives **29a** as a pale yellow oil: 5.73g, 70%. ^{1}H NMR ($CDCl_3$, 300 MHz) δ 2.80-3.05 (2 H, m, *J*=17.6, 4.4 Hz), 3.65 (3 H, d), 4.6 (1 H, s), 5.1 (2 H, s), 6.0 (1 H, dd), 7.3-7.4 (5 H, m), 7.8 (1H, br s).

1-*tert*-Butyl-4-methyl-2(S)-(N-benzyloxycarbonyl)amino-butanoate **30.** 4-Methyl-2(S)-(N-benzyloxycarbonyl)amino-butanoate **29a** (1.4 g, 5.0 mmol) was placed in a 300mL RBF and cooled to -20 °C (ice/acetone bath). Isobutylene was distilled into the flask (~50 mL). To this solution was added concentrated H_2SO_4 (2 drops) with stirring. Solution was allowed to gradually warm to RT and stirred for a further 2 days. Excess isobutylene was released, and solid Na_2CO_3 was added to reaction mixture. After bubbling ceased, residue dissolved in H_2O and extracted 3X with EtOAc. Organic layer was washed once with an aqueous saturated $NaHCO_3$ solution, and dried with $MgSO_4$. Removal of solvent under reduced pressure gives **30** as a colorless oil: 0.756 g, 45%; $[\alpha]_D^{20}$ +15.6° (*c*=7.6 g/100 mL, $CHCl_3$); IR (neat) υ 3357, 2979, 1732, 1504, 1455, 1439, 1370, 1222, 1156, 1047, 847 cm^{-1}; ^{1}H NMR ($CDCl_3$, 300 MHz) δ 1.2 (9 H, s), 2.75-3.0 (2 H, m, *J*=16.6 Hz, *J*=4.6 Hz), 3.6 (3 H, s), 4.5-4.6 (1 H, m, *J*=3.7 Hz), 5.05 (2 H, s), 5.9 (1 H, d, *J*=8.3), 7.15-7.20 (5 H, m); ^{13}C NMR ($CDCl_3$, 75.4 MHz) δ 27.74, 36.48, 51.38, 51.54, 66.61, 82.12, 127.79, 127.82, 128.20, 128.80, 136.07, 155.68, 169.30, 170.85; MS (FAB) *m/e* (relative intensity) 338 (33), 282 (89), 238 (62), 184 (59), 91 (100); HRMS exact mass calcd.

for $C_{17}H_{24}NO_6$ (m+1) requires 338.1604, found 338.1653 (FAB NBA).

1-*tert*-Butyl 2(S)-(N-benzyloxycarbonyl)amino-3(R,S)-carbomethoxy-4-phenyl-butanoate **30a**. A solution of LiHMDS (1.0 M in THF) (4.5 mL, 4.5 mmol) dissolved in dry THF (20 mL) was cooled to -78 °C before the addition of diester **30** (0.73 g, 2.17 mmol) dissolved in dry THF (20 mL) to give a pale-yellow solution. The reaction mixture was stirred at -78 °C for 30 min, then warmed slowly to -30 °C, and stirred for 45 min. to ensure formation of the dianion. After recooling the resulting orange solution to -78 °C, distilled benzyl bromide (0.75 mL, 6.3 mmol) was added at such a rate that the solution temperature did not exceed -74 °C. Stirring was continued for 10 min., at -78 °C, before the reaction was allowed to warm to RT and stirred for a further 60 min. The reaction was quenched by pouring it into aqueous 1 M HCl (120 mL) at RT. After extraction using Et_2O (3 x 30 mL), the organic phases were dried ($MgSO_4$) and the solvent evaporated under reduced pressure. The crude material was purified by flash chromatography (eluant: 30% Et_2O/hexanes) to yield a clear oil, which was a 60:40 mixture of epimers at C-3: 103 mg, 11%; ^1H NMR ($CDCl_3$, 300 MHz) δ 1.41 and 1.49 (2 x 9 H, s, major and minor diastereomers), 2.76-3.20 (2H, m, $PhC\underline{H}_2$), 3.25-3.40 (1 H, m, $C\underline{H}CO_2Me$), 3.62 and 3.63 (2 x 3 H, s, minor and major dias.), 4.45, (1 H, dd, *J*=9.76, 3.66 Hz, NC<u>H</u> major dia.), 4.58, (1 H, dd, *J*=8.54, 3.91 Hz, NC<u>H</u> minor dia.), 5.10

and 5.15 (2 x 2 H, s, minor and major dias.), 5.57, (1 H, d, J=8.54 Hz, NH minor dia.), 5.75 (1 H, d, J=9.76 Hz, NH major dia.), 7.15-7.45 (20 H, m, ArH); ^{13}C NMR ($CDCl_3$, 75.4 MHz) δ 27.79 and 27.97 (major and minor dias.), 34.98 and 34.43 (minor and major dias.), 48.75 and 50.24 (major and minor dias.), 51.88 (both dias.), 54.63 and 55.24 (major and minor dias.), 67.03, 82.54 and 83.09 (major and minor dias.), 126.67, 128.08, 128.49, 128.84, 128.90, 128.96, 136.35 and 138.13, 156.39, 169.63, 169.68, 172.24, 173.14.

1,5-di-*tert*-butyl-2(S)-amino-3(R)-carbomethoxypentanoate **33**. Ten percent (10%) Pd/C (4 mg) was added to a solution of the N-protected ester **28** (44 mg, 0.98 mmol) dissolved in MeOH (10 mL). The reaction mixture was placed under a hydrogen atmosphere and allowed to stir for 12 hours at RT. Filtration through celite, followed by removal of the solvent under reduced pressure, yielded the **33** as a clear oil, which was used without further purification. 21 mg, 66%; ^{1}H NMR (CD_3OD, 500 MHz) δ 1.45 (9 H, s), 1.49 (9 H, s), 2.67 (2 H, d, J=6.84 Hz), 3.49-3.54 (1 H, m), 3.74 (3 H, s), 4.23 (1 H, d, J=3.91 Hz); ^{13}C NMR (CD_3OD, 75.4 MHz) δ 28.12 (q), 28.26 (q), 33.59 (t), 43.79 (d), 52.99 (q), 55.17 (d), 82.53 (s), 85.16 (s), 168.95 (s), 171.75 (s), 172.17 (s); MS (EI) *m/e* (relative intensity) 318 (MH^+, 3), 205 (9), 188 (33), 160 (100), 142 (12), 128 (77), 114 (17), 100 (32); HRMS exact mass calcd. for MH^+, $C_{15}H_{28}NO_6$ requires 318.1917, found 318.1917.

Enantiomeric Purity of 1,5-di-*tert*-butyl-2(S)-amino-3(R)-carbo-methoxypentanoate **33**. (S)-α-methylbenzyl isocyanate (0.12 mL, 0.84 mmol) was added to a solution of **33** (0.08 g, 0.25 mmol) in dry THF (10 mL) under a nitrogen atmosphere, and the resulting solution was refluxed for 3 hours. Removal of the volatiles under reduced pressure left a residue which was directly examined by ^{1}H NMR. Similarly, (R)-α-methylbenzyl isocyanate (0.16 mL, 1.10 mmol) was added to a solution of **33** (0.13 g, 0.40 mmol) in dry THF (10 mL) under a nitrogen atmosphere, and the resulting solution was refluxed for 3 hours. Removal of the volatiles under reduced pressure left a residue which was directly examined by ^{1}H NMR in which the methyl ester peaks were clearly differentiated. The limits of detection were determined through incremental doping experiments with ureas (R) and (S). **Urea (R)-31:** ^{1}H NMR ($CDCl_3$, 500 MHz) δ 1.41 (9 H, s), 1.43 (9 H, s), 1.58 (3 H, d, *J*=7.00 Hz), 2.30 (1 H, m), 2.51 (1 H, dd, *J*=17.09, 9.76 Hz), 3.47 (1 H, dt, *J*=8.79, 4.88 Hz), 3.61 (3 H, s), 4.08 (1 H, m, *J*=6.84 Hz), 4.82 (1 H, q, *J*=3.91 Hz), 5.02 (1 H, br s), 5.52 (1 H, br s), 7.20-7.40 (5 H, m); ^{13}C NMR ($CDCl_3$, 75.4 MHz) δ 22.38 (q), 27.72 (q), 27.91 (q), 33.80 (d), 44.08 (d), 50.22 (t), 51.73 (q), 54.46 (d), 80.75 (s), 82.40 (s), 125.19 (d), 126.67 (d), 128.48 (d), 142.32 (s), 156.92 (s), 170.27 (s), 170.65 (s), 172.47 (s). **Urea (S)-32:** ^{1}H NMR ($CDCl_3$, 500 MHz) δ 1.41 (2 x 9 H, s), 1.58 (3 H, d, *J*=6.84 Hz), 2.44 (1 H, dd, *J*=16.6, 4.88 Hz), 2.63 (1 H, dd, *J*=17.09, 9.28 Hz), 3.49 (1 H, m, *J*=4.88 Hz), 3.63 (3 H, s), 4.08 (1 H, m, *J*=6.84

Hz), 4.85 (1 H, q, J=6.84 Hz), 5.02 (1 H, br s), 5.48 (1 H, br s), 7.28-7.38 (5 H, m); ^{13}C NMR ($CDCl_3$, 75.4 MHz) δ 23.02 (q), 27.73 (q), 27.89 (q), 34.06 (d), 43.98 (d), 49.93 (t), 51.72 (q), 54.48 (d), 80.78 (s), 82.32 (s), 125.20 (d), 126.94 (d), 128.48 (d), 142.33 (s), 157.08 (s), 170.37 (s), 170.68 (s), 172.58 (s).

2-Iodoadenosine-5'-phosphate **44.** Dry 2-Iodoadenosine **43** (0.017 g, 0.044 mmol) was added to a solution of phosphoryl chloride ($POCl_3$) (0.2 mL, 0.21 mmol), distilled H_2O (0.1 mL, 0.14 mmol), and pyridine (0.2 mL, 0.25 mmol) in dry acetonitrile (0.5 mL, 18.9 mmol) at 0 °C. After stirring at 0° C for 4 hours, the solution was diluted with distilled H_2O (2.5 mL) and stirred at 0° C for a further 1 hour. The reaction mixture was then concentrated and purified by anion exchange HPLC; mobile phase A) distilled H_2O, B) 15% MeOH/H_2O; gradient, 0% B for 8 min., then 50% B in 2 min.; temperature, ambient; flow-rate, 0.5 mL/min. Peak 1 (3.8 min) collected: 0.007 g, 34%; m.p. 210 °C (dec) (SM m.p.=140 °C); IR (neat) υ cm^{-1}; ^1H NMR (CD_3OD, 300 MHz) δ 1.20 (3 H, t, J=7.1 Hz), 1.25 (6 H, t, J=7.1 Hz), 3.45 (2 H, q, J=7.1 Hz), 3.53 (2 H, q, J=7.1 Hz); ^{31}P NMR (CD_3OD, 121.4 MHz) δ 2.69 (s); MS (Neg. Ion Electrospray) *m/e* (relative intensity) 455 (-H_2O) (67), 427 (33), 394, (11), 260 (100).

L-4,4-Difluoroglutamic Acid **65.** DL-N-Acetyl-4,4-difluoroglutamic acid **87** (25 mg, 0.11 mmol) was dissolved in distilled H_2O (2 mL) under nitrogen and the pH was adjusted

to 7.5 with 0.5 M LiOH. Porcine kidney acylase I (4.0 mg) was added and the solution was maintained at 40 °C for 72 hours. Periodic addition of base was required to maintain pH=7.5-8.0, followed by addition of more enzyme (1.0 mg). The reaction was adjusted to pH=5 with 3 M HCl, heated to 60 °C with decolorizing charcoal, and filtered through celite. The filtrate was acidified to pH=1.5 with 3 M HCl and extracted with EtOAc (2 x 30 mL). The aqueous layer was applied to a column of Dowex-50 (H^+) cation exchange resin, and the column was rinsed with H_2O until neutral, then eluted with 1 M ammonia. The ammonia-containing fractions were collected and lypholyzed to give the product as a whitish solid: 0.43 mg, 2.1%; $[\alpha]_D^{22}$ +2.1° (*c*=0.04 g/100 mL, 6M HCl); ^1H NMR (D_2O, 500 MHz) δ 2.58-2.86 (2 H, m), 4.20 (1 H, m); ^{19}F NMR (D_2O, 282.2 MHz) δ -103.24 (dd, *J*=19.2, 14.5 Hz), -103.05 (dd, *J*=19.4, 12.1 Hz).

DL-4,4-Difluoroglutamic Acid **81**. N,N-Diethyl-4-carbethoxy-2,2-difluoro-4-aminobutanamide **85** (0.16 g, 0.58 mmol) was dissolved in 12 M HCl (10 mL) and refluxed at 100° C for 15 hours. The solution was then evaporated to dryness, and the yellow residue was dissolved in H_2O, neutralized with $NaHCO_3$, and purified by chromatography on an anion-exchange resin (BioRad AG1 X8, 20 mL wet volume) with H_2O and 4M HOAc as the eluants. The ninhydrin-positive fractions were collected and lypholyzed to give the product as a whitish solid: 0.11 g, 77%; mp 173-175° C, dec. (lit. 174-176° C, dec.); IR (KBr) υ

3420, 3140, 1710 cm^{-1}; ^1H NMR (D_2O, 300 MHz) δ 2.60-2.90 (2 H, m), 4.24 (1 H, dd, *J*=8.3, 3.9 Hz); ^{13}C NMR (D_2O, 75.4 MHz) δ 34.45 (t, *J*=26.4 Hz), 48.24, 50.57, 116.13 (t, *J*=251.9 Hz), 168.61, 170.89; ^{19}F NMR (D_2O, 282.2 MHz) δ -103.24 (dd, *J*=19.5, 14.6 Hz), -103.05 (dd, *J*=19.5, 12.2 Hz); MS (CI) *m/e* (relative intensity) 184 (9), 166 (100), 120 (12); HRMS exact mass calcd. for $C_5H_8F_2NO_4$ requires (m+1) 184.0421, found 184.0474 (CI).

N,N-Diethyl-4-carbethoxy-2,2-difluoro-3-hydroxy-4-nitro-butanamide **83**. Diethylamine (0.2 mL, 2.7 mmol) was added to a solution of 3-Ethoxy-N,N-diethyl-2,2-difluoro-3-hydroxy-propionamide **90** (0.25 g, 1.1 mmol) in dry THF (10 mL, 112 mmol) at 0° C. After stirring for 10 minutes, the solution was allowed to warm to RT and stirred at ambient temperature for a further 5 hours. The reaction mixture was then cooled to 0° C and diluted with ethyl acetate (15 mL) and poured into a 0.5 M HCl solution (15 mL). The organic layer was separated, and the aqueous layer was extracted with ethyl acetate (20 mL x 3). The combined organic layers were dried with anhydrous $MgSO_4$ and evaporated to give a pale yellow oil which was used without further purification: 0.344 g, 99%; IR (neat) υ 2983, 1758, 1654, 1531, 1349 cm^{-1}; ^1H NMR ($CDCl_3$, 300 MHz) δ 1.18 (3 H, t, *J*=7.1 Hz), 1.23 (3 H, t, *J*=7.1 Hz), 1.34 (3 H, t, *J*=6.8 Hz), 3.36-3.46 (2 H, q, *J*=7.1 Hz), 3.48-3.58 (2 H, q, *J*=7.1 Hz), 4.32 (2 H, q, *J*=6.8 Hz), 5.52 (1 H, d, *J*=6.4 Hz), 5.58 (1 H, d, *J*=7.6 Hz); ^{13}C NMR ($CDCl_3$, 75.4

MHz) δ 12.06, 13.85, 14.02, 41.64 (d, *J*=4.5 Hz), 41.88, 63.19, 70.89, 86.20 (d, *J*=137.9 Hz), 116.63 (t, *J*=268.3 Hz), 161.50, 162.04; ^{19}F NMR ($CDCl_3$, 282.2 MHz) δ -112.92 (dd, *J*=293.0, 14.7 Hz), -105.72 (dd, *J*=293.0, 4.9 Hz); MS (FAB NBA) *m/e* (relative intensity) 313 (100), 265 (7), 180 (26), 137 (82), 120 (13), 107 (22); HRMS exact mass calcd. for $C_{11}H_{19}F_2N_2O_6$ requires 313.1211, found 313.1210 (FAB).

N,N-Diethyl-4-carbethoxy-2,2-difluoro4-nitrobutanamide **84**. Sodium borohydride (0.083 g, 2.2 mmol) was added to a solution of N,N-Diethyl-4-carbethoxy-2,2-difluoro-3-acetoxy-4-nitrobutanamide **91** (0.37 g, 1.1 mmol) in dry THF (10 mL, 112 mmol) at 0° C. The reaction mixture was allowed to warm to RT and stirred at ambient temperature for a further 45 minutes. The reaction mixture was cooled to 0° C and diluted with ethyl acetate (30 mL) and 0.5 M HCl (15 mL) was added. The organic layer was separated, and the aqueous layer was extracted with ethyl acetate (30 mL x 3). The combined organic layers were dried with anhydrous $MgSO_4$ and evaporated to give a pale yellow oil. Purification by column chromatography on silica (eluants: 20% EtOAc/ 40-60 °C petroleum ether) afforded a clear oil: 0.2 g, 64%; IR (neat) υ 2985, 1755, 1659, 1571, 1375, 1273 cm^{-1}; ^1H NMR ($CDCl_3$, 300 MHz) δ1.17 (3 H, t, *J*=7.1 Hz), 1.20 (3 H, t, *J*=7.1 Hz), 1.32 (3 H, t, *J*=7.1 Hz), 3.11-3.35 (2 H, m), 3.38 (2 H, q, *J*=7.1 Hz), 3.50 (2 H, q, *J*=7.1 Hz), 4.32 (2 H, q, *J*=7.1 Hz), 5.54 (1 H, dd, *J*=8.8, 3.9 Hz); ^{13}C NMR ($CDCl_3$, 75.4 MHz) δ 11.95,

13.54, 13.86, 35.40 (t, J=24.7 Hz), 41.32, 41.47, 63.41, 85.50, 117.32 (t, J=258.2 Hz), 160.86 (t, J=28.2 Hz), 163.25; ^{19}F NMR ($CDCl_3$, 282.2 MHz) δ -100.13 (dt, J=288.1, 17.1 Hz), -97.74 (ddd, J=288.1, 19.5, 12.2 Hz); MS (CI) *m/e* (relative intensity) 297 (9), 279 (14), 250 (100); HRMS exact mass calcd. for $C_{11}H_{19}F_2N_2O_5$ requires 297.1262, found 297.1247 (CI).

N,N-Diethyl-4-carbethoxy-2,2-difluoro-4-aminobutanamide **85.** Raney Nickel (wet volume of 1 mL) was added to a solution of N,N-Diethyl-4-carbethoxy-2,2-difluoro-4-nitrobutanamide **84** (0.335 g, 1.1 mmol) in absolute ethanol (6 mL, 110 mmol), and the reaction mixture was stirred under H_2 (40 psi) at ambient temperature for 36 hours. The catalyst was removed by filtration through celite, washed with ethanol, washed with ethyl acetate, and the washings were then evaporated to dryness. Purification by flash column chromatography on alumina (eluants: 50% EtOH/$CHCl_3$) afforded a clear oil: 0.16 g, 52%; IR ($CHCl_3$) υ 3391, 2985, 1735, 1658, 1466, 1384, 1366, 1193 cm^{-1}; ^1H NMR ($CDCl_3$, 300 MHz) δ 1.16 (3 H, t, J=7.1 Hz), 1.21 (3 H, t, J=7.1 Hz), 1.28 (3 H, t, J=7.1 Hz), 2.45 (1 H, dq, J=15.6, 7.8 Hz), 2.79 (1 H, m), 3.38 (2 H, q, J=7.1 Hz), 3.52 (2 H, q, J=7.1 Hz), 3.85 (1 H, m, J=7.8 Hz), 4.20 (2 H, q, J=7.1 Hz); ^{13}C NMR ($CDCl_3$, 75.4 MHz) δ 11.93, 13.79, 14.64, 39.26 (t, J=26.2 Hz), 41.35, 41.56, 49.49, 61.04, 118.70 (t, J=255.8 Hz), 174.01, 205.40; ^{19}F NMR ($CDCl_3$, 282.2 MHz) δ -98.55 (t, J=19.5 Hz), -98.42 (t, J=19.5 Hz); MS (CI)

m/e (relative intensity) 267 (100), 249 (85), 193 (9); HRMS exact mass calcd. for $C_{11}H_{21}F_2N_2O_3$ requires 267.1520, found 267.1480 (CI).

Chloro-N,N-diethyldifluoroacetamide **88**. Diethylamine (1.5 mL, 14.5 mmol) was added to a solution of chlorodifluoroacetic anhydride **87** (2.6 mL, 14.9 mmol) in dry diethyl ether (15 mL, 145 mmol) at 0° C. After stirring for 30 minutes, the solution was allowed to warm to RT and stirred at ambient temperature for a further 6 hours. The mixture was then diluted with diethyl ether and poured into a sat. $NaHCO_3$ solution. The organic layer was separated, and the aqueous layer was extracted with ether (50 mL x 3). The combined organic layers were dried with anhydrous $MgSO_4$ and evaporated to give a pale yellow oil which was used without further purification: 2.77 g, 97%; b.p. 86° C/30 mm Hg; IR (neat) υ 2983, 1689 cm^{-1}; ^1H NMR ($CDCl_3$, 300 MHz) δ 1.20 (3 H, t, *J*=7.1 Hz), 1.25 (6 H, t, *J*=7.1 Hz), 3.45 (2 H, q, *J*=7.1 Hz), 3.53 (2 H, q, *J*=7.1 Hz); ^{13}C NMR ($CDCl_3$, 75.4 MHz) δ 11.32, 13.24, 41.50, 42.09 (t, *J*=3.9 Hz), 118.49 (t, 301.0 Hz), 157.59 (t, 29.1 Hz); ^{19}F NMR ($CDCl_3$, 282.2 MHz) δ -57.60 (s); MS (CI) *m/e* (relative intensity) 187 (12), 185 (49), 172, (21), 170 (72), 143, (12), 141 (42), 100 (100); HRMS exact mass calcd. for $C_6H_{10}ClF_2NO$ requires 185.0419, found 185.0417 (CI).

3-(Dimethylamino)-3-ethoxy-N,N-diethyl-2,2-difluoropropionamide **89**. A solution of diethyl sulfate (2 mL, 15.3 mmol) in

DMF (4 mL, 51.8 mmol) was stirred at 90° C for 2.5 hours. To that solution was added zinc powder (1.32 g, 20.2 mmol) and chloro-N,N-diethyldifluoroacetamide **88** (1.76 g, 9.5 mmol) at 70° C, and the mixture was stirred at that temperature for 4.5 hours. Solution was cooled to RT, filtered to remove the excess zinc, diluted with pentane (30 mL), and poured into a 3M ammonium chloride solution (30 mL). The organic layer was separated, and the aqueous layer was extracted with pentane (30 mL x 3). The combined organic layers were washed with 10% $NaHCO_3$ solution, dried with anhydrous $MgSO_4$, and evaporated. Purification by vacuum distilled afforded a clear oil: 0.4173 g, 24%; b.p. 95° C/5 mm Hg; IR ($CHCl_3$) υ 2990, 1650, 1453, 1210 cm^{-1}; ^1H NMR ($CDCl_3$, 500 MHz) δ 1.15 (3 H, t, J=6.8 Hz), 1.18 (3 H, t, J=6.3 Hz), 1.21 (3 H, t, J=6.8 Hz), 2.55 (6 H, s), 3.25-3.38 (2 H, m), 3.46-3.50 (1 H, m), 3.55 (1 H, dq, J=9.4, 7.1 Hz), 3.62-3.70 (1 H, m), 3.73 (1 H, dq, J=9.4, 7.1 Hz), 4.48 (1 H, dd, J=16.6, 5.3 Hz); ^{13}C NMR ($CDCl_3$, 75.4 MHz) δ 11.80, 14.27, 14.84, 39.67 (2 C, s), 41.83, 42.09 (t, J=3.9 Hz), 65.48, 91.30 (dd, J=28.6, 20.6 Hz), 117.62 (dd, J=268, 254 Hz), 162.97 (t, 27.4 Hz); ^{19}F NMR ($CDCl_3$, 282.2 MHz) δ -114.33 (dd, J=263.7, 17.1 Hz), -105.83 (d, J=263.7 Hz); MS (CI) *m/e* (relative intensity) 253 (14), 207 (84), 102, (100); HRMS exact mass calcd. for $C_{11}H_{23}F_2N_2O_2$ requires 253.1728, found 253.1701 (CI).

3-Ethoxy-N,N-diethyl-2,2-difluoro-3-hydroxypropionamide **90.** To a solution of 3-(Dimethylamino)-3-ethoxy-N,N-diethyl-2,2-

difluoropropionamide **89** (0.377 g, 1.5 mmol) in absolute ethanol (2.5 mL, 42.6 mmol) and water (0.5 mL, 27.7 mmol) was added 3 drops of conc. sulfuric acid, and the mixture was stirred at RT for 35 minutes. After dilution with diethyl ether (30 mL), the reaction mixture was poured into water (30 mL). The organic layer was separated, and the aqueous layer was extracted with Et_2O (30 mL x 3). The combined organic layers were dried with anhydrous $MgSO_4$ and evaporated to give a pale yellow oil which was used without further purification: 0.2494 g, 75%; ^1H NMR ($CDCl_3$, 300 MHz) δ 1.17 (6 H, t, J=7.1 Hz), 1.24 (3 H, t, J=7.1 Hz), 3.26-3.38 (2 H, q, J=7.1 Hz), 3.40-3.53 (2 H, q, J=7.1 Hz), 3.54-3.70 (2 H, dq, J=9.5, 7.1 Hz), 3.93 (1 H, dq, J=9.5, 7.1 Hz); ^{13}C NMR ($CDCl_3$, 75.4 MHz) δ 11.98, 14.18, 14.88, 41.66, 41.85, 64.39, 95.76 (t, J=31.7 Hz), 112.38 (dd, J=264.3, 257.8 Hz), 162.68 (t, 27.2 Hz); ^{19}F NMR ($CDCl_3$, 282.2 MHz) δ -111.43 (2 F, dd, J=459.0, 280.5 Hz) (ethyl hemiaminal), -111.35 (2 F, d, J=4.8 Hz) (hydrate).

N,N-Diethyl-3-acetoxy-4-carbethoxy-2,2-difluoro-4-nitrobutanamide **91**. Acetic anhydride (0.5 mL, 5.3 mmol) was added to a solution of N,N-Diethyl-4-carbethoxy-2,2-difluoro-3-hydroxy-4-nitrobutanamide **83** (0.34 g, 1.1 mmol) in dry dichloromethane (10 mL, 156 mmol) at 0° C. To that solution was added 3 drops of concentrated sulfuric acid, after which the reaction mixture was allowed to warm to RT and stirred at ambient temperature for a further 13 hours. The reaction

mixture was diluted with dichloromethane (30 mL) and poured into distilled H_2O (40 mL). The organic layer was separated, and the aqueous layer was extracted with dichloromethane (25 mL x 2). The combined organic layers were dried with anhydrous $MgSO_4$ and evaporated to give a pale yellow oil which was used without further purification: 0.38 g, 83%; IR (neat) υ 2983, 1755, 1721, 1660, 1531, 1349, 1280 cm^{-1}; ^1H NMR ($CDCl_3$, 300 MHz) δ 1.16 (3 H, t, *J*=7.1 Hz), 1.22 (3 H, t, *J*=7.1 Hz), 1.33 (3 H, t, *J*=7.1 Hz), 2.14 (3 H, s), 3.34-3.44 (2 H, q, *J*=7.1 Hz), 3.45-3.55 (2 H, q, *J*=7.1 Hz), 4.25-4.38 (2 H, q, *J*=7.1 Hz), 5.80 (1 H, dd, *J*=27.8, 6.6 Hz), 6.44 (1 H, dt, *J*=16.1, 6.6 Hz), 6.60 (1 H, ddd, *J*=17.1, 7.8, 4.4); ^{13}C NMR ($CDCl_3$, 75.4 MHz) δ 12.04, 14.06, 13.61, 20.19, 41.66 (d, *J*=8.5 Hz), 41.78, 63.51 (d, 25.6 Hz), 68.23, 85.34 (d, *J*=23.1 Hz), 114.26 (dd, *J*=265.3, 258.2 Hz), 160.18, 161.02, 168.15; ^{19}F NMR ($CDCl_3$, 282.2 MHz) δ -109.27 (dd, *J*=306.3, 18.3 Hz), -105.68 (dd, *J*=306.3, 7.8 Hz); MS (FAB) *m/e* (relative intensity) 355 (100), 313 (38), 295 (34), 180 (21), 137 (67), 120, (9), 107 (17); HRMS exact mass calcd. for $C_{13}H_{21}F_2N_2O_7$ requires 355.1317, found 355.1307 (FAB NBA).

DL-N-Acetyl-4,4-Difluoroglutamic Acid **92.** DL-4,4-Difluoroglutamic acid **81** (0.045 g, 0.25 mmol) was suspended in EtOAc (2 mL, 18.2 mmol) and sonicated for 45 minutes at ambient temperature. Addition of triethylamine (0.1 mL, 0.72 mmol) and acetic anhydride (0.05 mL, 0.40 mmol) was followed by reflux at 80° C for 4 hours. Completion of the reaction

was revealed by TLC and ninhydrin stain. The reaction mixture was then evaporated to dryness to give a yellowish oil which was used without further purification: 0.052 g, 94%; IR ($CHCl_3$) υ 3631, 3429, 3015, 1741, 1664, 1016 cm^{-1}; ^1H NMR (D_2O, 500 MHz) δ 1.95 (3 H, s), 2.25-2.54 (2 H, m), 4.30 (1 H, dd, J=10.3, 3.5 Hz); ^{13}C NMR (D_2O, 75.4 MHz) δ 21.57, 35.84, 49.63, 63.61, 80.35, 117.00, 171.05, 173.04, 179.73; ^{19}F NMR ($CDCl_3$, 282.2 MHz) δ -103.75 (dd, J=15.3, 12.2 Hz), -103.40 (t, J=18.3 Hz); MS (CI) *m/e* (relative intensity) 226 (88), 208 (35), 188 (2), 166 (17), 120 (5), 102. (100); HRMS exact mass calcd. for $C_7H_{10}F_2NO_5$ requires (m+1) 226.0527, found 226.0547 (CI).

Dimethyl (3(S)-(N-benzyloxycarbonyl)amino-2(R,S)-hydroxy-4-carbobutoxybutyl) phosphonate **98**. The N-protected silyl ether **102** (0.09 g, 0.17 mmol) was dissolved in conc. acetic acid (5 mL, 90 mmol) and stirred at RT for 24 hours. The solvent was removed under reduced pressure, and the residue dissolved into EtOAc. The organic layer was washed with H_2O (2 x 20 mL), then dried with anhydrous $MgSO_4$. Removal of the solvent under reduced pressure afforded **98** as an oil:. 0.065g, 92%; ^1H NMR ($CDCl_3$, 300 MHz) δ 1.45 (9 H, s), 1.8-2.5 (2 H, m), 3.6-3.7 (6 H, dd, $3J_{PH}$=10.2 Hz), 3.9-4.7 (2 H, m), 5.1 (2 H, s), 5.9 (1 H, m), 7.25-7.40 (5 H, m); ^{13}C NMR ($CDCl_3$, 75.4 MHz) δ 28.01, 34.52, 52.02, 53.46, 64.83, 67.19, 128.52, 128.65, 128.85, 135.25, 156.68, 172.68; ^{31}P NMR

($CDCl_3$, 121.43 MHz) δ 26.5; MS (FAB) *m/e* (relative intensity) 418 (28), 390 (18), 326 (10), 183 (6), 91 (22).

1-*tert*-Butyl 2(S)-(N-benzyloxycarbonyl)amino-4-oxo-butanoate **99**. Anhydrous pyridine (1.3 mL, 16.1 mmol) was added to dry CH_2Cl_2 (10 mL) under nitrogen. To this colorless solution was added dry CrO_3 (0.76 g, 7.6 mmol) and the resulting solution was allowed to stir at RT for 20 minutes. This orange colored solution was then cooled to 5 °C, and the N-protected ester **101** (0.38 g, 1.26 mmol) was added in one portion with stirring and the resulting solution was allowed to stir for 2 hours at RT. The resulting dark brown/red solution was poured through celite, which was then washed with copious amounts of CH_2Cl_2. The filtrate was concentrated under reduced pressure, the dark brown residue was dissolved in H_2O, and the solution was extracted with Et_2O. The organic layer was washed with 1N HCl (2 x 25 mL), 5% $NaHCO_3$ (1 x 30 mL), H_2O (1 x 30mL), and dried with anhydrous $MgSO_4$. Removal of solvent under reduced pressure gives a yellowish oil. Purification by flash column chromatography (eluant: 40% EtOAc/40-60 °C petroleum ether) gives the product as clear oil (Rf=0.40): 0.12g, 30%. $[\alpha]_D^{20}$ +0.2° (*c*=1.2 g/100 mL, $CHCl_3$); ^1H NMR ($CDCl_3$, 300 MHz) δ 1.4 (9 H, s), 2.90-3.10 (2 H, m, *J*=18.8, 4.9 Hz), 4.50-4.58 (1 H, m, *J*=4.9 Hz), 5.05 (2 H, s), 5.66 (1 H, d, *J*=7.6 Hz), 7.15-7.20 (5 H, m), 9.7 (1 H, s); ^{13}C NMR ($CDCl_3$, 75.4 MHz) δ 27.76, 46.12, 49.65, 67.01, 82.93, 128.04, 128.17, 128.49, 136.09, 140.22, 155.89,

169.49, 199.16; MS (FAB) *m/e* (relative intensity) 308 (10), 252 (27), 120 (8), 91 (100); HRMS exact mass calcd. for $C_{16}H_{22}NO_5$ (m+1) requires 308.1498, found 308.1538 (FAB NBA).

1-*tert*-Butyl 2(S)-(N-benzyloxycarbonyl)amino-butanoate **100.** The N-protected diester **30** (1.34 g, 3.97 mmol) was dissolved in MeOH (30 mL, 742 mmol) with stirring. To this solution 2M NaOH (8 mL, 16 mmol) was added and resulting solution was stirred at RT until reaction was completed, as determined by TLC (1.5 hr). Solution was concentrated, dissolved in H_2O, and extracted with Et_2O (1X). Aqueous layer was acidified with conc. HOAc (pH=3), extracted with EtOAc (3X), and dried with anhydrous $MgSO_4$. Removal of solvent under reduced pressure gives a colorless oil. Purification by flash column chromatography (eluant: 50% EtOAc/40-60 °C petroleum ether) affords the product as clear oil (Rf=0.45): 0.74g, 58%. $[\alpha]_D^{20}$ +16.1° (*c*=7.4 g/100 mL, $CHCl_3$); IR ($CHCl_3$) υ 3433, 3030, 2983, 1721, 1508, 1455, 1396, 1371, 1343, 1228, 1156, 1066, 845 cm^{-1}; ^1H NMR ($CDCl_3$, 300 MHz) δ 1.4 (9 H, s), 2.85-2.9 (2 H, m, *J*=17.3 Hz, *J*=4.0 Hz), 4.52-4.55 (1 H, m, *J*=4.2 Hz), 5.1 (2 H, s), 6.0 (1 H, d, *J*=8.3), 7.3 (5 H, m), 11.3 (1H, s); ^{13}C NMR ($CDCl_3$, 75.4 MHz) δ 27.74, 36.35, 66.86, 82.47, 127.80, 127.86, 128.20, 135.74, 135.85, 156.05, 169.39, 175.72, 176.89; MS (FAB) *m/e* (relative intensity) 324 (9), 268 (43), 224 (15), 184 (8), 91 (100); HRMS exact mass calcd. for $C_{16}H_{22}NO_6$ (m+1) requires 324.1447, found 324.1481 (FAB NBA).

1-*tert*-Butyl 2(S)-(N-benzyloxycarbonyl)amino-4-hydroxybutanoate **101.** The N-protected ester **100** (0.72 g, 2.23 mmol) was dissolved in THF (5 mL, 56 mmol) with stirring and cooled to -15 °C. To this solution N-methylmorpholine (0.25 mL, 2.27 mmol) was added and resulting yellowish solution was stirred for 15 minutes. Ethyl chloroformate (0.25 mL, 2.6 mmol) was then added dropwise, and solution was allowed to stir for a further 15 minutes, after which solid precipitate was removed by filtration. Filtrate was added dropwise to a prepared solution of $NaBH_4$ (0.211 g, 5.58 mmol) in H_2O (10 mL, 556 mmol) at 0 °C. (Observation - solution becomes cloudy white, bubbling occurs) Solution was allowed to stir for 4 hours, after which it was recooled to 0 °C, acidified to pH=2 with 1N HCl, and extracted with EtOAc (3 x 30 mL). The organic layer was washed with H_2O and dried with anhydrous $MgSO_4$. Removal of solvent under reduced pressure gives a colorless oil. Purification by flash column chromatography (eluant: 5% isopropanol/$CHCl_3$) gives the product as clear oil (Rf=0.65): 0.40g, 59%. $[\alpha]_D^{20}$ +2.45° (*c*=4.0 g/100 mL, $CHCl_3$); IR ($CHCl_3$) υ 3422, 3030, 3012, 1725, 1706, 1511, 1370, 1349, 1312, 1227, 1156, 1051, 843 cm^{-1}; ^1H NMR ($CDCl_3$, 300 MHz) δ 1.2 (9 H, s), 1.6 (1 H, m), 2.05 (1 H, m), 2.8-3.5 (1 H, br s), 3.5-3.7 (2 H, m), 4.25-4.45 (1 H, m), 5.05 (2 H, s), 5.8 (1 H, d, *J*=7.1 Hz), 7.15-7.20 (5 H, m); ^{13}C NMR ($CDCl_3$, 75.4 MHz) δ 27.74, 35.66, 51.62, 58.21, 66.99, 82.23, 127.97, 128.06, 128.38, 136.01, 156.72, 171.52; MS (FAB) *m/e* (relative intensity) 310 (7), 254 (31), 210 (34), 91 (100);

HRMS exact mass calcd. for $C_{16}H_{24}NO_5$ (m+1) requires 310.1654, found 310.1671 (FAB NBA).

Dimethyl (3(S)-(N-benzyloxycarbonyl)amino-2(R,S)-(trimethylsilyloxy)-4-carbobutoxybutyl) phosphonate **102.** The N-protected aldehydic ester **99** (0.114 g, 0.37 mmol) was dissolved in dry benzene (5 mL, 56 mmol). To this solution dimethyl trimethylsilylphosphite (0.12 mL, 0.62 mmol) was added, and resulting solution was refluxed at 85 °C for 1.5 hour. The solution was removed from heat, and allowed to stir for additional 2 hours at RT. The mixture was extracted with H_2O, washed with an aqueous saturated NaCl solution, and dried with anhydrous $MgSO_4$. Removal of solvent under reduced pressure gives a colorless oil as the crude product. Purification by flash column chromatography (eluant: 40% EtOAc/Hexanes) gives the product as clear oil: 0.10g, 56%; IR ($CHCl_3$) υ 3620, 3019, 2400, 1725, 1706, 1522, 1476, 1422, 1219, 1046, 752 cm^{-1}; ^1H NMR ($CDCl_3$, 300 MHz) δ 0.1 (9 H, s), 1.4 (9 H, s), 1.7-2.2 (2 H, m), 3.7-3.9 (8 H (3+3+2), m), 3.9-4.6 (2 H, m), 5.1 (2 H, s), 5.5 (1 H, d), 7.15-7.20 (5 H, m); ^{13}C NMR ($CDCl_3$, 75.4 MHz) δ 0.08, 27.97, 34.54, 51.79, 53.16, 64.72, 67.00, 82.20, 128.06, 128.37, 128.43, 135.00, 156.19, 171.27; ^{31}P NMR ($CDCl_3$, 121.43 MHz) δ 25.57, 25.77; MS (FAB) *m/e* (relative intensity) 490 (34), 434 (100), 390 (11), 326 (10), 183 (6), 137 (11), 91 (22); HRMS exact mass calcd. for $C_{21}H_{37}NO_8PSi$ (m+1) requires 490.2026, found 490.1933 (FAB NBA).

N-Benzyl-methoxy-(3(S)-(N-benzyloxycarbonyl)amino-4-carbethoxybutyl) phosphonamidate **103.** Distilled benzyl amine (0.15 mL, 1.37 mmol) was dissolved in THF and cooled to 0 °C under a N_2 atmosphere. Triethylamine (0.5 mL, 3.6 mmol) was added to the reaction, followed immediately by the dropwise addition by cannula of solution of methyl (3(S)-(N-benzyloxycarbonyl)amino-4-carbethoxybutyl) phosphonochloridate **104** (0.517 g, 1.37 mmol) dissolved in THF (15 mL, 168 mmol) under N_2. The resulting solution was allowed to warm to RT and stirred overnight. The $Et_3N{\cdot}HCl$ precipitate was removed by filtration, and the filtrate was concentrated in vacuo. The oily residue was dissolved in EtOAc and washed successively with aqueous 5% $NaHCO_3$ (1 x 30 mL), aqueous 5% $KHSO_4$ (1 x 30 mL), aqueous saturated NaCl (1 x 25 mL), and dried with anhydrous $MgSO_4$. Removal of solvent under reduced pressure afforded a yellowish oil which was purified by column chromatography on alumina (eluants: 10% EtOH/$CHCl_3$) to give white oil: 0.365g, 60%. ^1H NMR (CD_3OD, 500 MHz) δ 1.20 (3 H, m), 1.30-1.6 (2 H, m), 1.8-2.2 (2 H, m), 3.05 (2H, d), 3.6 (3 H, d, $^3J_{PH}$=10.8 Hz), 4.05 (2 H, m), 4.2 (1 H, m), 4.8 (2 H, s), 5.05 (2 H, s), 7.05-7.50 (10 H, m), 7.8 (1 H, s); ^{13}C NMR (CD_3OD, 75.4 MHz) δ 14.50, 26.82, 35.73 (d, *J*=125 Hz), 45.18, 51.27, 55.58 (d, *J*=17 Hz), 62.33, 67.56, 79.35 (d, *J*=6 Hz), 127.60, 128.05, 128.35, 128.64, 128.92, 129.07, 129.36, 129.41, 133.32, 137.95, 158.35, 173.09; ^{31}P NMR ($CDCl_3/CD_3OD$ 121.43 MHz) δ 34.36, 38.00; MS (FAB) *m/e* (relative intensity) 450 (6) (m+2), 449 (8), 276 (43), 200

(15), 136 (16), 109 (15), 91 (100); HRMS exact mass calcd. for $C_{22}H_{30}N_2O_6P$ (m+1) requires 449.1841, found 449.1852 (FAB NBA).

Methyl (3(S)-(N-benzyloxycarbonyl)amino-4-carbethoxybutyl) phosphonochloridate **104**. Oxalyl chloride (2.0 M in CH_2Cl_2) (0.7 mL, 1.4 mmol) was added dropwise to a solution of methyl (3(S)-(N-benzyloxycarbonyl)amino-4-carbethoxybutyl) phosphonic acid **110** (0.308 g, 0.86 mmol) and DMF (0.65 M in CH_2Cl_2) (0.07 mL, 0.045 mmol) dissolved in CH_2Cl_2 (5.0 mL, 78 mmol) at 0 °C under a nitrogen atmosphere. The solution was stirred at 0 °C for 20 min and then warmed to RT and stirred for a further 80 min. The reaction was concentrated, dissolved in toluene (2 mL), and then reconcentrated in vacuo to remove the volatile reagents. Yellowish oil was used immediately in the subsequent reaction without further purification. ^1H NMR ($CDCl_3$, 500 MHz) δ 1.30 (3 H, t, J=6.4 Hz), 2.05-2.38 (4 H, m), 3.90 (3 H, d, $^3J_{PH}$=11.8 Hz), 4.25 (2 H, q, J=6.4 Hz), 4.45 (1 H, m), 5.10 (2 H, s), 5.40-5.50 (1 H, br s), 7.20-7.35 (5 H, m); ^{31}P NMR ($CDCl_3$ 121.43 MHz) δ 42.3.

Dimethyl (3(S)-(N-benzyloxycarbonyl)amino-4-carbethoxybutyl) phosphonate **105**. 1-Ethyl 2(S)-(N-Benzyloxylcarbonyl)amino-4-bromobutanoate **106** (1.9 g, 5.7 mmol) was dissolved in trimethylphosphite (20 mL, 181 mmol) under an argon atmosphere, and the resulting solution was refluxed for 5 days. The reflux condensor was flushed continuously with

water at 50 °C, and an argon stream was maintained to remove the side product, methyl bromide, (bp=4 °C). Reaction was concentrated in vacuo, and immediately purified by column chromatography on silica (eluants: 1:1 EtOAc/$CHCl_3$, 9:9:2 EtOAc/$CHCl_3$/MeOH) to afford a yellowish oil: 1.914g, 92%. IR (KBr) υ 3156, 2958, 1725, 1574, 1379, 1096 cm^{-1}; ^1H NMR ($CDCl_3$, 500 MHz) δ 1.25-1.28 (3 H, m, *J*=7.8 Hz), 1.76-1.88 (2H, m, *J*=4.4, 11.8 Hz), 1.90-2.00 (1 H, m, *J*=4.9 Hz), 2.1-2.21 (1 H, m, *J*=5.9 Hz), 3.68-3.74 (6 H, dd, $^3J_{PH}$=11 Hz), 4.16-4.22 (2 H, q, *J*=6.8 Hz), 4.33-4.38 (1 H, m, *J*=4.9 Hz), 5.1 (2 H, s), 6.05 (1 H, d, *J*=8.3 Hz), 7.25-7.4 (5 H, m); ^{13}C NMR ($CDCl_3$, 75.4 MHz) δ 13.31, 20.06 (d, *J*=143 Hz), 24.23, 51.32 (5.5 Hz), 53.46 (d, 18 Hz), 60.56, 77.19, 127.22, 127.44, 127.62, 135.80, 155.67, 170.90; ^{31}P NMR ($CDCl_3$, 121.43 MHz) δ 34.16; MS (FAB) *m/e* (relative intensity) 374 (100), 330 (14), 300 (3), 256 (7), 167 (8), 146 (5), 91 (72); HRMS exact mass calcd. for $C_{16}H_{25}NO_7P$ (m+1) requires 374.1369, found 374.1369 (FAB NBA).

Methyl (3(S)-(N-benzyloxycarbonyl)amino-4-carbethoxybutyl) phosphonate, *tert*-butyl amine salt **105a**. Dimethyl (3-(S)-(N-(benzyloxycarbonyl)amino-4-carbethoxybutyl) phosphonate **105** (1.9 g, 6.5 mmol) was dissolved in distilled *tert*-butyl amine (10 mL, 95 mmol) under a nitrogen atmosphere, and the resulting solution was refluxed for 4 days. The reaction mixture was concentrated to provide product salt as a white solid: 1.13g, 99%. $[\alpha]_D^{20}$ -34.3° (*c*=8.6 g/100 mL, $CHCl_3$); IR

($CHCl_3$) υ 3500-2400, 1702, 1522, 1214, 1049 cm^{-1}; ^1H NMR ($CDCl_3$, 300 MHz) δ 1.20 (3 H, t), 1.25 (9 H, s), 1.5-1.95 (3 H, m), 1.95-2.2 (1 H, m), 3.51-3.58 (3 H, d, $^3J_{PH}$=11 Hz), 4.18-4.26 (1 H, m, J=7 Hz), 4.40-4.48 (1 H, m), 4.9-5.2 (2 H, m, J=11, 17 Hz), 6.88-6.95 (1 H, d, J=7.6 Hz), 7.2 (5 H, m), 7.8-7.95 (1 H, br s); ^{13}C NMR ($CDCl_3$, 75.4 MHz) δ 14.04, 22.07 (d, J=130 Hz), 26.50, 28.35, 50.05, 51.46, 54.42, 61.06, 66.58, 127.93, 128.08, 128.29, 136.45, 156.31, 172.19; ^{31}P NMR ($CDCl_3$, 121.43 MHz) δ 24.71; MS (FAB) *m/e* (relative intensity) 433 (7), 360 (15), 135 (6), 91 (37), 74 (100); HRMS exact mass calcd. for $C_{19}H_{34}N_2O_7P$ (m+1) requires 433.2103, found 433.1119 (FAB NBA).

1-Ethyl 2(S)-(N-Benzyloxylcarbonyl)amino-4-bromobutanoate **106**. The N-protected ester **109** (4.84 g, 15.64 mmol) was dissolved in dry CH_2Cl_2 (30 mL, 470 mmol) under dry argon at RT with stirring. After addition of triethylamine (2.8 mL, 20 mmol), the solution was covered with aluminum foil to shield from light and stirred for a further 10 minutes at RT. Addition of 1-oxa-2-oxo-3-thiaindolizinium chloride (3.22 g, 16.95 mmol) was followed by stirring for a further 15 minutes. The solution was diluted with bromotrichloromethane (70 mL, 710 mmol), the foil was removed, and the solution was irradiated with 150W flood lamp while stirring for 20 minutes. The cloudy yellow solution was observed to slowly became more orange in color and clear as reaction progressed. The solution was filtered, and the filtrate was concentrated

to give an oil. Purification by flash column chromatography (eluants: 100% hexane, 50% hexane/CH_2Cl_2, 100% CH_2Cl_2) (TLC R_f=0.6) afforded an oil: 2.004g, 38%. $[\alpha]_D^{20}$ +8.2° (*c*=2.4 g/100 mL, $CHCl_3$) (lit. $[\alpha]_D^{21}$ -33° (c=6.8, abs. MeOH)[2]; IR ($CHCl_3$) υ 3428, 3033, 1723, 1510, 1342, 1227, 698 cm^{-1}; ^1H NMR ($CDCl_3$, 300 MHz) δ 1.22-1.26 (3 H, m, *J*=7.1 Hz), 2.14-2.26 (1 H, m, *J*=7.3 Hz), 2.33-2.42 (1 H, m, *J*=7.8 Hz), 3.36-3.42 (2 H, m, 6.8 Hz), 4.13-4.4.22 (2 H, q, *J*=7.1 Hz), 4.42-4.50 (1 H, m, *J*=5.6 Hz), 5.05 (2 H, s), 5.82-5.88 (1 H, d, *J*=8.1 Hz), 7.3 (5 H, s); ^{13}C NMR ($CDCl_3$, 75.4 MHz) δ 13.84, 28.14, 35.15, 52.70, 61.51, 66.77, 127.81, 127.90, 128.23, 135.95, 155.83, 171.32; MS (FAB) *m/e* (relative intensity) 344 (38), 302 (15), 274 (3), 137 (95), 91 (100); HRMS exact mass calcd. for $C_{14}H_{19}BrNO_4$ (m+1) requires 344.0498, found 344.0484 (FAB NBA).

3((S)-N-Benzyloxycarbonyl-5'-oxo-4'-oxazolidine)propanoic acid **108**. A mixture of N-benzyloxycarbonyl-L-glutamic acid **107** (10.2 g, 36.4 mmol), p-formaldehyde (2.19 g, 73 mmol), and p-toluenesulfonic acid (0.4 g, 2.3 mmol) were dissolved in dry benzene (220 mL, 2480 mmol) under a nitrogen atmosphere. The resulting solution was refluxed at 90 °C and water was removed duting the course of the reaction with a Dean-Stark trap. After 2 hours, the solution was concentrated to roughly 1/3 volume, dissolved in EtOAc (50 mL), and extracted with aqueous 5% $NaHCO_3$ (1 x 30 mL) and H_2O (3 x 25 mL). After drying with anhydrous $MgSO_4$, solvent was removed under reduced pressure to afford a colorless oil,

which was used without further purification: 9.34 g, 88%. IR (neat) υ 3500-3000, 3034, 2926, 1800, 1713, 1499, 1417, 1359, 1245, 1214, 1168, 1132, 1054, 751, 698 cm^{-1}; ^1H NMR ($CDCl_3$, 300 MHz) δ 2.15-2.25 (1 H, m, *J*=7.1 Hz), 2.25-2.35 (1 H, m, *J*=7.1 Hz), 2.45-2.57 (2 H, m), 4.38-4.44 (1 H, m, *J*=5.62 Hz), 5.18 (2 H, s), 5.22-5.24 (2 H, d, *J*=4.64 Hz), 5.50-5.58 (1 H, br s), 7.30-7.40 (5 H, m); ^{13}C NMR ($CDCl_3$, 75.4 MHz) δ 25.72, 29.02, 53.92, 68.25, 77.83, 128.39, 128.70, 128.72, 135.13, 155.6, 166.8, 177.25; MS (FAB) *m/e* (relative intensity) 294 (22), 250 (22), 138 (13), 107 (14), 91 (100); HRMS exact mass calcd. for $C_{14}H_{16}NO_6$ (m+1) requires 294.0978, found 294.0973 (FAB NBA).

1-Ethyl 2(S)-(N-benzyloxycarbonyl)aminopentanoate **109**. The N-protected 5-oxazolidinone **108** (1.9 g, 6.5 mmol) was dissolved in absolute EtOH (130 mL, 2220 mmol) under a nitrogen atmosphere and the resulting solution was cooled to 0 °C. Dropwise addition of NaOEt (3.3M) (4.0 mL, 13.2 mmol) over 20 minutes formed a clear solution which was stirred at 0 °C for a further 100 minutes. Solution was removed from cooling bath and H_2O was added immediately, followed by EtOAc. The solution was acidified with 3N HCl (pH1), then concentrated under reduced pressure without heat. The resulting oil was dissolved in EtOAc, extracted with H_2O (1 x 30 mL), aqueous saturated NaCl solution (1 x 25 mL), and dried with anhydrous $MgSO_4$. Removal of solvent under reduced pressure afforded a yellowish oil. Purification by flash

column chromatography (eluant: 10% EtOH/$CHCl_3$) afforded a white oil: 1.73g, 87%. IR (KBr) υ 3327, 2982, 1732, 1715, 1694, 1682, 1538, 1505, 1455, 1416, 1212, 1056, 781, 698 cm^{-1}; ^1H NMR ($CDCl_3$, 300 MHz) δ 1.20 (3 H, m, *J*=7.1 Hz), 1.90-2.02 (1 H, m, *J*=8.1 Hz), 2.1-2.25 (1 H, m, *J*=7.8 Hz), 2.3-2.5 (2 H, m), 4.12-4.20 (2 H, q, *J*=7.1 Hz), 4.34-4.42 (1 H, m, *J*=5.1 Hz), 5.05 (2H, s), 6.0 (1 H, d, *J*=8.3 Hz), 7.2-7.3 (5 H, m), 8.8 (1 H, br s); ^{13}C NMR ($CDCl_3$, 75.4 MHz) δ 13.67, 26.90, 29.63, 53.03, 61.38, 66.71, 127.69, 127.80, 128.14, 135.86, 156.02, 171.88, 176.57; MS (FAB) *m/e* (relative intensity) 310 (40), 266 (31), 107 (8), 91 (100); HRMS exact mass calcd. for $C_{15}H_{20}NO_6$ (m+1) requires 310.1291, found 310.1422 (FAB NBA).

Methyl (3(S)-(N-benzyloxycarbonyl)amino-4-carbethoxybutyl) phosphonic acid **110.** The *tert*-butyl amine salt **105a** (1.13 g, 2.61 mmol) was dissolved in $CHCl_3$ and treated with washed cation exchange resin (Dowex 50W-X8 (H^+ form) 200-400 mesh, 10 g (dry)). After stirring for 2 hours, the resin was removed by filtration, and the filtrate was concentrated in vacuo to afford the product as an oil: 0.922g, 94%. $[\alpha]_D^{20}$ +7.5° (*c*=9.21 g/100 mL, $CHCl_3$); IR (KBr) υ 3428, 3020, 1720, 1508, 1220, 1050, 928 cm^{-1}; ^1H NMR ($CDCl_3$, 300 MHz) δ 1.20 (3 H, t, *J*=7 Hz), 1.68-2.05 (3 H, m), 2.10-2.20 (1 H, m), 3.61-3.68 (3 H, d, $^3J_{PH}$=11 Hz), 4.10-4.18 (1 H, m, *J*=7 Hz), 4.30-4.38 (1 H, m), 5.05 (2 H, s), 5.8-6.0 (1 H, br s), 7.25 (5 H, m), 11.8-12.5 (1 H, br s); ^{13}C NMR ($CDCl_3$, 75.4 MHz) δ 13.85,

21.27 (d, *J*=140 Hz), 25.24, 51.55 (d, *J*=7 Hz), 53.85 (d, *J*=20 Hz), 61.44, 66.77, 77.20, 127.82, 127.92, 128.26, 136.03, 155.87, 171.33; ^{31}P NMR ($CDCl_3$, 121.43 MHz) δ 34.19; MS (FAB) *m/e* (relative intensity) 360 (40), 136 (100), 107 (8), 91 (100); HRMS exact mass calcd. for $C_{15}H_{23}NO_7P$ (m+1) requires 360.1212, found 360.1212 (FAB NBA).

Diethyl 2(S)-N-[methoxy-(3'(S)-(N-benzyloxycarbonyl)amino-4'-carbethoxybutyl)phosphinyl]aminopentan-1,5-dioate **111**. L-glutamic acid hydrochloride, diethyl ester (0.118 g, 0.50 mmol) was dissolved in THF and cooled to 0 °C under a nitrogen atmosphere. Triethylamine (0.2 mL, 1.4 mmol) was added to the reaction, followed immediately by the dropwise addition by cannula of solution of methyl (3(S)-(N-benzyloxycarbonyl)amino-4-carbethoxybutyl) phosphonochloridate **104** (0.324 g, 0.86 mmol) dissolved in THF (30 mL, 224 mmol) under a nitrogen atmosphere. After stirring at 0 °C for 20 minutes, the resulting solution was allowed to warm to RT and stirred overnight. The $Et_3N{\cdot}HCl$ precipitate was removed by filtration, and the filtrate was concentrated in vacuo. The oily residue was dissolved in EtOAc and washed successively with aqueous 5% $NaHCO_3$ (1 x 30 mL), aqueous 5% $KHSO_4$ (1 x 30 mL), aqueous saturated NaCl (1 x 25 mL), and dried with anhydrous $MgSO_4$. Removal of solvent under reduced pressure afforded a yellowish oil: 0.03g, 11%. ^1H NMR ($CDCl_3$, 300 MHz) δ 1.15-1.35 (9 H, m), 2.35-2.45 (2 H, m), 3.12 (1 H, t), 3.64 (3 H, d), 3.85-4.00 (1 H, m), 4.05-4.25

(6 H, m), 4.35-4.45 (1 H, m), 5.11 (2 H, s), 5.61 (1 H, d), 7.35 (5 H, m).

N-Methyl-methoxy-(3(S)-(N-benzyloxycarbonyl)amino-4-carbethoxybutyl) phosphonamidate **112**. Methyl amine (2.0 M in THF) (0.45 mL, 0.9 mmol) was cooled to 0 °C under a nitrogen atmosphere. Triethylamine (0.24 mL, 1.72 mmol) was added to the reaction, followed immediately by the dropwise addition by cannula of solution of methyl (3(S)-(N-benzyloxycarbonyl)amino-4-carbethoxybutyl)phosphonochloridate **104** (0.324 g, 0.86 mmol) dissolved in THF (20 mL, 224 mmol) under N_2. The resulting solution was allowed to warm to RT and stirred overnight. The $Et_3N{\cdot}HCl$ precipitate was removed by filtration, and the filtrate was concentrated in vacuo. The oily residue was dissolved in EtOAc and washed successively with aqueous 5% $NaHCO_3$ (1 x 30 mL), aqueous 5% $KHSO_4$ (1 x 30 mL), aqueous saturated NaCl (1 x 25 mL), and dried with anhydrous $MgSO_4$. Removal of solvent under reduced pressure afforded a yellowish oil which was purified by column chromatography on alumina (eluants: 10% EtOH/$CHCl_3$) to give a white oil: 0.130g, 42%. ^1H NMR ($CDCl_3$, 300 MHz) δ 1.18-1.21 (3 H, d), 1.22-1.32 (2 H, m), 1.4-2.1 (2 H, m), 2.48-2.58 (3 H, m), 3.6-3.65 (3 H, dd, $^3J_{PH}$=10, 4 Hz), 4.3-4.4 (1 H, m), 5.1 (2 H, s), 6.00-6.05 (1 H, m, J=6.6 Hz), 7.20-7.40 (5 H, m), 7.6 (1 H, br s); ^{13}C NMR ($CDCl_3$, 75.4 MHz) δ 14.04, 26.85, 28.46, 33.93 (d, J=63 Hz), 51.07, 59.04, 63.71, 66.80, 126.53, 127.96, 128.36, 129.61, 132.24, 156.07, 171.71; ^{31}P

NMR ($CDCl_3$ 121.43 MHz) δ 33.32, 36.17; MS (FAB) *m/e* (relative intensity) 373 (7), 307 (28), 200 (9), 136 (66), 107 (22), 91 (100); HRMS exact mass calcd. for $C_{16}H_{26}N_2O_6P$ (m+1) requires 373.1529, found 373.1525 (FAB NBA).

Dimethyl (2(S)-(N-benzyloxycarbonyl)amino-3-carbomethoxypropyl) phosphonate **117**. Solid 2(S)-(N-benzyloxycarbonyl) amino-3-hydroxypropanoic acid lactone **119** (0.31 g, 1.4 mmol) was refluxed in trimethylphosphite (5 mL, 42.4 mmol) at 70 °C for 72 hours. Removal of excess trimethylphosphite under reduced pressure gave a clear oil. Purification by flash column chromatography (eluant: 5% isopropanol/$CHCl_3$) (Rf=0.35) afforded a clear oil: 0.417 g, 87%; $[\alpha]_D^{20}$ +9.4° (*c*=4.2 g/100 mL, $CHCl_3$); IR (KBr) υ 3431, 3009, 1749, 1721, 1511, 1455, 1345, 1248, 1039, 853 cm^{-1}; ^1H NMR ($CDCl_3$, 300 MHz) δ 2.35-2.45 (2 H, m), 3.67 (3 H, d, $^3J_{PH}$=11.1 Hz), 3.75 (3 H, d, $^3J_{PH}$=11.2 Hz), 4.5-4.7 (1 H, dq, *J*=19.5, 6.4 Hz), 5.15 (2 H, s), 6.15 (1 H, d, *J*=8.3 Hz), 7.30-7.4 (5 H, m); ^{13}C NMR ($CDCl_3$, 75.4 MHz) δ 25.79, 27.66, 49.11, 51.87, 52.55, 66.77, 127.85, 127.93, 128.25, 136.04, 155.60, 170.79, 170.92; ^{31}P NMR ($CDCl_3$ 121.43 MHz) δ 29.99; MS (FAB) *m/e* (relative intensity) 346 (70), 302 (19), 91 (100); HRMS exact mass calcd. for $C_{14}H_{21}NO_7P$ requires 346.1056, found 346.1064 (FAB NBA).

Dimethyl (2(S)-(N-benzyloxycarbonyl)amino-3-carboxypropyl) phosphonate. Methyl 2-(S)-(N-(benzyloxycarbonyl) amino)-3-(dimethylphosphono)propanoate **117** (0.417 g, 1.21 mmol) was

dissolved in distilled H_2O (25 mL, 1389 mmol) at 0 °C. After dropwise addition of 2M NaOH (1.3 mL, 2.6 mmol), solution was allowed to stir for a further 10 at 0 °C, and then stirred at RT until no more starting material was observed by TLC (1:9 MeOH/$CHCl_3$) (approx. 100 min). Solution was washed with $CHCl_3$, acidified to pH=1 with 3M HCl, extracted into $CHCl_3$, and dried with anhydrous magnesium sulfate. Removal of solvent under reduced pressure yielded a clear oil: 0.235 g, 59%; $[\alpha]_D^{20}$ +37.6° (*c*=2.354 g/100 mL, $CHCl_3$) IR (KBr) υ 3423, 3020, 1719, 1510, 1421, 1215, 1043, 762 cm^{-1}; ^1H NMR ($CDCl_3$, 300 MHz) δ 2.40-2.6 (2 H, m), 3.62-3.65 (3 H, d, *J*=11 Hz), 3.65-3.72 (3 H, d, *J*=11 Hz), 4.5-4.65 (1 H, m, *J*=6 Hz), 5.03-5.18 (2 H, m, *J*=12 Hz), 6.16 (1 H, d, *J*=7.3 Hz), 7.25-7.4 (5 H, m), 9.4 (1 H, br s); ^{13}C NMR ($CDCl_3$, 75.4 MHz) δ 25.89, 27.79, 49.19, 52.86, 66.89, 77.19, 127.97, 128.05, 128.40, 136.19, 155.19, 171.76, 171.87; ^{31}P NMR ($CDCl_3$ 121.43 MHz) δ 31.14; MS (FAB) *m/e* (relative intensity) 332 (80), 288 (40), 107 (32), 91 (100); HRMS exact mass calcd. for $C_{13}H_{19}NO_7P$ (m+1) requires 332.0899, found 332.0923 (FAB NBA).

2(S)-(N-benzyloxycarbonyl)amino-3-hydroxypropanoic acid lactone **119**. Triphenylphosphine (1.8 g, 7.2 mmol) was dissolved in tetrahydrofuran (45 mL, 553 mmol) under a nitrogen atmosphere. The reaction flask was cooled to -78 °C and dimethyl azodicarboxylate (1.0 mL, 7.53 mmol) was added dropwise. Dropwise addition of 2(S)-(N-benzyloxycarbonyl) amino-3-hydroxypropanoic acid **121** (1.70 g, 7.12 mmol)

dissolved in THF to this mixture was followed by stirring at -78 °C for 0.5 hr, followed by stirring at RT for 6 hours. Removal of solvent under reduced pressure gives a pale yellow solid. Purification by flash column chromatography (eluant: 60% EtOAc/40-60 °C petroleum ether) afforded a white solid: 0.7 g, 45%; mp 136-137 °C; IR (KBr) υ 3366, 1846, 1687, 1533, 1267, 1110, 1019, 884, 754 cm^{-1}; ^1H NMR (Acetone-d_6, 300 MHz) δ 4.40-4.52 (2 H, m), 5.1 (2 H, s), 5.25-5.35 (1 H, m), 7.26-7.4 (5 H, m); ^{13}C NMR (Acetone-d_6, 75.4 MHz) δ 60.41, 66.4, 67.32, 128.60, 128.77, 128.80, 129.17, 137.38, 156.34, 170.37; MS (EI) *m/e* (relative intensity) 177 (4); HRMS exact mass calcd. for $C_{11}H_{11}NO_4$ requires 221.2126, found 221.0688 (EI butane).

2(S)-(N-benzyloxycarbonyl)amino-3-hydroxypropanoic acid **121.** Solid L-serine (10.8 g, 103 mmol) was dissolved in a mixture of H_2O (170 mL, 9440 mmol) and Et_2O (80 mL, 772 mmol) with stirring. Magnesium oxide (10.0 g, 248 mmol) was added to mixture and flask was cooled to 0 °C. Benzyl chloroformate (21 mL, 147 mmol) was added dropwise over a period of 15 minutes. Mixture stirred in bath for 4 hours and then stirred at RT overnight. Workup involved removal of excess MgO by gravity filtration followed by extraction of aqueous solution twice with Et_2O. Aqueous layer was acidified with 3M HCl (pH1) with 3M HCl, extracted with EtOAc (3 x 40 mL), and the organic layer was dried with $MgSO_4$. Removal of solvent under reduced pressure afforded a white solid. The

product was obtained as a pale white solid after recrystallization from EtOAc/hexane: 18.6 g, 76%; mp 116-118 °C (lit. 119 °C); IR (KBr) υ 3337, 3329, 1747, 1691, 1534, 1305, 1247, 1208, 1060, 1029, 749, 697 cm^{-1}; ^1H NMR (DMSO-d_6, 300 MHz) δ 3.2-3.4 (1 H, br s), 3.65 (2 H, d), 4.0 (1 H, m), 5.05 (2 H, s), 7.25-7.40 (5 H, m), 12.6-12.8 (1H, br s); MS (FAB) *m/e* (relative intensity) 240 (95), 196 (35), 153 (100), 136 (79), 91 (100); HRMS exact mass calcd. for $C_{11}H_{14}NO_5$ (m+1) requires 240.0872, found 240.0893 (FAB NBA).

N-Benzyl-methoxy-(2(S)-(N-benzyloxycarbonyl)amino-3-carbobenzoxypropyl) phosphonamidate **123.** Distilled benzyl amine (0.015 mL, 0.14 mmol) was dissolved in THF and cooled to 0 °C under a N_2 atmosphere. Triethylamine (0.3 mL, 11 mmol) was added to the reaction flask, followed immediately by the dropwise addition by cannula of solution of methyl (2(S)-(N-benzyloxycarbonyl)amino-3-carbobenzoxypropyl) phosphonochloridate **130** (0.05 g, 0.11 mmol) dissolved in THF (15 mL, 168 mmol) under N_2. The resulting solution was allowed to warm to RT and stirred overnight. The $Et_3N{\cdot}HCl$ precipitate was removed by filtration, and the filtrate was concentrated in vacuo. The oily residue was dissolved in EtOAc and washed successively with aqueous 5% $NaHCO_3$ (1 x 30 mL), aqueous 5% $KHSO_4$ (1 x 30 mL), aqueous saturated NaCl (1 x 25 mL), and dried with anhydrous $MgSO_4$. Removal of solvent under reduced pressure afforded a yellowish oil which was purified by column chromatography on alumina (eluants: 10% EtOH/$CHCl_3$)

to give an oil: 0.03 g, 52%. IR ($CHCl_3$) υ 3402, 3032, 1717, 1679, 1510, 1455, 1405, 1326, 1260, 1024, 909 cm^{-1}; ^1H NMR ($CDCl_3$, 500 MHz) δ 2.2-2.4 (2 H, m), 3.6 (3 H, d, $^3J_{PH}$=10.8 Hz), 4.05 (2 H, m), 4.4 (1 H, m), 5.05 (2 H, s), 5.10 (2 H, s), 6.25 (1 H, br s), 7.1-7.2 (10 H, m), 7.8 (1 H, s); ^{13}C NMR (CD_3OD, 75.4 MHz) δ 29.70, 31.08, 43.72 (d, J=9.2 Hz), 44.61 (d, J=9.2 Hz), 50.00, 50.41, 51.35, 62.70, 65.98, 67.12, 127.26, 127.46, 127.64, 127.73, 127.85, 128.08, 128.22, 128.52, 128.66, 128.82, 128.98, 136.06, 137.89, 156.07, 159.62, 170.10; ^{31}P NMR ($CDCl_3/CD_3OD$ 121.43 MHz) δ 33.17, 33.97; MS (FAB) *m/e* (relative intensity) 496 (8), 389 (13), 290 (9), 137 (100), 91 (60); HRMS exact mass calcd. for $C_{26}H_{29}N_2O_6P$ (m+1) requires 496.1763, found 496.1851 (FAB NBA).

Dimethyl (2(S)-(N-benzyloxycarbonyl)amino-3-carbobenzoxypropyl) phosphonate **124**. Solid benzyl 2(S)-N-(benzyloxycarbonyl)amino)-3-bromopropionate **125** (0.31 g, 1.4 mmol) was refluxed in trimethylphosphite (5 mL, 42.4 mmol) under an argon atmosphere at 70 °C for 72 hours. Removal of excess trimethylphosphite under reduced pressure gave a clear oil. Purification by flash column chromatography (eluant: 5% isopropanol/$CHCl_3$) (Rf=0.65) afforded a clear oil: 0.112 g, 96%; IR (KBr) υ 3430, 3015, 1750, 1720, 1515, 1455, 1345, 1253, 1040, 853 cm^{-1}; ^1H NMR ($CDCl_3$, 300 MHz) δ 2.30-2.45 (2 H, ddd, J=17.3, 5.4, 1.7 Hz), 3.70 (3 H, m, $^3J_{PH}$=11.0 Hz), 3.76 (3 H, m, $^3J_{PH}$=11.0 Hz), 4.5-4.75 (1 H, dq, J=26.9, 8.3, 5.9 Hz), 5.11 (2 H, s), 5.17 (2 H, s), 6.33 (1 H, d, J=8.1

Hz), 7.20-7.45 (10 H, m); ^{13}C NMR ($CDCl_3$, 75.4 MHz) δ 25.91, 27.80, 49.46, 52.46, 54.21, 67.61, 128.00, 128.08, 128.32, 128.41, 128.46, 128.52, 135.03, 136.13, 155.68, 170.35; ^{31}P NMR ($CDCl_3$ 121.43 MHz) δ 29.87.

Benzyl 2(S)-(N-benzyloxycarbonyl)amino-3-bromopropanoate **125.** Under a nitrogen atmosphere, solid N-protected tosylate **127** (0.1844 g, 0.4 mmol) was dissolved in dry acetone (5 mL, 68 mmol). After addition of solid tetrabutylammonium bromide (0.135 g, 0.41 mmol), solution was stirred for 96 hours at RT (reaction followed by TLC). Solid was filtered off, and solution was concentrated and immediately purified using column chromatography (eluant: 20% EtOAc/40-60 °C petroleum ether). Recrystallization from EtOAc/40-60 °C petroleum ether yielded a white solid: 0.14 g, 93%; mp 82-84 °C; $[\alpha]_D^{20}$ +13.9° (*c*=1.42 g/100 mL, $CHCl_3$); IR ($CHCl_3$) υ 3430, 3033, 1749, 1721, 1508, 1456, 1377, 1304, 1189, 1065, 908 cm^{-1}, ^1H NMR ($CDCl_3$, 300 MHz) δ 3.7-3.85 (2 H, m, *J*=10.8, 2.9 Hz), 4.8 (1 H, m), 5.1 (2 H, s), 5.2 (2 H, s), 5.7 (1 H, d), 7.3-7.4 (10 H, m); ^{13}C NMR ($CDCl_3$, 75.4 MHz) δ 33.69, 54.34, 67.29, 68.07, 128.11, 128.28, 128.46, 128.56, 128.65, 129.02, 134.71, 135.87, 155.51, 168.71, 205.5; MS (EI) *m/e* (relative intensity) 394 (5), 392 (5), 181 (6), 154 (19), 137 (14), 136 (14), 107 (11), 91 (100); HRMS exact mass calcd. for $C_{18}H_{19}BrNO_4$ requires 392.0498, found 392.0490 (EI butane).

Benzyl 2(S)-(N-benzyloxycarbonyl)amino-3-hydroxypropanoate **126.** Solid N-protected L-serine **121** (4.66 g, 14 mmol) was

added to solution of Cs_2CO_3 (5.07 g, 15.6 mmol) dissolved in H_2O (70 mL, 3900 mmol). The solution was lypholyzed overnight and residue was dissolved in N,N-dimethylformamide (75 mL, 970 mmol) followed by addition of benzyl bromide (2 mL, 16.8 mmol). Resulting solution was stirred for 24 hours at RT. Removal of solvent under reduced pressure yielded an oil which was dissolved in H_2O and extracted three times with EtOAc. The organic layer was washed once with aqueous 5% $NaHCO_3$, water, and dried with anhydrous $MgSO_4$. Removal of solvent under reduced pressure yielded a yellowish oil which solidified on standing. Purification using flash column chromatography (eluant: 50% EtOAc/40-60 °C petroleum ether) followed by recrystallization from EtOAc/40-60 °C petroleum ether afforded a white solid: 9.47 g, 60%; mp 81-82 °C (lit. 84-85 °C); ^1H NMR ($CDCl_3$, 300 MHz) δ 3.30 (1 H, br s), 3.7-3.9 (2 H, m), 4.2 (1 H, m), 5.00 (2 H, s), 5.05 (2 H, s), 6.05 (1 H, m), 7.2-7.3 (10 H, m); MS (FAB) *m/e* (relative intensity) 330 (77), 286 (100), 196 (23), 181 (51), 151 (34); HRMS exact mass calcd. for $C_{18}H_{20}NO_5$ requires 330.1341, found 330.1280 (FAB NBA).

Benzyl 2(S)-(N-benzyloxycarbonyl)amino-3-(4'-toluenesulfonoyl)propanoate **127**. Solid benzyl 2(S)-(N-benzyloxycarbonyl) amino-3-hydroxypropanoate **126** (0.508 g, 1.5 mmol) was dissolved in anhydrous pyridine (5 mL, 62 mmol) under a nitrogen atmosphere, and the solution was cooled to -10 °C. After addition of solid tosyl chloride (0.5 g, 2.6 mmol), the

solution was stirred for 4 hours at -10 °C (reaction followed by TLC). Solution was concentrated and immediately purified using column chromatography (eluant: 50% EtOAc/40-60 °C petroleum ether). Recrystallization from EtOAc/40-60 °C petroleum ether yielded a white solid: 0.33 g, 43%; mp 70-72 °C (lit. 75-77 °C); ^{1}H NMR ($CDCl_3$, 300 MHz) δ 2.35 (3 H, s), 4.25-4.45 (2 H, m), 4.6 (1 H, m), 5.05 (2 H, s), 5.10 (2 H, d), 5.75 (1 H, m), 7.2-7.4 (12 H, m), 7.65 (2H, d); ^{13}C NMR ($CDCl_3$, 75.4 MHz) δ 21.43, 53.32, 66.98, 67.75, 68.99, 127.76, 127.78, 128.03, 128.07, 128.34, 128.38, 128.44, 129.41, 129.74, 132.02, 134.54, 135.78, 144.99, 155.44, 167.96; MS (FAB) *m/e* (relative intensity) 484 (4), 440 (9), 181 (15), 151 (12), 135 (9), 91 (100); HRMS exact mass calcd. for $C_{25}H_{26}NSO_7$ (m+1) requires 484.1430, found 484.1427 (FAB NBA).

Methyl (2(S)-(N-benzyloxycarbonyl)amino-3-carbobenzoxypropyl) phosphonic acid **129.** Dimethyl (2(S)-(N-benzyloxycarbonyl)amino-3-carbobenzoxypropyl) phosphonate **124** (0.199 g, 0.47 mmol) was dissolved in distilled *tert*-butyl amine (6 mL, 57 mmol) under a nitrogen atmosphere, and the resulting solution was refluxed for 4 days. The reaction mixture was concentrated to provide the *tert*-butyl amine salt as a white solid. This salt was dissolved in $CHCl_3$ and treated with washed cation exchange resin (Dowex 50W-X8 (H^+ form) 200-400 mesh, 10 g (dry)). After stirring for 2 hours, the resin was removed by filtration, and the filtrate was concentrated in vacuo to afford the product as an oil:

0.164g, 85%. IR (KBr) υ 3428, 3032, 1720, 1510, 1455, 1342, 1224, 1194, 1051, 989 cm^{-1}; ^1H NMR ($CDCl_3$, 300 MHz) δ 2.30-2.45 (2 H, dd, *J*=17.8, 5.6 Hz), 3.56 (3 H, d, $^3J_{PH}$=11.1 Hz), 3.60 (3 H, s), 4.60 (1 H, m), 5.06 (2 H, s), 5.14 (2 H, d, 4.2 Hz), 6.00 (1 H, m), 7.25-7.4 (5 H, m), 9.3 (1 H, br s); ^{13}C NMR ($CDCl_3$, 75.4 MHz) δ 26.62, 28.51, 49.43, 51.91, 67.00, 67.70, 126.96, 127.57, 128.00, 128.08, 128.36, 128.43, 128.53, 135.03, 136.15, 155.76, 170.24; ^{31}P NMR ($CDCl_3$, 121.43 MHz) δ 30.94; MS (FAB) *m/e* (relative intensity) 408 (1), 391 (MH^+-H_2O) (43), 369 (3), 279 (5), 149 (77), 91 (22); HRMS exact mass calcd. for $C_{19}H_{23}NO_7P$ (m+1).requires 408.1212, found 408.1210 (FAB NBA).

Methyl (2(S)-(N-benzyloxycarbonyl)amino-3-carbobenzoxypropyl) phosphonochloridate **130.** Oxalyl chloride (2.0 M in CH_2Cl_2) (0.28 mL, 0.56 mmol) was added dropwise to a solution of methyl (2(S)-(N-(benzyloxycarbonyl)amino)-3-carbobenzoxypropyl) phosphonic acid **129** (0.09 g, 0.21 mmol) and DMF (0.65 M in CH_2Cl_2) (0.01 mL, 7.5 μol) dissolved in CH_2Cl_2 (5.0 mL, 78 mmol) at 0 °C under a nitrogen atmosphere. The solution was stirred at 0 °C for 20 min and then warmed to RT and stirred for a further 80 min. The reaction was concentrated, dissolved in toluene (2 mL), and then reconcentrated in vacuo to remove the volatile reagents. Yellowish oil was used immediately in the subsequent reaction without further purification. ^1H NMR ($CDCl_3$, 300 MHz) δ 2.30-2.40 (2 H, m), 3.68 (3 H, d, $^3J_{PH}$=11.5 Hz), 4.50 (1 H, m), 5.12 (2 H, s),

5.14 (2 H, s), 7.30-7.40 (10 H, m); ^{31}P NMR ($CDCl_3$, 121.43 MHz) δ 41.5.

N-Methyl-methoxy-(2(S)-(N-benzyloxycarbonyl)amino-3-carbobenzoxypropyl) phosphonamidate **131.** Methyl amine (2.0 M in THF) (0.16 mL, 0.32 mmol) was cooled to 0 °C under a nitrogen atmosphere. Triethylamine (0.01 mL, 0.72 mmol) was added to the reaction flask, followed immediately by the dropwise addition by cannula of solution of methyl (2(S)-(N-benzyloxycarbonyl)amino-3-carbobenzoxypropyl) phosphonochloridate **130** (0.09 g, 0.21 mmol) dissolved in THF (15 mL, 168 mmol) under N_2. The resulting solution was allowed to warm to RT and stirred overnight. The $Et_3N{\cdot}HCl$ precipitate was removed by filtration, and the filtrate was concentrated in vacuo. The oily residue was dissolved in EtOAc and washed successively with aqueous 5% $NaHCO_3$ (1 x 30 mL), aqueous 5% $KHSO_4$ (1 x 30 mL), aqueous saturated NaCl (1 x 25 mL), and dried with anhydrous $MgSO_4$. Removal of solvent under reduced pressure afforded a yellowish oil which was purified by column chromatography on alumina (eluants: 10% EtOH/$CHCl_3$) to give an oil: 0.080 g, 89%. IR ($CHCl_3$) υ 3427, 3032, 1719, 1513, 1455, 1404, 1261, 1232, 1198, 1049, 911 cm^{-1}; ^1H NMR ($CDCl_3$, 300 MHz) δ 2.20-2.60 (2 H, m), 3.40-3.50 (3 H, dd, $^3J_{PH}$=11.2, 3.9 Hz), 3.62 (3 H, m), 4.50-4.62 (1 H, m), 5.00 (2 H, d), 5.14 (2 H, s), 6.00 (1 H, m), 6.15 (1 H, m), 7.15-7.4 (5 H, m); ^{13}C NMR (CD_3OD, 75.4 MHz) δ 13.54, 28.44, 49.69, 66.95, 67.53, 79.39, 113.76, 128.08, 128.29, 128.36,

128.43, 128.52, 128.59, 131.10, 134.37, 135.13, 159.40, 172.10; ^{31}P NMR ($CDCl_3$ 121.43 MHz) δ 25.94, 27.51; MS (FAB) *m/e* (relative intensity) 421 (3) (m+1), 364 (13), 149 (11), 137 (14), 91 (100); HRMS exact mass calcd. for $C_{20}H_{27}N_2O_6P$ (m+1) requires 421.1528, found 421.1524 (FAB NBA).

APPENDIX A
ABBREVIATIONS FOR AMINO ACIDS

Amino acid	Three-letter Abbreviation	One-letter Symbol
Alanine	Ala	A
Arginine	Arg	R
Asparagine	Asn	N
Aspartic Acid	Asp	D
Cysteine	Cys	C
Glutamine	Gln	Q
Glutamic Acid	Glu	E
Glycine	Gly	G
Histidine	His	H
Isoleucine	Ile	I
Leucine	Leu	L
Lysine	Lys	K
Methionine	Met	M
Phenylalanine	Phe	F
Proline	Pro	P
Serine	Ser	S
Threonine	Thr	T
Tryptophan	Trp	W
Tyrosine	Tyr	Y
Valine	Val	V

APPENDIX B
CALCULATED PARAMETERS FOR FORMAMIDE AND TAUTOMERS

Table 7. SCF Calculated Interatomic Distances (Å) for Formamide (**45**) and Tautomers (**46-49**)

species	H-C	C-O	C-N	N-H	O-H
45	1.0955	1.1934	1.3544	(a) 0.9936 (b) 0.9965	
45 (expt)[a]	1.098	1.219	1.352	(a) 1.002 (b) 1.002	
46	1.0843	1.3297	1.2505	1.0032	0.9484
47	1.0891	1.3377	1.2477	1.0036	0.9423
48	1.0841	1.3447	1.2457	1.0080	0.9432
49	1.0799	1.3391	1.2505	1.0080	0.9459

[a] Taken from reference 147.

Table 8. SCF Calculated Interatomic Angles (deg) for Formamide (**45**) and Tautomers (**46-49**)

species	∠HCO	∠OCN	∠CNH	∠HOC
45	122.4	125.0	(a) 119.37 (b) 121.23	
45 (expt)[a]	122.5	124.7	(a) 118.5 (b) 120.0	
46	110.72	122.63	111.45	108.50
47	114.24	120.82	110.56	110.95
48	115.21	124.66	111.41	111.17
49	110.39	129.08	113.49	111.40

[a] Taken from reference 147.

Table 9. Comparison of Calculated and Experimental Vibrational Frequencies (cm^{-1}) of Formamide **45** and Deuterated Formamide

H_2NCHO (calc)	H_2NCHO (expt)[a]	H_2NCDO (calc)	H_2NCDO (expt)[b]	D_2NCHO	D_2NCDO	assignment
44	289	44		33	33	N-H(D) wag
614	581	606	563	509	488	NCO bending
654	603	641	591	531	525	$NH(D)_2$ twist
1147	1046	1050	1142	972	949	$NH(D)_2$ rock
1169	1021	983	955	1165	981	CH(D) out-of-plane deflection
1362	1258	1353	1242	1422	1438	C-N stretch
1547	1390	1231		1557	1206	C-H(D) bend
1759	1577	1754	1582	1190	1123	$NH(D)_2$ scissoring
1979	1754	1949	1740	1970	1942	C-O stretch
3195	2854	2373	2135	3195	2372	C-H(D) stretch
3838	3439	3838	3438	2774	2774	N-H(D) sym. stretch
3985	3563	3984	3563	2995	2955	N-H(D) antisym stretch

[a] Taken from reference 148. [b] Taken from reference 149.

APPENDIX C
CALCULATED PARAMETERS FOR FORMIMIDE AND TAUTOMERS

Table 10. SCF Calculated Interatomic Distances (Å) for Formimide **50-52** and Tautomers **53-60**

species	H-C	C-O	C-N	N-H	O-H
50	1.0956	1.1802	1.3888	0.9969	
53	(a) 1.0804 (b) 1.0921	(a) 1.3184 (b) 1.1868	(a) 1.2598 (b) 1.4063		0.9439
54	(a) 1.0804 (b) 1.0891	(a) 1.3009 (b) 1.2035	(a) 1.2782 (b) 1.3841		0.9595
51	(a) 1.0929 (b) 1.0878	(a) 1.1874 (b) 1.1865	(a) 1.3766 (b) 1.3854	0.9990	
55	(a) 1.0796 (b) 1.1011	(a) 1.3267 (b) 1.1824	(a) 1.2607 (b) 1.3964		0.9441
56	(a) 1.0836 (b) 1.0891	(a) 1.3337 (b) 1.2035	(a) 1.2538 (b) 1.3841		0.9438
57	(a) 1.0908 (b) 1.0811	(a) 1.1905 (b) 1.3103	(a) 1.4027 (b) 1.2653		0.9497
58	(a) 1.0905 (b) 1.0854	(a) 1.1918 (b) 1.3170	(a) 1.4032 (b) 1.2598		0.9439
52	1.0933	1.1851	1.3757	1.0016	
59	(a) 1.1013 (b) 1.0853	(a) 1.1820 (b) 1.3126	(a) 1.3994 (b) 1.2592		0.9498
60	(a) 1.1027 (b) 1.0903	(a) 1.1816 (b) 1.3194	(a) 1.3999 (b) 1.2544		0.9436

Table 11. SCF Calculated Interatomic Angles (deg) for Formimide **50-52** and Tautomers **53-60**

species	∠HCO	∠OCN	∠CNC	∠CNH	∠HOC
50	122.76	126.65	128.02	115.98	
53	(a) 115.16 (b) 121.40	(a) 127.43 (b) 128.15	122.45		110.94
54	(a) 112.48 (b) 120.49	(a) 128.82 (b) 126.62	118.50		109.49
51	(a) 122.90 (b) 124.26	(a) 124.82 (b) 122.42	124.20	119.28	
55	(a) 110.02 (b) 118.83	(a) 131.07 (b) 122.93	121.79		113.91
56	(a) 115.24 (b) 121.16	(a) 125.88 (b) 121.88	119.39		111.38
57	(a) 121.61 (b) 125.14	(a) 126.64 (b) 121.96	116.06		109.13
58	(a) 121.49 (b) 116.35	(a) 126.79 (b) 120.42	115.25		111.29
52	122.76	126.65	128.02	115.98	
59	(a) 120.79 (b) 111.61	(a) 123.61 (b) 122.76	122.45		109.14
60	(a) 120.50 (b) 115.22	(a) 123.77 (b) 121.06	118.50		111.60

Table 12. Vibrational Frequencies (cm^{-1}) of Formimide conformers (50-52)

$HN(CHO)_2$				$DN(CHO)_2$				$DN(CDO)_2$				
50	51	52	expt[a]	50	51	52	expt[a]	50	51	52	expt[a]	assignment[a]
149	169	131		149	168	131		168	1554	163		
224	255	277	262	223	253	277		238	244	287		NCO γ
280	288	303		278	286	303		291	246	297		
568	553	578	513	459	518	578		296	508	375	501	CNC in-plane def.
614	682	658	638	567	538	685		492	530	415	589	NCO γ
979	861	742	785	956	858	742		668	812	676	754	CNC sym. stretch[a]
1047	1156	1152	1030	1017	991	1152		862	959	936	873	CH γ
1131	1167	1166	1178	1043	1155	1166		970	980	977	967	NH γ
1157	1173	1287	1253	1131	1172	1287		1024	988	998	1322	CNC antisym. stretch
1268	1298	1361	1363	1157	1211	1361		1081	1108	1091	1038	CH in-plane def.
1550	1512	1472	1401	1499	1460	1472		1171	1149	1174	1070	NH in-plane def.
1577	1554	1571	1466	1552	1551	1571		1383	1263	1417	1228	NH in-plane def.
1660	1635	1617	1679	1575	1556	1617		1465	1485	1454	1650	CO stretch
1982	1974	1989	1740	1970	1972	1989		1647	1930	1691	1714	CO stretch
2075	2023	2034	2775	2072	2014	2034		1990	1983	1968	2070	CH stretch
3191	3226	3210	2910	2843	2832	3210		2302	2400	2322	2202	CH stretch
3193	3297	3233	3100	3190	3225	3233		2375	2458	2398	2325	NH stretch
3874	3852	3834	3255	3193	3297	3834		2941	2832	3897	2415	NH stretch

[a] Taken from reference 158.

APPENDIX D
CALCULATED REACTION COORDINATE TABLES

Table 13. Semi-empirical (AM1) Calculated Relative Energies (kcal/mol) for the Nucleophilic Attack of (Methyl)Thiolate on Formimide (gas phase)

C-S distance (Å)	**50** with -SH	**51** with -SH	**50** with CH_3S^-	**51** with CH_3S^-
1.50		+18.51		
2.00	-2.05	-15.91	-9.15	-13.47
2.63	-17.10	-19.27	-18.57	-19.35
2.68	-17.87	-22.10	-19.63	-20.13
3.00	-23.75	-24.54	-24.52	-24.59
3.45	-22.26	-21.53	-21.16	-20.30
3.87	-16.29	-15.94	-16.31	-15.64
4.00	-15.21	-14.75	-15.24	-14.50
6.00	-7.23	-6.35	-7.24	-6.26

Table 14. Total Energies (atomic units) for SCF and Correlated Wave Functions and Relative Energy Differences (kcal/mol) for the Nucleophilic Attack of Methylthiolate on Formamide **45**

	Nonprotonated **45**			Protonated **45**		
C–S dist.(Å)	SCF[a]	MP2[b]	Relative Energy[c]	SCF[a]	MP2[b]	Relative Energy[c]
1.35				-606.26820	-607.21829	-46.83
1.50	-605.78344	-606.71799	59.96	-606.40058	-607.33037	-117.91
1.75	-605.87044	-606.78521	17.18	-606.48451	-607.39613	-159.46
2.00	-605.89856	-606.80287	6.00	-606.48692	-607.39043	-156.44
2.50	-605.92859	-606.81646	-2.48	-606.46570	-607.35629	-135.53
3.00	-605.95810	-606.83114	-11.96	-606.46997	-607.38465	-156.00
3.50	-605.96877	-606.84247	-19.18			
4.00	-605.97181	-606.84673	-21.99	-606.47247	-607.38595	-157.22
4.50	-605.97077	-606.84525	-21.15			
5.00	-605.96602	-606.8387	-17.20			
5.50	-605.96038	-606.83193	-13.11			
6.00	-605.95557	-606.82657	-9.86			

[a] Calculated using the 6-31G basis set. [b] Using second-order Møller-Plesset perturbation theory using the 6-31G** basis set. [c] Zero-point corrected MP2 energy of species less energies of isolated reactants.

Table 15. Total Energies (atomic units) for SCF and Correlated Wave Functions and Relative Energy Differences (kcal/mol) for the Nucleophilic Attack of Methylthiolate on Formimide **50**

	Nonprotonated **50**			Protonated (0°) **50**			Protonated (180°) **50**		
C-S dist (Å)	SCF[a]	MP2[b]	Relative Energy[c]	SCF[a]	MP2[b]	Relative Energy[c]	SCF[a]	MP2[b]	Relative Energy[c]
1.50				-719.04012	-720.33708	-108.15	-719.04012	-720.33708	-114.03
1.75				-719.1491	-720.42275	-161.92	-719.14910	-720.42274	-167.80
2.00	-718.5937	-719.85864	-14.39	-719.1598	-720.42451	-163.23	-719.15796	-720.42046	-167.09
2.50				-719.13187	-720.38868	-141.51	-719.12496	-720.38029	-142.67
2.63	-718.61582	-719.85976	-15.59	-719.12422	-720.37818	-135.00	-719.10822	-720.36363	-132.22
2.68	-718.61764	-719.85989	-15.66	-719.12145	-720.37414	-132.50	-719.10629	-720.36001	-129.95
3.00	-718.62831	-719.86315	-17.84	-719.1046	-720.3601	-126.39	-719.09987	-720.35333	-128.13
3.50				-719.11511	-720.36874	-132.13	-719.11157	-720.36341	-134.64
3.87	-718.63684	-719.86696	-20.47				-719.07763	-720.31232	-100.22
4.00	-718.63534	-719.86512	-19.36	-719.07886	-720.31285	-94.34	-719.07215	-720.30632	-96.49
4.50							-719.05191	-720.28468	-82.95
5.00									
6.00	-718.61573	-719.84554	-7.51						

[a] Calculated using the 6-31G basis set. [b] Using second-order Møller-Plesset perturbation theory and the 6-31G** basis set. [c] Zero-point corrected MP2 energy of species less energies of isolated reactants.

Table 16. Total Energies (atomic units) for SCF and Correlated Wave Functions and Relative Energy Differences (kcal/mol) for the Nucleophilic Attack of Methylthiolate on Formimide **51**

	Nonprotonated **51**			Protonated (0°) **51**			Protonated (180°) **51**		
C–S dist (Å)	SCF[a]	MP2[b]	Relative Energy[c]	SCF[a]	MP2[b]	Relative Energy[c]	SCF[a]	MP2[b]	Relative Energy[c]
1.50				-718.92737	-720.26555	-76.61	-718.91131	-720.24769	-58.95
1.75				-719.14532	-720.41900	-170.11	-719.12871	-720.40271	-153.94
2.00	-718.59813	-719.86004	-9.88	-719.15794	-720.42134	-171.98	-719.14691	-720.41018	-159.30
2.50				-719.07316	-720.33138	-119.31	-719.08996	-720.34287	-120.01
2.63	-718.62818	-719.86830	-15.34	-719.08089	-720.33681	-122.82	-719.09974	-720.35285	-126.53
2.68	-718.63003	-719.86874	-15.62	-719.08335	-720.33859	-123.97	-719.10215	-720.35395	-127.35
3.00	-718.64019	-719.87245	-18.13	-719.09057	-720.34572	-128.55	-719.11176	-720.35992	-130.83
3.50				-719.10067	-720.35420	-134.16	-719.12272	-720.36973	-137.32
3.87	-718.64755	-719.87443	-19.63						
4.00	-718.64597	-719.87260	-18.53	-719.05704	-720.29316	-93.12			
4.50							-719.05360	-720.30574	-95.01
6.00	-718.62620	-719.85293	-6.58						

[a] Calculated using the 6-31G basis set. [b] Using second-order Møller-Plesset perturbation theory using the 6-31G** basis set. [c] Zero-point corrected MP2 energy of species less energies of isolated reactants.

Table 17. Total Energies (atomic units) for SCF and Correlated Wave Functions and Relative Energy Differences (kcal/mol) for the Breakdown of the Tetrahedral Intermediate formed by the Nucleophilic Attack of Methylthiolate on Formamide **45**

	Nonprotonated **45**			Protonated (0°) **45**			Protonated (180°) **45**		
C-N dist (Å)	SCF[a]	MP2[b]	Relative Energy[c]	SCF[a]	MP2[b]	Relative Energy[c]	SCF[a]	MP2[b]	Relative Energy[c]
1.35	-606.41693	-607.33506	-316.62	-606.83092	-607.74027	-364.97	-606.83092	-607.74026	-361.83
1.50	-606.44024	-607.35850	-332.31	-606.84651	-607.75680	-376.44	-606.84651	-607.75681	-373.32
1.75	-606.45026	-607.37077	-341.91	-606.83668	-607.74988	-373.31	-606.83668	-607.74988	-370.19
2.00	-606.46042	-607.38107	-349.27	-606.82223	-607.73929	-367.91	-606.81848	-607.73769	-363.94
2.50	-606.48012	-607.39751	-360.57	-606.81228	-607.73407	-365.78	-606.81228	-607.73408	-362.66
3.00	-606.48838	-607.40361	-364.73	-606.84625	-607.77324	-389.15	-606.84624	-607.77324	-386.03
3.50	-606.48860	-607.40252	-364.72	-606.86303	-607.78161	-394.66	-606.81068	-607.73469	-363.46
4.00	-606.48664	-607.40006	-363.46	-606.80583	-607.73005	-363.77	-606.80583	-607.73006	-360.65
4.50	-606.48483	-607.39774	-362.20	-606.80219	-607.72651	-361.78	-606.81365	-607.73527	-364.19
5.00	-606.48354	-607.39590	-361.25	-606.80281	-607.72916	-363.34	-606.80280	-607.72921	-360.25
5.50	-606.48267	-607.39494	-360.80	-606.80236	-607.72730	-362.22	-606.80236	-607.72732	-359.10
6.00				-606.80110	-607.72508	-360.98	-606.80111	-607.72508	-357.86

[a] Calculated using the 6-31G basis set. [b] Using second-order Møller-Plesset perturbation theory using the 6-31G** basis set. [c] Zero-point corrected MP2 energy of species less energies of isolated reactants.

Table 18. Total Energies (atomic units) for SCF and Correlated Wave Functions and Relative Energy Differences (kcal/mol) for the Breakdown of the Tetrahedral Intermediate formed by the Nucleophilic Attack of Methylthiolate on Formimide **50**

	Nonprotonated **50**			Protonated **50**		
C-S dist.(Å)	SCF[a]	MP2[b]	Relative Energy[c]	SCF[a]	MP2[b]	Relative Energy[c]
1.35	-718.65165	-719.88602	-32.16	-719.17215	-720.43322	-168.15
1.50	-718.64101	-719.87807	-27.81			
1.75	-718.58551	-719.85271	-12.53	-719.12832	-720.40168	-150.42
2.00	-718.56981	-719.84272	-6.71	-719.13085	-720.40569	-152.96
2.50				-719.14817	-720.42247	-163.62
3.00	-718.57611	-719.84467	-8.73	-719.15733	-720.43030	-168.66
3.50	-718.57594	-719.84522	-8.87	-719.15729	-720.42956	-168.51
4.00	-718.57612	-719.84428	-8.32	-719.15426	-720.42600	-166.55
4.50	-718.57566	-719.84280	-7.42	-719.15198	-720.42349	-165.13
5.00	-718.57462	-719.84093	-6.26			
5.50	-718.57006	-719.83845	-4.76	-719.15076	-720.42261	-164.59
6.00	-718.56274	-719.83177	-0.75			

[a] Calculated using the 6-31G basis set. [b] Using second-order Møller-Plesset perturbation theory using the 6-31G** basis set. [c] Zero-point corrected MP2 energy of species less energies of isolated reactants.

Table 19. Total Energies (atomic units) for SCF and Correlated Wave Functions and Relative Energy Differences (kcal/mol) for the Breakdown of the Tetrahedral Intermediate formed by the Nucleophilic Attack of Methylthiolate on Formimide **51**

	Nonprotonated **51**			Protonated (0°) **51**			Protonated (180°) **51**		
C-N dist (Å)	SCF[a]	MP2[b]	Relative Energy[c]	SCF[a]	MP2[b]	Relative Energy[c]	SCF[a]	MP2[b]	Relative Energy[c]
1.35				-719.08607	-720.35126	-127.17	-719.09190	-720.35492	-123.67
1.50				-719.10465	-720.37101	-140.26	-719.10960	-720.37407	-136.36
1.75				-719.10965	-720.38196	-148.48	-719.11291	-720.38374	-143.80
2.00	-718.55624	-719.81062	15.92	-719.11772	-720.39332	-156.09	-719.11984	-720.39427	-150.92
2.50	-718.63237	-719.86433	-15.61	-719.13625	-720.41176	-168.06	-719.13793	-720.41223	-162.64
3.00	-718.58454	-719.85090	-6.90	-719.14242	-720.41634	-171.26	-719.14447	-720.41695	-165.88
3.50	-718.57885	-719.84516	-3.31	-719.14306	-720.41547	-171.06	-719.14492	-720.41732	-166.40
4.00	-718.57192	-719.83848	0.81	-719.13970	-720.41292	-169.73	-719.14278	-720.41520	-165.26
4.50	-718.56640	-719.83283	4.23	-719.13791	-720.41105	-168.67	-719.14147	-720.41395	-164.53
5.00	-718.56297	-719.82909	6.50				-719.14690	-720.42134	-168.45
5.50	-718.56086	-719.82715	7.63				-719.14818	-720.41964	-167.54
6.00	-718.55963	-719.82615	8.22	-719.13560	-720.40865	-167.36			

[a] Calculated using the 6-31G basis set. [b] Using second-order Møller-Plesset perturbation theory using the 6-31G** basis set. [c] Zero-point corrected MP2 energy of species less energies of isolated reactants.

APPENDIX E
CALCULATED REACTION COORDINATE FIGURES

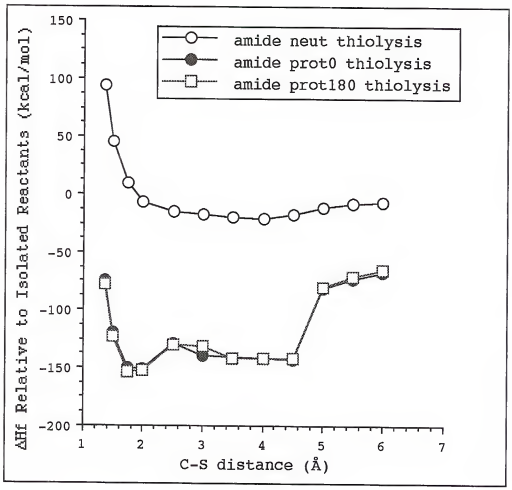

Figure AE-1. Gas phase AM1-calculated reaction coordinate for methylthiolate ion + formamide **45.**

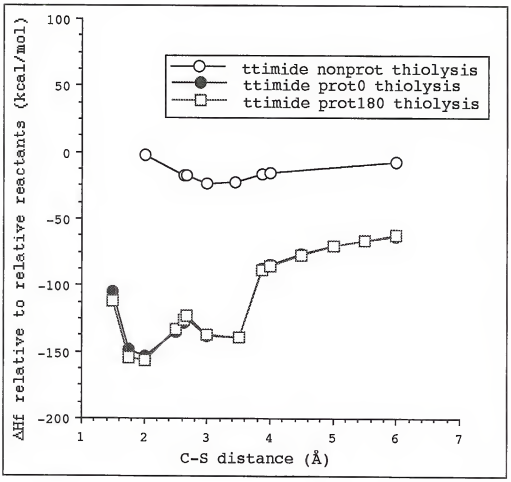

Figure AE-2. Gas phase AM1-calculated reaction coordinate for methylthiolate ion + formimide **50.**

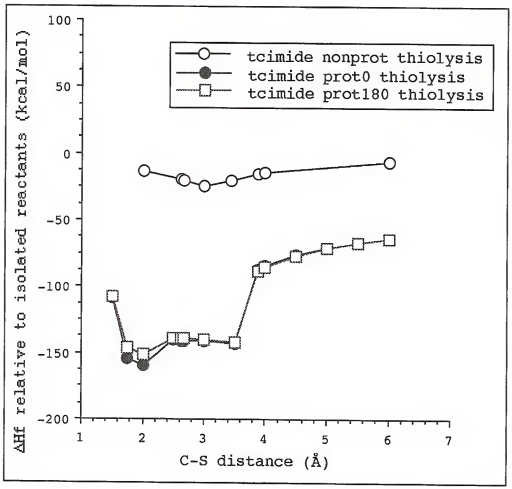

Figure AE-3. Gas phase AM1-calculated reaction coordinate for methylthiolate ion + formimide **51.**

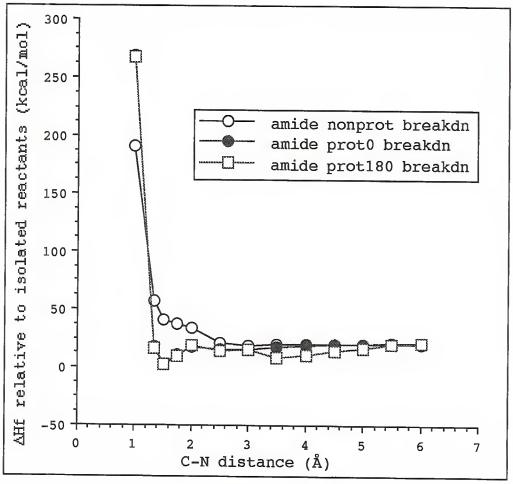

Figure AE-4. Gas phase AM1-calculated reaction coordinate for breakdown of methylthiolate ion + formamide 45 tetrahedral intermediate.

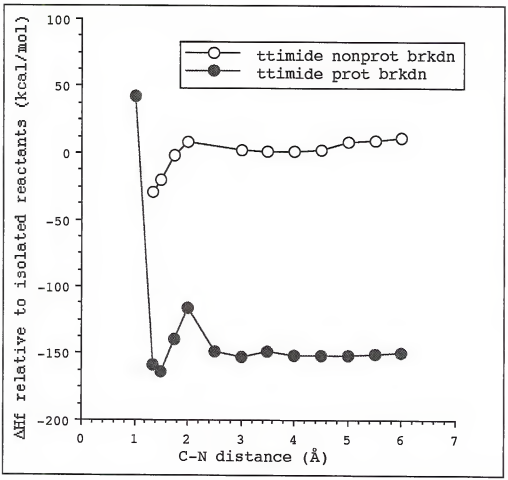

Figure AE-5. Gas phase AM1-calculated reaction coordinate for breakdown of methylthiolate ion + formimide **50** tetrahedral intermediate.

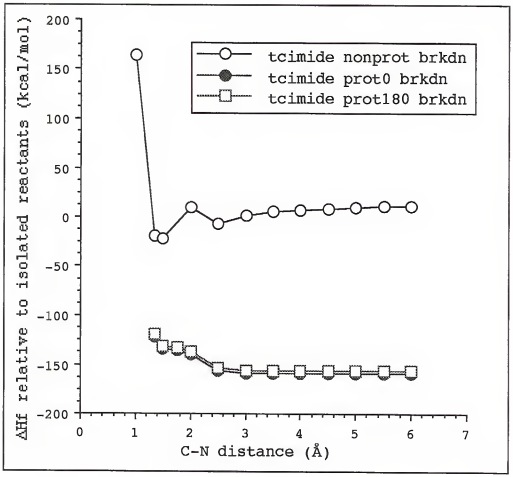

Figure AE-6. Gas phase AM1-calculated reaction coordinate for breakdown of methylthiolate ion + formimide **51** tetrahedral intermediate.

LIST OF REFERENCES

1. Carlomago, M. S.; Chiariotti, L.; Alifano, P.; Nappo, A. G.; Bruni, C. B. *J. Mol. Biol.* **1988**, *203*, 586.

2. Koshland, D. E.; Levitzky, A. In *The Enzymes*; Boyer, P. D., Ed.; Academic Press: New York, 1974; p. 539.

3. Badet, B; Vermoote, P.; Haumont, P.-Y. *Biochemistry* **1987**, *26*, 1940.

4. Blanche, F.; Couder, M.; Debusshe, L.; Thibaut, D.; Cameron, B.; Crouzet, J. *J. Bacteriol.* **1991**, *173*, 6046.

5. McGrath, R.; Vining, L. C.; Sala, F.; Westlake, D. W. S. *Can. J. Biochem.* **1968**, *46*, 587.

6. Buchanan, J.M.; *Adv. Enzymol. Relat. Areas Mol. Biol.* **1973**, *39*, 91.

7. Zalkin, H. *Adv. Enzymol. Relat. Areas Mol. Biol.* **1993**, *66*, 203.

8. Mei, B.; Zalkin, H. *J. Biol. Chem.* **1989**, *264*, 16613.

9. Mei, B.; Zalkin, H. *J. Bacteriol.* **1990**, *172*, 3512.

10. Andrulis, I. L.; Chen, J.; Ray, P. N. *Mol. Cell. Biol.* **1987**, *7*, 2435.

11. Tempest, D. W.; Meers, J. L. *Biochem. J.* **1970**, *117*, 405.

12. Hartman, S. C.; *J. Biol. Chem.* **1963**, *238*, 3024.

13. Zalkin, H. *Adv. Enzymol. Relat. Areas Mol. Biol.* **1973**, *38*, 1.

14. Meister, A. *Adv. Enzymol. Relat. Areas Mol. Biol.* **1989**, *62*, 315.

15. Sampei, G.; Mizobuchi, K. *J. Biol. Chem.* **1989**, *264*, 21230.

16. Tiedeman, A. A.; Smith, J. M.; Zalkin, H. *J. Biol. Chem.* **1985**, *260*, 8676.

17. Kaplan, J. B.; Nichols, B. P. *J. Mol. Biol.* **1983**, *168*, 451.

18. Jah, D.; Kim, Y.-C.; Ishino, Y.; Chen, M.-W.; Soll, D. *J. Biol. Chem.* **1990**, *265*, 8059.

19. Yi, C. K.; Dietrich, L. S. *J. Biol. Chem.* **1972**, *247*, 4794.

20. Crouzet, J.; Cauchois, L.; Blanche, F.; Debussche, L; Thibaut, D.; Rouyez, M.-C.; Rigault, S.; Mayaux, J.-F.; Cameron, B. *J. Bacteriol.* **1990**, *172*, 5968.

21. Crouzet, J.; Levy-Schil, S.; Cameron, B.; Cauchois, L.; Rouyez, M.-C.; Blanche, F.; Debussche, L; Thibaut, D. *J. Bacteriol.* **1991**, *173*, 6074.

22. Levitzki, A.; Koshland, D. E. *Biochemistry* **1971**, *10*, 3365.

23. Zalkin, H.; Truitt, C. D. *J. Biol. Chem.* **1977**, *252*, 5431.

24. Zalkin, H.; Murphy, T. *Biochem. Biophys. Res. Commun.* **1975**, *67*, 1370.

25. Mantsala, P.; Zalkin, H. *J. Biol. Chem.* **1984**, *259*, 14230.

26. Rubino, S. D.; Nyunoya, H.; Lusty, C. J. *J. Biol. Chem.* **1986**, *261*, 11320.

27. Humbert, R.; Simoni, R. D. *J. Bacteriol.* **1980**, *142*, 212.

28. Burchall, J. J.; Reichelt, E. C.; Wolin, M. J. *J. Biol. Chem.* **1964**, *239*, 1794.

29. Cedar, H.; Schwartz, J. H. *J. Biol. Chem.* **1969**, *244*, 4112.

30. Ravel, J. M.; Norton, S. J.; Humphreys, J. S.; Shive, W. *J. Biol. Chem.* **1962**, *237*, 2845.

31. Reitzer, L. J.; Magasanik, B. *J. Bacteriol.* **1982**, *151*, 1291.

32. McPhee, K. G.; Nelson, R.; Schuster, S. M. *J. Bacteriol.* **1983**, *156*, 475.

33. Ramos, F.; Wiame, J. M. *Eur. J. Biochem.* **1979**, *94*, 409.

34. Surin, B. P.; Downie, J. A. *Mol. Microbiol.* **1988**, *2*, 173.

35. Hongo, S.; Matsumoto, T.; Sato, T. *Biochim. Biophys. Acta.* **1978**, *552*, 258.

36. Huang, Y.-Z.; Knox, E. W. *Enzymes.* **1975**, *19*, 314.

37. Luehr, C. A.; Schuster, S. M. *Arch. Biochem. Biophys.* **1985**, *237*, 335.

38. Andrulis, I. L.; Shotwell, M.; Evans-Blacker, S.; Zalkin, H.; Siminovitch, L.; Ray, P. N. *Gene* **1989**, *80*, 75.

39. Boehlein, S. K.; Richards, N. G. J.; Schuster, S. M. *J. Biol. Chem.* **1994**, *269*, 7450.

40. Smith, J. L.; Zaluzec, E. J.; Wery, J.-P.; Niu, L.; Switzer, R. L.; Zalkin, H.; Satow, Y. *Science* **1994**, *264*, 1427.

41. Kim, J. H.; Krahn, J. M.; Tomchick, D. R.; Smith, J. L.; Zalkin, H. *J. Biol. Chem.* **1996**, *271*, 15549.

42. Isupov, M. N.; Obmolova, G.; Butterworth, S.; Badet-Denisot, M.-A.; Badet, B.; Polikarpov, I.; Littlechild, J. A.; Teplyakov, A. *Structure* **1996**, *4*, 801.

43. Tesmer, J. J. G.; Klem, T. J.; Deras, M. L.; Davisson, V. J.; Smith, J. M. *Nat. Struct. Biol.* **1996**, *3*, 74.

44. Van Heeke, G.; Schuster, S. M. *J. Biol. Chem.* **1989**, *264*, 5503.

45. Van Heeke, G.; Schuster, S. M. *J. Biol. Chem.* **1989**, *264*, 19475.

46. Pfeiffer, N. E.; Melhaff, P. M.; Wylie, D. E.; Schuster, S. M. *J. Biol. Chem.* **1987**, *262*, 11565.

47. Cedar, H.; Schwartz, J. H. *J. Biol. Chem.* **1969**, *244*, 4122.

48. Tso, J. Y.; Hermodson, M. A. ; Zalkin, H. *J. Biol. Chem.* **1982**, *257*, 3532.

49. Vollmer, S. J.; Switzer, R. L.; Hermodson, M. A.; Bower, S. G.; Zalkin, H. *J. Biol. Chem.* **1983**, *258*, 10582.

50. Sheng, S.; Moraga-Amador, D.; Van Heeke, G.; Allison, R. D.; Richards, N. G. J.; Schuster, S. M. *J. Biol. Chem.* **1993**, *268*, 16771.

51. Drenth, J.; Jansonius, J. N.; Koebek, R.; Worthers, B. G. *The Enzymes* **1971**, *3*, 485.

52. Richards, N. G. J.; Schuster, S. M. unpublished results, 1996.

53. Milman, H. A.; Cooney, D. A.; Huang, C. Y. *J. Biol. Chem.* **1980**, *255*, 1862.

54. Roberts, D. V. *Enzyme Kinetics*; Cambridge University Press: London; 1977.

55. Markin, R. S.; Luehr, C. A.; Schuster, S. M. *Biochemistry*, **1981**, *20*, 7226.

56. Habibzadegah-Tari, P., Ph.D. Dissertation, University of Florida, 1996.

57. Felton, J.; Michaelis, S.; Wright, A. *J. Bacteriol.* **1980**, *142*, 221.

58. Nakamura, M.; Yamada, M.; Hirota, Y.; Sugimoto, K.; Oka, A.; Takanami, M. *Nucleic Acids Res.* **1981**, *9*, 4669.

59. Scofield, M. A.; Lewis, W. S.; Schuster, S. M. *J. Biol. Chem.* **1990**, *265*, 12895.

60. Richards, N. G. J.; Schuster, S. M. *FEBS Lett.* **1992**, *313*, 98.

61. Gibbs, R. A.; Taylor, S.; Benkovic, S. J. *Science* **1992**, *258*, 803.

62. Kornfield, R.; Kornfield, S. *Annu. Rev. Biochem.* **1985**, *54*, 631.

63. Geiger, R.; Konig, W. In *The Peptides, Analysis, Synthesis, Biology*, vol. 3; Gross, E.; Meienhofer, J., Eds.; Academic Press: New York, 1981; p. 50.

64. Boehlein, S. K.; Richards, N. G. J.; Walworth, E. S.; Schuster, S. M. *J. Biol. Chem.* **1994**, *269*, 26789.

65. Lusty, C. J.; Liao, M. *Biochemistry* **1993**, *32*, 1278.

66. Boehlein, S. K.; Rosa-Rodriguez, J. G.; Schuster, S. M.; Richards, N. G. J. *J. Am. Chem. Soc.* **1997**, *119*, in press.

67. Cleland, W. W.; Kreevoy, M. M. *Science* **1994**, *264*, 1887.

68. Etter, M. C.; Reutzel, S. M. *J. Am. Chem. Soc.* **1991**, *113*, 2586.

69. Boehlein, S. K.; Schuster, S. M.; Richards, N. G. J. *Biochemistry* **1996**, *35*, 3031.

70. Imperiali, B.; Shannon, K. L.; Rickert, K. W. *J. Am. Chem. Soc.* **1992**, *114*, 7942.

71. Imperiali, B.; Shannon, K. L.; Unno, M.; Rickert, K. W. *J. Am. Chem. Soc.* **1992**, *114*, 7944.

72. Hendrickson, T. L.; Spencer, J. R.; Kato, M.; Imperiali, B. *J. Am. Chem. Soc.* **1996**, *118*, 7636.

73. Stoker, P. W.; O'Leary, M. H.; Boehlein, S. K.; Schuster, S. M.; Richards, N. G. J. *Biochemistry* **1996**, *35*, 3024.

74. Rosa-Rodriguez, J. G., Ph.D. Dissertation, University of Florida, 1996.

75. Broome, J. D. *J. Exp. Med.* **1963**, *118*, 99.

76. Burchenal, J. H. *Rec. Results Canc. Res.* **1970**, *33*, 350.

77. Cooney, D. A.; Handschumacher, R. E. *Annu. Rev. Pharmacol.* **1970**, *10*, 421.

78. Broome, J. D. *J. Exp. Med.* **1968**, *127*, 1055.

79. Kiriyama, Y.; Kubota, M.; Takimoto, T.; Kitoh, J.; Tanizawa, A.; Akiyama, Y.; Mikawa, H. *Leukemia* **1989**, *3*, 294.

80. Broome, J. D.; Schwartz, J. H. *Biochim. Biophys. Acta.* **1967**, *138*, 637.

81. Hersh, E. M. *Transplantation* **1971**, *12*, 368.

82. Goodbourn, S. *Curr. Biol.* **1994**, *4*, 930.

83. Clipstone, N. A.; Crabtree, G. R. *Nature* **1992**, *357*, 92.

84. Ornstein, P. L.; Arnold, M. B.; Augenstein, N. K.; Paschal, J. W. *J. Med. Chem.* **1991**, *34*, 90.

85. Bridges, R. J.; Stanley, M. S.; Anderson, M. W.; Cotman, C. W.; Chamberlin, A. R. *J. Med. Chem.* **1991**, *34*, 717.

86. Gmeiner, P.; Feldman, P. L.; Chu-Mover, M. Y.; Rapoport, H. *J. Org. Chem.* **1990**, *55*, 3068.

87. Wang, S.; Gisin, B. F.; Winter, D. P.; Makofske, R.; Kulesha, I. D.; Tzougraki, C.; Meienhofer, J. *J. Org. Chem.* **1977**, *42*, 1286.

88. Baldwin, J. E.; Moloney, M. G.; North, M. *Tetrahedron* **1989**, *45*, 6309.

89. Baldwin, J. E.; Moloney, M. G.; North, M. *Tetrahedron* **1989**, *45*, 6319.

90. Baldwin, J. E.; Moloney, M. G.; North, M. *J. Chem. Soc., Perkin Trans. 1* **1989**, 833.

91. Pappo, R.; Allen, D. S., Jr.; Lemieux, R. U.; Johnson, W.S. *J. Org. Chem.* **1956**, *21*, 478.

92. Inomata, K.; Nakayama, Y.; Kotake, H. *Bull. Chem. Soc. Japan* **1980**, *53*, 565.

93. West, C. T.; Donnelly, S. J.; Kooistra, D. A.; Doyle, M. P. *J. Org. Chem.* **1973**, *38*, 2675.

95. Anantharamaiah, G.M.; Sivanandaiah, K.M. *J. Chem. Soc., Perkin Trans. 1* **1977**, 490

96. Jackson, A. E.; Johnstone, R. A. W. *Synthesis* **1976**, 685.

97. Humphrey, J. M.; Bridges, J. M.; Hart, J. A.; Chamberlin, A. R. *J. Org. Chem.* **1994**, *59*, 2467.

98. Seebach, D.; Wasmuth, D. *Angew. Chem. Int. Ed. Eng.* **1981**, *20*, 971.

99. Dener, J. M.; Zhang, L. H.; Rapoport, H. *J. Org. Chem.* **1993**, *58*, 1159.

100. Dunn, P. J.; Haner, R.; Rapoport, H. *J. Org. Chem.* **1990**, *55*, 5017.

101. Ireland, R. E.; Daub, J. P. *J. Org. Chem.* **1981**, *46*, 479.

102. Parr, I. B., Ph.D. Dissertation, University of Southampton, UK, 1994.

103. Seebach, D.; Wasmuth, D. *Helv. Chim. Acta.* **1980**, *63*, 197.

104. Lubell, W. D.; Rapoport, H. *J. Am. Chem. Soc.* **1988**, *22*, 7447.

105. Asao, N.; Uyehara, T.; Yamamoto, Y. *Tetrahedron* **1990**, *46*, 4572.

106. Derome, A. E. *Modern NMR Technigues for Chemistry Research*; Pergamon: Oxford, 1987.

107. Sanders, J. K. M.; Mersh, J. D. *Prog. NMR Spectrosc.* **1982**, *4*, 353.

108. Mauger, A. B. *J. Am. Chem.Soc.* **1966**, *88*, 2019.

109. Ibrahim, H. H.; Lubell, W. D. *J. Org. Chem.* **1993**, *58*, 6438.

110. Ramalingham, K.; Woodward, R. W. *J. Org. Chem.* **1988**, *53*, 1900.

111. Anderson, G. W.; Callahan, F. M. *J. Am. Chem. Soc.* **1960**, *82*, 786.

112. Dewar, M. J. S.; Zoebisch, E. G.; Healy, E. F.; Stewart, J. J. P. *J. Am. Chem. Soc.* **1985**, *107*, 3902.

113. MOPAC: Stewart, J. J. P. Quantum Chemistry Exchange Program, University of Indiana, Bloomington, IN 1993, Program 455. Version: 6.0.

114. Gill, P.; Lubell, W. D. *J. Org. Chem.* **1995**, *60*, 2658.

115. Parr, I. B.; Boehlein, S. K.; Dribben, A. B.; Schuster, S. M.; Richards, N. G. J. *J. Med. Chem.* **1996**, *39*, 2367.

116. Horowitz, B.; Meister, A. *J. Biol. Chem.* **1972**, *247*, 6708.

117. Mokotoff, M.; Bagaglio, J. F.; Parikh, B. S. *J. Med. Chem.* **1975**, *18*, 354.

118. Segel, I. H. *Enzyme Kinetics*; Wiley-Interscience: New York, 1975, pp. 100-160.

119. Danishefsky, A. T.; Onnufer, J. J.; Petsko, G. A.; Ringe, D. *Biochemistry* **1991**, *30*, 1980.

120. Yeh, J. I.; Biemann, H.-P.; Pandit, J.; Koshland, D. E.; Kim, S.-H. *J. Biol. Chem.* **1993**, *268*, 9787.

121. Wang, W.; Poland, B. W.; Honzatko, R. B.; Fromm, H. J. *J. Biol. Chem.* **1995**, *270*, 13160.

122. Blow, D. M.; Rossmann, M. G. *Acta Cryst.* **1961**, *14*, 1195.

123. Glusker, J. P.; Lewis, M.; Rossi, M. *Crystal Structure Analysis for Chemists and Biologists*; VCH Publishers, Inc.: New York, 1994, pp. 320-327.

124. Lebioda, L.; Zhang, E. *Nature* **1992**, *25*, 323.

125. Tesmer, J. J. G.; Stemmler, T. L.; Penner-Hahn, J. E.; Davisson, V. J.; Smith, J. L. *Proteins* **1994**, *18*, 394.

126. Glusker, J. P.; Lewis, M.; Rossi, M. *Crystal Structure Analysis for Chemists and Biologists*; VCH Publishers, Inc.: New York, 1994, pp. 731-782.

127. Yoshikawa, M.; Kato, T.; Takenishi, T. *Bull. Chem. Soc., Jpn.* **1969**, *42*, 3505.

128. Sowa, T.; Ouchi, S. *Bull. Chem. Soc., Jpn.* **1975**, *48*, 2084.

129. Bartlett, R. J.; Stanton, J. F. In *Reviews in Computational Chemistry*; Volume V. Lipkowitz, K. B.; Boyd, D. B., Eds.; VCH Publishers, Inc.: New York, 1994; pp. 65-169.

130. Kwiatkowski, J. S.; Zielinski, T. J.; Rein, R. *Adv. Chem. Phys.* **1986**, *18* .

131. Minkin, V. I.; Olekhnovich, L. P.; Zhdanov, Y. A. *Molecular Design of Tautomeric Compounds*; D. Reidel Publishing Co.: Dordrecht, Holland; 1988.

132. Kwiatkowski, J. S.; Bartlett, R. J.; Person, W. B. *J. Am. Chem. Soc.* **1988**, *110*, 2353.

133. Nagaoka, M.; Okuna, Y.; Yambe, T. *J. Am. Chem. Soc.* **1991**, *113*, 769.

134. Schegel, H. B.; Gund, P.; Fluder, E. M. *J. Am. Chem. Soc.* **1982**, *104*, 5347.

135. Carlsen, N. R.; Radom, L.; Riggs, N. V.; Rodwell, W. R. *J. Am. Chem. Soc.* **1979**, *101*, 2233.

136. Radom, L.; Riggs, N. V. *Aust. J. Chem.* **1980**, *33*, 249.

137. Wang, X.-C.; Nichols, J.; Feyereisen, M.; Gutowski, M.; Boatz, J.; Haymet, A. D. J.; Simons, J. *J. Phys. Chem.* **1991**, *95*, 10419.

138. Dunning, T. H. *J. Chem. Phys.* **1989**, *90*, 1007.

139. Møller, C.; Plesset, M. S. *Phys. Rev.* **1934**, *46*, 618.

140. Binkley, J. S.; Pople, J. A. *Int. J. Quantum Chem.* **1975**, *9*, 229.

141. Krishnan, R.; Fritsch, M. J.; Pople, J. A. *J. Chem. Phys.* **1980**, *72*, 4244.

142. Dunning, T. H. *J. Chem. Phys.* **1970**, *53*, 2823.

143. Redmon, L. T.; Purvis III, G. D.; Bartlett, R. J. *J. Am. Chem. Soc.* **1979**, *101*, 2856.

144. Bartlett, R. J.; Watts, J. D.; Kucharski, S. A.; Noga, J. *Chem. Phys. Lett.* **1990**, *165*, 513.

145. ACES II: Stanton, J. F.; Gauss, J.; Watts, J. D.; Lauderdale, W. J.; Bartlett, R. J. Quantum Theory Project, University of Florida: Gainesville, FL, 1995. Version: 2.0.

146. Stanton, J. F.; Gauss, J.; Watts, J. D.; Lauderdale, W. J.; Bartlett, R. J. *Int. J. Quant. Chem.* **1992**, *S26*, 879.

147. Hirota, E.; Sugiasaki, R.; Nielsen, C. J.; Sorensen, G. O. *J. Mol. Spectrosc.* **1974**, *49*, 251.

148. King, S. T. *J. Phys. Chem.* **1975**, *75*, 405.

149. Sugawara, Y.; Hamada, Y.; Tsuboi, M. *Bull. Chem. Soc. Jpn.* **1983**, *56*, 1045.

150. Radom, L.; Riggs, N. *Aust. J. Chem.* **1980**, *33*, 1635.

151. Hehre, W. J.; Stewart, R. F.; Pople, J. A.. *J. Chem. Phys.* **1969**, *51*, 2657.

152. Kupfer, R.; Nagel, M.; Wurthwein, E.; Allman, R. *Chem. Ber.* **1985**, *118*, 3089.

153. Stanton, J. F.; Gauss, J.; Bartlett, R. J. *Chem. Phys. Lett.* **1992**, *195*, 194.

154. Dunning, T. H. *J. Chem. Phys.* **1971**, *55*, 716.

155. Binkley, J. S.; Pople, J. A.; Hehre, W. J. *J. Am. Chem. Soc.* **1980**, *102*, 939.

156. Steinmetz, W. *J. Am. Chem. Soc.* **1973**, *95*, 2777.

157. Noe, E. A.; Raban, M. *J. Am. Chem. Soc.* **1975**, *97*, 5811.

158. Allenstein, E.; Beyl, V. *Chem. Ber.* **1967**, *100*, 3551.

159. Weiner, S.; Singh, U. C.; Kollman, P. A. *J. Am. Chem. Soc.* , **1985**, *107*, 2219.

160. Howard, A.E.; Kollman, P. A. *J. Am. Chem. Soc.* , **1988**, *110*, 7195.

161. Arad, D.; Langridge, R.; Kollman, P. A. *J. Am. Chem. Soc.* , **1990**, *112*, 491.

162. Ditchfield, R.; Hehre, W. J.; Pople, J. A. *J. Chem. Phys.* **1971**, *54*, 724.

163. Francl, M. M.; Pietro, W. J.; Hehre, W. J.; Binkley, J. S.; Gordon, M. S.; DeFrees, D. J.; Pople, J. A. *J. Chem. Phys.* **1982**, *77*, 3654.

164. GAMESS: Dupuis, M.; Spangler, D.; Wendoloski, J. J. National Resource for Computations in Chemistry Software Catalog, University of California, Berkeley, CA 1980, Program QG01. Version: 22 June 1996.

165. Schmidt, M. W.; Baldridge, K. K.; Boatz, J. A.; Elbert, S. T.; Gordon, M. S.; Jensen, J. H.; Koseki, S.; Matsunaga, N.; Nguyen, K. A.; Su, S. J.; Windus, T. L.; Dupuis, M.; Montgomery, J. A. *J. Comput. Chem.* **1993**, *14*, 1347.

166. Krishnan, R.; Binkley, J. S. ;Seeger, R.; Pople, J. A. *J. Chem. Phys.* **1980**, *72*, 650.

167. Francl, M. M.; Pietro, W. J.; Hehre, W. J.; Binkley, J. S.; Gordon, M. S.; DeFrees, D. J.; Pople, J. A. *J. Chem. Phys.* **1982**, *77*, 3654.

168. Kollman, P. A.; Hayes, D. M. *J. Am. Chem. Soc.* **1981**, *103*, 2955.

169. Fersht, A. *Enzyme Structure and Mechanism*, 2nd Ed.; W. H. Freeman & Co.: New York, 1985; pp. 413-416.

170. Fried, J.; Sabo, E. F. *J. Am. Chem. Soc.* **1954**, *76*, 1455.

171. Welch, J. T.; Eswarakrishnan, S. *Fluorine in Bioorganic Chemistry*; John Wiley & Sons: New York, 1991.

172. Welsh, J. T. In *Selective Fluorination in Organic and Bioorganic Chemistry*; Welsh, J. T., Ed.; American Chemical Society Symposium Series, #456: Washington, DC, 1991; pp. 1-15.

173. Baker, A. W.; Shulgin, A. T. *Nature* **1965**, *206*, 712.

174. Doddrell, S.; Wenkert, E.; Demarco, P. V. *J. Mol. Spectorsc.* **1969**, *32*, 162.

175. Goldman, P. *Science* **1969**, *164*, 1123.

176. Kollonitsch, J.; Perkins, L. M.; Patchett, A. A.; Doldouras, G. A.; Marburg, S.; Duggan, D. E.; Maycock, A. L.; Aster, S. D. *Nature* **1978**, *274*, 906.

177. Walsh, C. *Tetrahedron* **1982**, *38*, 871.

178. McDonald, I. A.; Palfreyman, M. G.; Jung, M.; Bey, P. *Tetrahedron Lett.* **1985**, *26*, 4091.

179. Abeles, R. H.; Maycock, A. L. *Acc. Chem. Res.* **1976**, *9*, 906.

180. Walsh, J. T.; Gyenes, A.; Jung, M. J. In *Fluorine-containing Amino Acids, Synthesis and Properties*; Kukhar', V. P.; Soloshonok, V. A., Eds.; John Wiley & Sons: New York, 1995; pp. 311-332.

181. Thaisrivongs, S.; Pals, D. T.; Kati, W. M.; Turner, S. R.; Thomasco, L. M. *J. Med. Chem.* **1985**, *28*, 1553.

182. Buchanan, R. L.; Dean, F. H.; Pattison, F. L. M. *Can. J. Chem.* **1962**, *40*, 1571.

183. Foy, S.; Hudlicky, M. *J. Fluorine Chem.* **1976**, *7*, 421.

184. Galivan, J.; Inglese, J.; McGuire, J. J.; Nimec, Z.; Coward, J. K. *Proc. Nat. Acad. Sci. USA* **1985**, *82*, 2598.

185. McGuire, J. J.; Graber, M.; Licato, N.; Vincenz, C.; Coward, J. K.; Nimec, Z.; Galivan, J. *Cancer Res.* **1989**, *49*, 4517.

186. Balcar, V. J.; Johnston, G. A. R. *J. Neurochem.* **1972**, *19*, 2657.

187. Foster, G. A.; Roberts, P. J. *Life Sci.* **1980**, *27*, 215.

188. McGuire, J. J.; Coward, J. K. *J. Biol. Chem.* **1985**, *260*, 6747.

189. Coward, J. K.; McGuire, J. J.; Galivan, J. In *Selective Fluorination in Organic and Bioorganic Chemistry*; Welsh, J. T., Ed.; American Chemical Society Symposium Series, #456: Washington, DC, 1991; pp. 196-204.

190. Hart, B. P.; Haile, W. H.; Licato, N. J.; Bolanowska, W. E.; McGuire, J. J.; Coward, J. K. *J. Med. Chem.* **1996**, *39*, 56.

191. Tsukamoto, T.; Kitazume, T.; McGuire, J. J.; Coward, J. K. *J. Med. Chem.* **1996**, *39*, 66.

192. Coward, J. K.; McGuire, J. J. In *Folates and Pterins*; Blakley, R. L.; Benkovic, S. J., Eds.; John Wiley & Sons: New York, 1984; pp. 135-190.

193. Voet, D.; Voet, J. G. *Biochemistry*; John Wiley & Sons: New York, 1990, pp. 740-768.

194. Tsushima, T.; Kawada, K.; Ishihara, S.; Uchida, N.; Shiratori, O.; Higaki, J.; Hirata, M. *Tetrahedron* **1988**, *44*, 5375.

195. Kirk, K. L. In *Fluorine-containing Amino Acids, Synthesis and Properties*; Kukhar', V. P.; Soloshonok, V. A., Eds.; John Wiley & Sons: New York, 1995; pp. 343-401.

196. Tsukamoto, T.; Coward, J. K. *J. Org. Chem.* **1996**, *61*, 2497.

197. Kitagawa, O.; Hashimoto, A.; Kobayashi, Y.; Taguchi, T. *Chem. Lett.* **1990**, 1307.

198. Yang, Z. Y.; Burton, D. J. *J. Org. Chem.* **1991**, *56*, 5125.

199. Taguchi, T.; Kitagawa, O.; Morikawa, T.; Nishiwaki, T.; Uehara, H.; Endo, H.; Kobayashi, Y. *Tetrahedron Lett.* **1986**, *27*, 6103.

200. Evans, D. E.; Ellman, J. A.; Dorow, R. L. *Tetrahedron Lett.* **1987**, *28*, 1123.

201. Hudlicky, M. *J. Fluorine Chem.* **1993**, *60*, 193.

202. Hudlicky, M.; Merola, J. S. *Tetrahedron Lett.* **1990**, *31*, 7403.

203. Sufrin, J. R.; Balasubramanaian, T. M.; Vora, c. M.; Marshall, G. R. *Int. J. Pept. Protein Res.* **1982**, *20*, 438.

204. Tsukamoto, T.; Kitazume, T. *J. Chem. Soc. Perkin Trans. 1* **1993**, 1177.

205. Rathke, M. W. *Org. React.* **1975**, *22*, 423.

206. Jones, G. *Org. React.* **1967**, *15*, 204.

207. Wollenberg, R. H.; Miller, S. J. *Tetrahedron Lett.* **1978**, 3219.

208. Still, W.C.; Kah, M.; Mitra, A. *J. Org. Chem.* **1978**, *43*, 2923.

209. Miyazawa, T. In *Fluorine-containing Amino Acids, Synthesis and Properties*; Kukhar', V. P.; Soloshonok, V. A., Eds.; John Wiley & Sons: New York, 1995; pp. 267-294.

210. Wong, C. -H.; Whitesides, G. M. *Enzymes in Synthetic Organic Chemistry*; Pergamon: New York, 1994; pp. 41-130.

211. Greenstein, J. P.; Winitz, M. *Chemistry of the Amino Acids*, Volume 2; John Wiley & Sons: New York, 1961; p. 1753.

212. Chenault, H. K.; Dahmer, J.; Whitesides, G. M. *J. Am. Chem. Soc.* **1989**, *111*, 6354.

213. Fu, S. -C.; Birnbaum, S. M. *J. Am. Chem. Soc.* **1953**, *75*, 918.

214. Anuradha, M. V.; Ravindranath, B. *Tetrahedron* **1997**, *53*, 1123.

215. Lide, D., R. *CRC Handbook of Chemistry and Physics*, 71st Ed.; CRC Press, Inc.: Boca Raton, FL, 1991; p. 3-258.

216. Hirschmann, R.; Yager, K. M.; Taylor, C. M.; Moore, W.; Sprengeler, P. A.; Witherington, J.; Phillips, B. W.; Smith, A. B. *J. Am. Chem. Soc.* **1995**, *117*, 6370.

217. Elliott, R. L.; Marks, N.; Berg, M. J.; Portoghese, P. S. *J. Med. Chem.* **1985**, *28*, 1208.

218. Blundell, T. L.; cooper, J.; Foundling, S. I.; Jones, D. M.; Atrash, B.; Szelke, M. *Biochemistry* **1987**, *26*, 5585.

219. Holden, H. M.; Tronrud, D. E.; Mozingo, A. F.; Weaver, L. H.; Matthews, B. W. *Biochemistry* **1987**, *26*, 8542.

220. Logusch, E. W.; Walker, D. M.; McDonald, J. F.; Franz, J. E. *Biochemistry* **1989**, *28*, 3043.

221. Logusch, E. W.; Walker, D. M.; McDonald, J. F.; Franz, J. E.; Villafranca, J. J.; DiIanni, C. L.; Colanduoni, J. A.; Li, B.; Schineler, J. B. *Biochemistry* **1990**, *29*, 366.

222. Logusch, E. W.; Walker, D. M.; McDonald, J. F.; Franz, J. E. *Plant Physiol.* **1991**, *95*, 1057.

223. Logusch, E. W.; Walker, D. M.; McDonald, J. F.; Leo, G. C.; Franz, J. E. *J. Org. Chem.* **1988**, *53*, 4069.

224. Jacobsen, N. E.; Bartlett, P. A. *J. Am. Chem. Soc.* **1981**, *103*, 654.

225. Bartlett, P. A.; Marlowe, C. K. *Science* **1987**, *235*, 569.

226. Bartlett, P. A.; Marlowe, C. K. *Biochemistry* **1987**, *26*, 8553.

227. Lerner, R. A.; Benkovic, S. J.; Schultz, P. G. *Science* **1991**, *252*, 659.

228. Benkovic, S. J. *Annu. Rev. Biochem.* **1992**, *61*, 29.

229. Bartlett, P. A.; Marlowe, C. K. *Biochemistry* **1983**, *22*, 4618.

230. Rogers, R. S. *Tetrahedron Lett.* **1992**, *33*, 7473.

231. Davidson, S. K.; Phillips, G. W.; Martin, S. F. *Org. Synth.* **1987**, *65*, 119.

232. Malachowski, W. P.; Coward, J. K. *J. Org. Chem.* **1994**, *59*, 7616.

233. Sampson, N. S.; Bartlett, P. A. *J. Org. Chem.* **1988**, *53*, 4500.

234. Valerio, R. M.; Alewood, P. F.; Johns, R. B. *Synthesis* **1988**, 786.

235. Evans, D. A.; Hurst, K. M.; Takacs, J. M. *J. Am. Chem. Soc.* **1978**, *100*, 3467.

236. Ramsamy, K.; Olsen, R. K.; Emery, T. *Synthesis* **1982**, 42.

237. Collins, J. C.; Hess, W. W.; Frank, F. J. *Tetrahedron Lett.* **1968**, 3363.

238. Hart, T. W.; Metcalfe, D. A.; Scheinmann, F. *J. Chem. Soc. Chem. Commun.* **179**, 156.

239. Malachowski, W. P.; Coward, J. K. *J. Org. Chem.* **1994**, *59*, 7625.

240. Musiol, H. J.; Grams, F.; Bohner, S. R.; Moroder, L. *J. Org. Chem.* **1994**, *59*, 6144.

241. Barton, D. H. R.; Crich, D.; Motherwell, W. B. *Tetrahedron* **1985**, *41*, 3901.

242. Scholtz, J. M.; Bartlett, P. A. *Synthesis* **1989**, 542.

243. Hanessian, S.; Sahoo, S. P. *Tetrahedron Lett.* **1984**, *25*, 1425.

244. Barton, D. H. R.; Herve, Y.; Potier, P.; Thierry, J. *J. Chem. Soc.; Chem. Commun.* **1983**, 1298.

245. Barton, D. H. R.; Herve, Y.; Potier, P.; Thierry, J. *Tetrahedron* **1988**, *44*, 5479.

246. Bhattacharya, A. K.; Thyagarajan, G. *Chem. Rev.* **1981**, *81*, 415.

247. Kosolapoff, G. M. *J. Am. Chem. Soc.* **1944**, *66*, 109.

248. Gray, M. D. M.; Smith, D. J. H. *Tetrahedron Lett.* **1980**, *21*, 859.

249. Baer, E.; Maurukas, J. *J. Biol. Chem.* **1955**, *212*, 39.

250. Pansare, S. V.; Huyer, G.; Arnold, L. D.; Vedras, J. C. *Org. Synth.* **1991**, *70*, 1.

251. Arnold, L. D.; Kalantar, T. H.; Vedras, J. C. *J. Am. Chem. Soc.* **1985**, *107*, 7105.

252. Smith, E. C. R.; McQuaid, A.; Paschal, J. W.; DeHoniesto, J. *J. Org. Chem.* **1990**, *55*, 4472.

253. McKenna, C. E.; Higa, M. T.; Cheung, N. H.; McKenna, M. -C. *Tetrahedron Lett.* **1977**, 155.

254. Theodoropoulos, D.; Schwartz, I. L.; Walter, R. *Biochemistry* **1967**, *6*, 3927.

255. Kagan, H. M.; Manning, L. R.; Meister, A. *Biochemistry* **1965**, *4*, 1063.

256. Yamauchi, K.; Kinoshita, M.; Imoto, M. *Bull. Chem. Soc. Jpn.* **1972**, *45*, 2528.

257. Yamauchi, K.; Ohtsuki, S.; Kinoshita, M. *J. Org. Chem.* **1984**, *49*, 1158.

258. Price, N. C.; Stevens, L. *Fundamentals of Enzymology*, Oxford Science: Oxford, UK, 1989; pp. 23-25.

259. Fieser, L. F.; Fieser, M. *Reagents for Organic Synthesis;* John Wiley & Sons: New York, 1967; p. 1276.

BIOGRAPHICAL SKETCH

Anthony Brian Dribben, son of Albert F. and Mary Jo Dribben, was born in Hattiesburg, MS, on January 6, 1970. After obtaining his early education in the public schools of Purvis, MS, he graduated with honors in 1988 from McComb High School, McComb, MS. He was awarded a Presidential Scholarship for undergraduate education at Mississippi College, Clinton, MS, and he graduated with distinction in 1992 with a Bachelor of Science degree in ACS chemistry. That same year he was awarded a Grinter Fellowship for graduate education in chemistry from the University of Florida, Gainesville, FL. In the summer of 1997, Anthony completed his Doctor of Philosophy degree in organic chemistry. His hobbies include cycling, discussing politics and sports, reading, listening to music, and contemplative introspection.

I certify that I have read this study and that in my opinion it conforms to acceptable standards of scholarly presentation and is fully adequate, in scope and quality, as a dissertation for the degree of Doctor of Philosophy.

Nigel G. J. Richards, Chair
Associate Professor of
Chemistry

I certify that I have read this study and that in my opinion it conforms to acceptable standards of scholarly presentation and is fully adequate, in scope and quality, as a dissertation for the degree of Doctor of Philosophy.

Rodney J. Bartlett
Graduate Research Professor
of Chemistry

I certify that I have read this study and that in my opinion it conforms to acceptable standards of scholarly presentation and is fully adequate, in scope and quality, as a dissertation for the degree of Doctor of Philosophy.

Wallace S. Brey
Professor of Chemistry

I certify that I have read this study and that in my opinion it conforms to acceptable standards of scholarly presentation and is fully adequate, in scope and quality, as a dissertation for the degree of Doctor of Philosophy.

William R. Dolbier, Jr.
Professor of Chemistry

I certify that I have read this study and that in my opinion it conforms to acceptable standards of scholarly presentation and is fully adequate, in scope and quality, as a dissertation for the degree of Doctor of Philosophy.

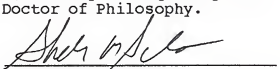

Sheldon M. Schuster
Professor of Biochemistry
and Molecular Biology

This dissertation was submitted to the Graduate Faculty of the Department of Chemistry in the College of Liberal Arts and Sciences and to the Graduate School and was accepted as partial fulfillment of the requirements for the degree of Doctor of Philosophy.

August, 1997

Dean, Graduate School